

**COMPUTATIONAL ANALYSIS OF AN ECCENTRIC
ROTOR THROUGH BONDGRAPH**

A THESIS SUBMITTED IN PARTIAL FULFILLMENT OF THE
REQUIREMENT FOR THE DEGREE OF

MASTER OF TECHNOLOGY

IN

COMPUTATIONAL
DESIGN

SUBMITTED BY

RISHIR KUMAR
(2K15/CDN/13)

UNDER THE SUPERVISION OF

DR. VIKAS RASTOGI

PROFESSOR



DEPARTMENT OF MECHANICAL ENGINEERING

DELHI TECHNOLOGICAL UNIVERSITY

JULY-2017

STUDENT'S DECLARATION

I hereby declare that the thesis entitled “**COMPUTATIONAL ANALYSIS OF AN ECCETRIC ROTOR THROUGH BONDGRAPH**” which is being submitted to the Delhi Technological University in partial fulfillment of the requirement for the award of the degree of Master of Technology in Computational Design is an authentic work carried out by me.

Rishir Kumar

2K15/CDN/13

CERTIFICATE

This is to certify that the dissertation entitled “**Computational Analysis of an Eccentric Rotor through Bondgraph**” produced by Rishir Kumar (M.Tech) (2K15/CDN/13) in the partial fulfillment of the requirements for the award of the degree of Master of Technology, Delhi Technological University (Formerly Delhi College of Engineering), is an authentic record of the candidate’s own work carried out by him under our guidance. The information and data enclosed in this report are original and has not been submitted elsewhere for honoring of any other degree to the best of our knowledge and belief.

Dr. Vikas Rastogi
Professor
(Project Mentor)

ACKNOWLEDGEMENT

Research is a higher concept. It brings to test our patience, vigor, and dedication. Every result arrived is a beginning for a higher achievement. My project is a small drop in an ocean. It needs the help of friends and guidance of experts in the field, to achieve something new.

I found my pen incompetent to express my thanks to my guide and mentor Dr. Vikas Rastogi, Professor, DTU under whose kind and worthy guidance and supervision, I had the opportunity to carry out this work. It was only due to his advice, thoughtful comments, constructive criticism, and continuous vigil over the progress of my work with a personal interest that it has taken this shape. They have been a great source of encouragement.

To get an opportunity to carry out the project work in the well-equipped, ever developing laboratories in our institution, I would like to pay my deep sense of thankfulness to Prof. R. S. Mishra, HOD, Department of Mechanical Engineering, DTU.

I am especially thankful to Mr. Ashish Gupta and Mr. Anuj Sharma, Ph.D. Scholar, DTU as I have completed my project under their worthy guidance and supervision. Their advice and thoughtful comments inspired me and were very helpful to complete my project.

I am very much thankful to my parents for their moral support and encouragement, which was giving me the strength to chase my goal. Without their support and inspiration, I would not able to complete my degree.

I would especially like to acknowledge my gratitude to all my dear friends for their consistent support, valuable suggestions from time to time to make this project worthy.

With a silent prayer to the Almighty, I take this opportunity to express my gratitude to all those who have supported me in completing my fourth-semester project work as a part of my degree program.

RISHIR KUMAR
(2K15/CDN/13)

LIST OF ABBREVIATIONS

E- Young's Modulus

I- Moment of Inertia

ρ - Density

A- Area

y- Displacement

γ - Separation Constant

M- Internal Bending Moment

θ - Angle of Rotation

T- Torque

R- Resilience

C- Damper

TF- Transfer Function

GY- Gyrator

SE- Source of Effort

SF-Source of Flow

V- Internal Shear Force

w- External Distributed Loading

e- Effort

f- Flow

I_d = Rotary inertia of the rotor

L_{beam} = Length of beam

N_{elem} = Number of elements

EI = Rigidity of the continuous rotor

D_i = Internal Diameter

D_o = External Diameter

μ_i = Internal Damping Coefficient

ABSTRACT

The computational analysis of an eccentric rotor is based on the bondgraph approach where the eccentricity of the rotor is analysed using bondgraph. This approach is used in this experiment to justify the displacements in shaft rotation which is occurring due to eccentricity introduced in the shaft. The computational analysis is necessary because by getting these results, a graph can be plotted which will give an accurate result of the bondgraph approach and it can be seen that by how much the displacement is occurring when the eccentricity is increased.

The modelling technique used in this approach introduces two shafts connected through a hub and is provided rotor excitation by connecting it through an external source that rotates it at different angular velocities. The shafts are connected in such a manner that it has displacements in radial axis and the displacement is noted.

The bond graph modelling of shaft and spinning hub is done using symbol sonata software bond pad. Simulation of this model has been carried out on Symbols sonata software which uses the fourth order Runge-Kutta method. The variation in the position of centre mass of rotor with change in various parameters such as speed, clearance is observed. The data obtained is used to get plots.

Keywords: Bondgraph modelling, Bondpad, Spinning hub, Spinning Shaft, Eccentricity, Simulation.

CONTENTS

STUDENT’S DECLARATION.....	i
CERTIFICATE.....	ii
ACKNOWLEDGEMENTS.....	iii
LIST OF ABBREVIATIONS.....	iv
ABSTRACT.....	v
LIST OF FIGURES	1
LIST OF TABLES	3
CHAPTER 1.....	4
INTRODUCTION	4
1.1 Modelling of rotor.....	4
1.2 Significance of bondgraph modelling	5
1.3 Research objective	7
1.4 Organization of thesis	7
CHAPTER 2.....	8
Literature review.....	8
CHAPTER 3.....	19
MATHEMATICAL MODELLING.....	19
3.1 Introduction	19
3.2 Rayleigh beam model.....	19
3.3 Summary of chapter.....	22
CHAPTER 4.....	23
BONDGRAPH MODELLING	23
4.1 Introduction	23
4.1.1 Basics of bondgraph modelling.....	25
4.1.2 Junction structure in bondgraph modelling.....	26
4.1.3 Concept of causality in bondgraph modelling.....	27
4.1.4 Junction and causality	29
4.2 Assumptions taken during modelling through bondgraph	30
4.3 Bondgraph model of a transformation capsule.....	31

4.4 Bondgraph model of shaft	32
4.5 Bondgraph model of spinning hub.....	33
4.6 Summary of chapter	34
CHAPTER 5	35
SIMULATION STUDY	35
5.1 INTRODUCTION	35
5.2 Simulation environment	35
5.3 Simulation properties	36
5.4 Ranga kutta method	37
5.5 Simulation rig	37
5.5 Simulation parameters.....	38
CHAPTER 6.....	39
RESULTS AND DISCUSSION	39
6.1 Introduction.....	39
6.2 Various variable parameters	39
6.2.1 Angular speed with low eccentricity	39
6.2.2 Angular velocity at comparatively high eccentricity.....	42
6.3 Results and discussion.....	58
CHAPTER 7.....	59
CONCLUSION AND FUTURE SCOPE.....	59
7.1 Conclusion.....	59
7.2 Future scope.....	59
REFERENCES	60
APPENDIX A	63
APPENDIX B.....	75

LIST OF FIGURES

Fig. 1.1: Simulation process steps.....	5
Fig 3.1: Beam element with generalized forces and displacement.....	20
Fig. 4.1 (a) Bondgraph Approach (b) Classical Approach.....	24
Fig.4.2 Basic elements	26
Fig.4.3 Transformation Capsule (Sub system).....	31
Fig.4.4 Shaft Capsule	32
Fig.4.5 Spinning hub.....	33
Fig 5.1: Bondgraph model of a complete eccentric rotor rig	37
Fig 6.1: Displacement of rotor about X vs. Y axes about the centre of mass at Eccentricity= 0.001 and Angular velocity= 16 rad/sec.....	40
Fig 6.2: Displacement of rotor about X vs. Y axes about the centre of mass at eccentricity= 0.001 and angular velocity= 40 rad/sec.....	41
Fig 6.3: Displacement of rotor about X vs. Y axes about the centre of mass at eccentricity= 0.001 and angular velocity= 70 rad/sec.....	42
Fig 6.4: Displacement of rotor about X vs. Y axes about the centre of mass at eccentricity= 0.005 and angular velocity= 16 rad/sec.....	43
Fig 6.5: Displacement of rotor about X vs. Y axes about the centre of mass at eccentricity= 0.005 and angular velocity= 40 rad/sec.....	44
Fig 6.6: Displacement of rotor about X vs. Y axes about the centre of mass at eccentricity= 0.005 and angular velocity= 70 rad/sec.....	45
Fig 6.7: Displacement of rotor about X-axis vs. time at eccentricity= 0.001 and angular velocity= 16 rad/sec	46
Fig 6.8: Displacement of rotor about X-axis vs. time at eccentricity= 0.005 and angular velocity= 16 rad/sec	47
Fig 6.9: Displacement of rotor about Y-axis vs. time at eccentricity= 0.001 and angular velocity= 16 rad/sec	48
Fig 6.10: Displacement of rotor about X-axis vs. time at eccentricity= 0.001 and angular velocity= 16 rad/sec	49
Fig 6.11: Displacement of rotor about X-axis vs. time at eccentricity= 0.001 and angular velocity= 40 rad/sec	50
Fig 6.12: Displacement of rotor about X-axis vs. time at eccentricity= 0.005 and angular velocity= 40 rad/sec	51

Fig 6.13: Displacement of rotor about Y-axis vs. time at eccentricity= 0.001 and angular velocity= 40 rad/sec	52
Fig 6.14: Displacement of rotor about Y-axis vs. time at eccentricity= 0.005 and angular velocity= 40 rad/sec	53
Fig 6.15: Displacement of rotor about X-axis vs. time at eccentricity= 0.001 and angular velocity= 70 rad/sec	54
Fig 6.16: Displacement of rotor about X-axis vs. time at eccentricity= 0.005 and angular velocity= 70 rad/sec	55
Fig 6.17: Displacement of rotor about Y-axis vs. time at eccentricity= 0.001 and angular velocity= 70 rad/sec	56
Fig 6.18: Displacement of rotor about Y-axis vs. time at eccentricity= 0.005 and angular velocity= 70 rad/sec	57

LIST OF TABLES

Table 4.1: Power terms in terms of effort and flow	24
Table 5.1: Parameter values for simulation.....	38
Table 6.1 Comparison among displacement and angular speed at different eccentricity	58

CHAPTER 1

INTRODUCTION

1.1 Modelling of rotor

Modelling is a process of producing model, whereas a model is representation of the working and construction of some system. Purpose of a model is to enable the analyst to predict the effect of changes to the system and it should be a close approximation to the real system and incorporate most of its salient features. Model should not be so complex that it is impossible to understand and experiment on it. A model is said to be good if it is judicious trade off between realism and simplicity. Model validity is an important issue in modelling. Validation techniques of model include simulating the model under known input conditions and comparing the output with the system output awesome experimental data available.

Most of the modern mechanical system form a part of multidisciplinary system and are closely coupled with the magnetic, hydraulic electrical or other kind of energy domains. Hierarchial approach is advantageous in modelling of an integrated dynamic system. Systematic approach minimises the modelling mistakes by breaking the system model into small components and subsystems, which are manageable in size and complexity. Same components can be used repeatedly without building blocks of the some part again. For example, an axle component in the Vehicle dynamics subsystem was built once and can be used for both rear and front axle. With hierarchial modelling, models of some component with different complexity can be easily be interchanged without changing the remaining structure of the model. The simulation process steps are shown in figure:

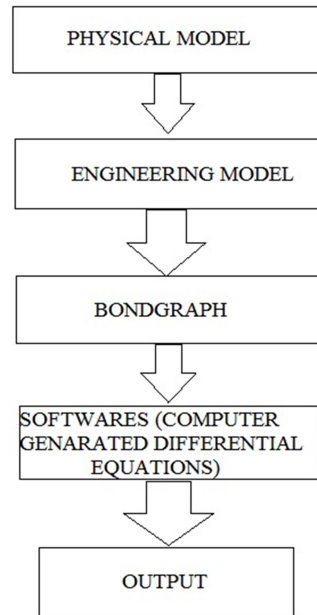


Fig. 1.1: Simulation process steps

The various approaches adopted in modelling of rotor with eccentricity are stated as follows:

- a) Ignoring body flexibility using a lumped mass model.
- b) Modelling the shaft as a regular beam using Rayleigh beam model and calculating, measuring or estimating model masses and stiffness.
- c) Modelling the mathematical model of different rotor.

1.2 Significance of bondgraph modelling

In the 1950s H.M. Paynter of MIT worked on various interdisciplinary engineering projects including digital and analogue computing, hydroelectric plants, nonlinear dynamics and control. He observed that the similar forms of equations were generated by dynamic system in a wide variety of domain (for example mechanical, fluid and electrical). He incorporated the notion of an energy port into his mythology and thus bond graph model was invented in 1959. Later bondgraph theory has been developed by many researchers.

Bondgraph model is a graphical model approach of modelling, in which component energy parts are connected by bonds which supply the transfer of energy between the system components.

The bondgraph language aspires to express general class of physical systems through the power interactions. Factor of power, i.e. Flow and Effort, have different interpretation in different physical domains. Hence power can be used as to generalized co-ordinate, to model coupled system residing in several energy domains in bondgraph. one only needs to recognize for groups of basic symbols in bondgraph, i.e., the three basic one port passive element inertance (I), Capacitance (C) Resistance (R) ; two basic active elements source of effort (SE) and source of flow (SF) ; two basic two port elements gyrator (GY) and transformer (TF) and two basic junctions i.e., constant flow junction(1) and constant effort junction (0); the basic variable of flow (f), effort (e), the time integral of flow (Q) and the time integral of effort (P). A physical system can be represented by lines and symbols, identifying the power flow by this approach. The lumped parameters element of inertance, capacitance and resistance are interconnected in the energy conserving way by junctions and bonds resulting in a network structure. The deviation of the system equation is so systematic that it can be algorithmized from the pictorial representation of bondgraph. Whole procedure of simulation and modelling of the system can be performed with some of the existing software example Camp-G, ENPORT, 20sim, SYMBOL-shakti, COSMO etc.

Main advantage of bondgraph techniques are-

- Bondgraphs can be used to describe simple linear and nonlinear systems.
- Bondgraph provides a useful notion for the purpose of modelling physical systems.
- Systems with diverse energy domain are treated in and unified manner.
- Easiest way to communicate the description of energy flow in dynamic systems.
- By using power conservation properties of bondgraph may need to constraint velocities only and the forces will be automatically balanced.
- Graphical representation of document complex models very easily and unambiguously.
- Model subsystems can be independently.

The present dissertation work explores the ability of bondgraph to obtain dynamic behaviour and modelling of rotor on physical paradigm of the system. Bondgraph technique generally offers flexibility in modelling and formulation of system equations. A very large system may also be modelled in a modular forms by creating subsystem models and then joining them together at their interaction port to create an integrated system model. Model is easy modified making it a powerful tool for system synthesis and consolidation of the

innovative ideas. Bondgraph equations normally used generalise displacement and generalized movement as state variables. The bondgraph modelling, their simulation and animation is performed using SYMBOLS Sonata, a bondgraph modelling software.

1.3 Research objective

The research's objective is:

- To create a dynamic model of an eccentric rotor by using bondgraph technique and to create its' mathematical model.
- Simulation of the bondgraph model of rotor for variable parameters to obtain behaviour of centre of mass of the rotor.

1.4 Organization of thesis

The chapters of the thesis are arranged in the following manner .*Chapter 1* discusses about the basic function and modelling of a bondgraph. The primary goal of this chapter is to provide the reader a rough idea about this thesis. *Chapter 2* discusses some literature reviews. *Chapter 3* presents the mathematical modelling of rigid rotor with eccentricity. *Chapter 4* presents the bondgraph modelling of shaft, hub and transformation element. *Chapter 5* presents simulation study .*Chapter 6* deals with results and discussion. *Chapter 7* concludes the thesis and also suggest some scope for future work.

CHAPTER 2

Literature review

Green K. and A.R. Champneys et al., [1] *Analysis of the transient response of an automatic dynamic balancer for eccentric rotor:* This paper investigates the transient response of a dynamical system modeling an automatic dynamic balancing mechanism for eccentric rotors. By using recently developed computational techniques, pseudo-spectra of the linearisation of the system about equilibrium are computed. This approach allows one to quantify which eigen values are most sensitive to perturbation. It is shown how the sensitivity of the eigen values directly influences the transient response. Furthermore, the effect which a variation of the damping coefficients has on the pseudo-spectra structure is considered. A transient growth due to the non-normality of the linearised system is shown to lead to an exponential decay or to a collapse back to the stable equilibrium; these effects are identified with the changes in the sensitivities of the eigen values under variation of the damping parameters. This provides a new insight into the full nonlinear system, in which qualitatively similar transient responses are shown to occur. In many applications involving rotating machinery it is important to know which frequencies may be excited after perturbation. In particular, the degree and nature of the transient response to perturbation can be highly unpredictable. This is evident in the non-normality of the damping and stiffness matrices describing such systems.

Tejas H. Patel et al., [2] *Experimental investigations on vibration response of misaligned rotors:* Misalignment is one of the most commonly observed faults in rotating machines. However, there have been relatively limited research efforts in the past to understand its effect on overall dynamics of the rotor system. In the existing literature, there is confusing spectral information on the rotor vibration characteristics of misalignment. The present study is aimed at understanding the dynamics of misaligned rotors and reducing the ambiguity so as to improve the reliability of the misalignment fault diagnosis. Influence of misalignment and its type on the forcing characteristics of flexible coupling is investigated followed by experimental investigation of the vibration response of misaligned coupled rotors supported on rolling element bearings. Steady-state vibration response at integer fraction of the first bending natural frequency is investigated. Effects of types of misalignments, i.e.

parallel and angular misalignments, are investigated. The conventional Fourier spectrum (i.e. FFT) has limitations in revealing the directional nature of the vibrations arising out of rotor faults. In addition, it has been observed that several other rotor faults generate higher harmonics in the Fourier spectrum and hence there could be a level of uncertainty in the diagnosis when other faults are also suspect. The present work through use of full spectra has shown possibility of diagnosing misalignment through unique vibration features exhibited in the full spectra (i.e. forward/backward whirl). This provides an important tool to separate faults that generate similar frequency spectra (e.g. crack and misalignment) and lead to a more reliable misalignment diagnosis. Full spectra and orbit plots are efficiently used to reveal the unique nature of misalignment fault not clearly brought out by the previous studies, and new misalignment diagnostics recommendations are proposed. The experimental investigation undertaken in this paper has contributed towards improvement in the misalignment diagnosis. Harmonic character of 3-pin-bush-type coupling is investigated experimentally under “no-misalignment” and “misalignment” conditions. From the measured forces, it has been found that the presence and type of misalignment (parallel and angular misalignment) have significant influence on harmonic content of the misalignment excitation forces.

Arun Kumar Samantaray et al., [3] *Sommerfeld effect in a gyroscopic overhung rotor-disk system*: Deflection of a rotor disk at the free end of a flexible overhung rotor shaft causes rotation about diametrical axis and consequently leads to a strong gyroscopic coupling in a spinning overhung rotor system. When the rotor is spun up about its axis, the unbalance in the rotor disc causes transverse and rotational vibrations to increase as the spin speed approaches the critical speed of the rotor. These transverse and rotational vibrations dissipate a lot of energy and if the rotor is driven through a non-ideal drive, i.e., a motor which can supply a limited amount of power, then the entire motor power may be spent to account for the energy dissipation. As a result, the rotor speed may get stuck in resonance at the critical speed or jump through the critical speed to a much higher speed with lower transverse and rotational vibration levels. These symptoms, normally referred to as the Sommerfeld effect, occur due to the intrinsic energetic coupling between the drive and the driven systems, and are important design considerations for development of various rotating machinery with flexible rotor shafts or supports (bearings). Sommerfeld effect in a strongly

gyroscopic rotor dynamic system is studied in this article. The dynamics of an overhung rotor system near the regimes of Sommerfeld effect is studied by using a discrete and a continuous shaft rotor model coupled with the model of the non-ideal motor drive. The models are developed using multi-energy domain modelling approach in bond graph model form. A steady state analysis of power transfer mechanism is used to postulate the ideal characteristics of Sommerfeld effect in the neighbourhood of the critical speed and thereafter, full transient analysis is performed with aid of the bond graph model generated coupled equations of motion to validate the postulated characteristics of the Sommerfeld effect.

Arun Kumar Samantaray et al., [4] *Bond Graph Modelling of an Internally Damped Non-ideal Flexible Spinning Shaft*: The rotating internal damping or non-conservative circulatory force in a rotor shaft system causes instability beyond a certain threshold rotor spinning speed. However, if the source loading of the drive is considered then the rotor spin is entrained at the stability threshold and a stable whirl orbit is observed about the unstable equilibrium. As we move towards the use of more and more lightweight rotor dynamic components such as the shaft and the motor, overlooking this frequency entrainment phenomenon while sizing the actuator in the design stage may lead to undesirable performance. This applies to many emerging areas of strategic importance such as in-vivo medical robots where flexible probes are used and space robotics applications involving rotating tools. We analyze this spin entrainment phenomenon in a distributed parameter model of a spinning shaft, which is driven by a non-ideal DC motor. A drive whose dynamics is influenced by the dynamics of the driven system is called a non-ideal source and the whole system is referred to as a non-ideal system. In particular, we show the advantages of representing such non-ideal drive–system interactions in a modular manner through bond graph modelling as compared to standard equation models where the energetic couplings between dynamic variables are not explicitly shown. The developed modular bond graph model can be extended to include rotor disks and bearings placed at different locations on the shaft. Moreover, the power conserving property of the junction structure of the bond graph model is exploited to derive the source loading expressions which are then used to analytically derive the steady-state spinning frequency and whirl orbit amplitude as functions of the drive and the rotor system parameters. We show that the higher transverse modes may become unstable before the lower ones under certain parametric conditions. The shaft spinning speed is entrained at the lowest stability threshold among all transverse modes. The

bond graph model is used for numerical simulation of the system to validate the steady-state results obtained from the theoretical study. The paper mentions the dynamics of an internally and externally damped flexible spinning shaft, which is driven through a non-ideal source (a DC motor). The stability threshold of all transverse vibration modes is determined and it is shown that the motor speed cannot pass the lowest stability threshold, i.e., the motor gets stuck at that threshold condition. If the power supply to the motor is increased further then the amplitude of transverse vibrations increase, but the motor speed remain stuck at the stability threshold. These are the classic symptoms associated with the Sommerfeld effect. The amplitudes and frequencies of the steady state transverse vibrations (whirl) are analytically obtained as functions of the system parameters.

G. Jacquet-Richardet et al., [5] *Rotating Internal Damping in the Case of Composite Shaft*: There is an increasing range of applications for rotors made of composite materials and operating at supercritical speeds. Design of such structures involves specific features which have to be accounted for in order to allow safe operations. A proper modelling of the mechanical characteristics of the composite is first needed. But, as far as the structure is rotating, the effect of stress stiffening and spin softening may be considered and the effect of internal damping has to be studied in order to avoid possible instability. Internal or rotating damping modelling remains an active field of research where both theoretical developments and experimental results are needed. The presented paper deals with the dynamical analysis of internally damped rotating composite shafts. Usual rotor dynamics modeling is based on beam theories. In this case, the General Homogenized Beam Theory is needed to avoid the main drawbacks associated with formulations that consider only symmetrical and balanced stacking sequences and do not take into account the distance of layers from the neutral axis.

Hsiang-Chieh Yu et al., [6] *Robust modal vibration suppression of a flexible rotor*: This study deals with active robust modal vibration control of rotor systems supported by magnetic bearings. The inherent divergent rigid body modes are suppressed by using a dual-level control approach. Finite element method is applied to formulate the rotor model. The Timoshenko beam theory, including the effects of shearing deformations and rotary inertia, is considered in this work. Because practical control systems are often limited by its sensing,

hardware, and computation speed capabilities, the reduced order approach is often used for a control system design. This study applies the independent modal space control (IMSC) approach to extract the accurate lower modes from the complex rotor systems with the gyroscopic effect considered. In practice, it is extremely difficult to model the complete dynamic characteristics of a rotor system. The model may contain un-modelled dynamics and parameter changes, which can be viewed as uncertainties of a system. As opposed to the conventional control approach, which requires fixed and accurate system parameters, this study considers robust control approach to design a controller capable of tolerating external disturbance and model uncertainties. It is demonstrated that the proposed approach is effective for vibration suppression when the system is subjected to impulsive or step loading, speed variation, and sudden loss of disk mass. Robust modal control design of a magnetically suspended rotor has been presented in this work using the finite element formulation. The original system is augmented using the direct output control in the first level, which removes the repeated rigid body modes of the uncontrolled system. In the second level design, a robust controller is implemented in the complex modal space. The vibration modes are controlled independently and hence for each mode controlled, the system matrix equation concerned is only of size 2×2 , against $2n \times 2n$ in the traditional coupled control approach. Significant reduction of the computational effort is evident by using the present approach. It has been shown that the present control design is robust for systems with uncertainties and parameter variations, such as disk mass variation, feedback gains variation, speed variation, and sudden disk mass loss, etc.

M. Karthikeyan, et al., [7] *Sommerfeld Effect Characterization in Rotors with Non-ideal Drive from Ideal Drive Response and Power Balance*, Rotor dynamic systems are often analyzed with ideal drive assumption. However, all drives are essentially non-ideal, i.e., they can only provide a limited amount of power. One basic fact often ignored in rotor dynamics studies is that the drive dynamics has complex coupling with the dynamics of the driven system. Increase in drive power input near resonance may contribute to increasing the transverse vibrations rather than increasing the rotor spin, which is referred to as the Sommerfeld effect. In this article, we generate the rotor response with finite element (FE) model by assuming an ideal drive. Thereafter, the rotor system's response with ideal drive is used in a power balance equation to theoretically predict the amplitude and speed characteristics of the same rotor system when it is driven through a non-ideal drive. The

integrated system with drive-rotor interaction is modelled in bond graph form and the transient analysis from the bond graph model is used to validate the theoretical results. The results are important from the point of actuator sizing for rotor dynamic systems.

Martin Donát et al., [8] *Eccentrically mounted rotor pack and its influence on the vibration and noise of an asynchronous generator:* Time-varying magnetic forces are the main source of vibrations in rotating electrical machines. A number of papers dealing with computational modelling of the dynamic behaviour of rotating electrical machines have been published. Almost all of these papers do not consider electro-mechanical interaction between the stator and the rotor of the machine. A computational model including electro-mechanical interaction is proposed in this paper. The influence of the air gap eccentricity due to eccentric mounting of the rotor pack on the shaft of the rotor is investigated. Electromagnetic coupled-field analysis was performed to obtain the dependence of the magnetic forces, which act on the stator and the rotor pack, on the time and air gap eccentricity. Attention has been paid to the air gap eccentricity due to the interaction between the stator and the rotor and the influence of the air gap eccentricity on the vibration and sound power of the machine. The obtained results show that the air gap eccentricity affects the amplitude spectrum of the magnetic forces. This change of amplitude spectrum causes a significant increase in the torsional vibration of the stator of the examined machine. The air gap eccentricity is also significantly reflected in the trajectory of the rotor centre line and radial load of bearings in the machine.

Vikas Rastogi, [9] *Effects of discrete damping on the dynamic behaviour of rotating shaft through extended Lagrangian formulation:* The main focus of the paper is touted as effects of discrete damping on the dynamic analysis of rotating shaft. The whole analysis is being carried out through extended Lagrangian formulation for a discrete-continuous system. The variation formulation for this system is possible, considering the continuous system as one-dimensional. The generalized formulation for one dimensional continuous rotary shaft with discrete external damper has been obtained through principle of variation. Using this extended formulation, the invariance of umbra-Lagrangian density through extended Noether's theorem is achieved. Rayleigh beam model is used to model the

shaft. Amplitude equation of rotor is obtained theoretically and validated through simulation results. The simulation results reveal the important phenomena of limiting dynamics of the rotor shaft, which is due to an imbalance of material damping and stiffness of the rotor shaft. The regenerative energy in the rotor shaft, induced due to elasticity/stiffness of the rotor shaft, is dissipated partially through the in-span discrete damper and also through the dissipative coupling between drive and the rotor shaft. In such cases, the shaft speed will not increase with increase in excitation frequency of the rotor but the slip between the drive and the shaft increases due to loading of drive. It has been demonstrated, that in-span discrete external damping as an isolated damper can be included in the extended Lagrangian-Hamiltonian formulation that permits a general formulation of the dissipation effects in this new extension. The theory is further used to illustrate the significance of complex modes in vibrations of rotating shafts, which has been taken as a case study. An interesting phenomenon of limiting dynamics of a rotor shaft with in-span external damper through a dissipative coupling has been obtained. The dynamic behaviour has been analysed through extended Lagrangian- Hamiltonian formulation for fields. The case study has been analysed theoretically and numerically. The study has further examined the various aspects of limiting dynamics of the rotor shaft and validated through simulation results. Further, the study demonstrated, that the regenerative energy in the shaft, due to elasticity/stiffness is dissipated partially through in-span external damper and the dissipative coupling. Limiting dynamics basically occurred due to the balance of power imported by internal damping from the shaft spin and dissipation of power by in-span external isolated discrete damper. Some portion of the energy has also been dissipated in the coupling and a part of action of internal damping, which acted as an external damping. The animation frames of the system have depicted the entrainment phenomenon of the whirl speed at different natural frequencies.

Xiangxi Kong et al., [10] *Synchronization analysis and control of three eccentric rotors in a vibrating system using adaptive sliding mode control algorithm*: In this paper, self- and controlled synchronizations of three eccentric rotors (ERs) inline driven by induction motors rotating in the same direction in a vibrating system are investigated. The vibrating system is a typical under actuated mechanical - electromagnetic coupling system. The analysis and control of the vibrating system convert to the synchronization motion problem of three ERs. Firstly, the self-synchronization motion of three ERs is analyzed according to self-synchronization theory. The criteria of synchronization and stability of

self-synchronous state are obtained by using a modified average perturbation method. The significant synchronization motion of three ERs with zero phase differences cannot be implemented according to self-synchronization theory through analysis and simulations. To implement the synchronization motion of three ERs with zero phase differences, an adaptive sliding mode control (ASMC) algorithm based on a modified master–slave control strategy is employed to design the controllers. The stability of the controllers is verified by using Lyapunov theorem. The performances of the controlled synchronization system are presented by simulations to demonstrate the effectiveness of controllers. Finally, the effects of reference speed and non-zero phase differences on the controlled system are discussed to show the strong robustness of the proposed controllers. Additionally, the dynamic responses of the vibrating system in different synchronous states are analyzed.

R. Whalley et al., [11] *Contoured shaft and rotor dynamics*: The dynamics of shaft–rotor systems, where the shaft profiles are contoured, are considered. Shafts with diameters which are functions of the shaft length are analysed. Procedures enabling the determination of the deflection, slope, bending moment and shear force at the extremities of the shaft are employed. Resonance, critical speed or whirling frequency conditions are computed using simple harmonic response methods. The response of the system for particular shaft–rotor dimensions and rotational speeds is determined, establishing the dynamic characteristics in the vicinity of the whirling speed. A cantilevered shaft–rotor system with an exponential – sinusoidal profile is investigated for purposes of illustration. The flexibility of the approach and the general applicability of the technique proposed is emphasised.

Lili Gu et al., [12] *An analytical study of rotor dynamics coupled with thermal effect for a continuous rotor shaft*: This paper presents an analytical analysis of a continuous rotor shaft subjected to universal temperature gradients. To this end, an analytical model is derived to investigate the generic thermal vibrations of rotor structures. The analytical solutions are obtained in a rotating frame and include parameters related with both the thermal environment and the rotor dynamic structures. This provides an insight into the mechanisms for the rotor thermal vibration. Furthermore, numerical results based on the analytical solutions are given. An index denoting the temperature gradients is proposed for the occasions with nonlinear cross-sectional temperature distributions. Finally, the factors

influencing the thermal vibrations are analyzed. The results show that the thermal vibration is affected by many factors including the shaft size, rotational speeds, heating locations, critical speed, etc. Moreover, it is investigated how the convection coefficient and the heat conductivity influence the thermal vibrations in order to provide an insight into the management of thermal vibrations from the perspective of thermal aspects.

Aydin Boyaci et al., [13] *Numerical continuation applied to nonlinear rotor dynamics:* Besides the synchronous oscillations due to unbalance, high-speed rotors in oil film bearings are known to show whirl/whip instabilities which exhibit various types of sub-synchronous oscillations. Here, the methods of numerical continuation are applied to study the sub-synchronous oscillations in detail. The main scope is to analyze the stability and bifurcation behaviour of the unbalanced Laval/Jeffcott rotor supported in semi-floating ring bearings. Characteristic bifurcation scenarios prove the existence of two different types of Hopf bifurcations which represent whirl/whip instabilities due to the inner or the outer oil films. Furthermore, it is shown that the critical limit cycle of non-tolerable amplitude is born at a saddle-node bifurcation. Finally, the influence of unbalance on the sub-synchronous oscillations is investigated by tracing the occurring bifurcations in the parameter plane of the unbalance load and the rotor speed. The obtained bifurcation curves provide extended stability charts which illustrate the global solution behaviour of the considered rotor bearing systems.

Evgueni V. Karpenko et al., [14] *Regular and chaotic dynamics of a discontinuously non-linear rotor system:* The non-linear vibrations are considered in a two-degree of freedom rotor dynamic system subjected to a bearing clearance effect. The excitation is provided by an out-of-balance within the system, and the non-linearity, in the form of a discontinuous stiffness, is effected by means of a radial clearance between the elastically supported rotor and the elastically supported outer ring. Different non-linear dynamic analysis techniques are employed to unveil the global dynamics of the rotor system. In particular, the system has been investigated with the help of time trajectories, phase portraits, bifurcation diagrams, Poincare maps, power spectrum analysis and construction of basins of attraction. A numerical study is presented which encompasses the effects of

different system parameters in order to demonstrate the severity of the vibrations. It is also shown that the response of the system can be extremely sensitive to changes in these parameters, and that chaos can exist over large regions of parameter space.

Eilif Pedersen et al., [15] *Bond graph modeling of rotordynamic systems with a flexible shaft including shear correction:* Rotor-dynamic analysis is of crucial importance in the design of rotor systems in order to prevent rotor instabilities. Detection of critical speeds, analysis of bearing stiffnesses or damping on the rotor stability and how unbalances, dynamic run-up, transient conditions or fault conditions influences the complete rotor system are some of the required areas that have to be thoroughly analyzed. Traditionally, rotor-dynamic analysis is carried out using the Finite Element approach, an approach having favorable properties, but also with some limitations especially related to computational time and system analysis. In this paper, a continuous shaft-disc system is modeled as a rotating Euler-Bernoulli beam, but shear stress corrections are added as a Timoshenko beam. The continuous shaft-disc system with imbalances is described using kinetic and potential energies including translational and rotational motion, gyroscopic coupling, shear and axial forces. The shaft model developed is based on the assumed mode approach for representing distributed systems and this is then combined with a standard rigid body disc model to form a complete rotor model. The derived model can be regarded as a mechatronic element where the focus is on control and connectivity to other models. The equations of motion are derived using the Lagrange approach and the model is presented in the bond graph formalism. Simulation examples are included for simple rotor configurations demonstrating most rotor dynamic phenomena together with more complex rotor dynamics features.

CHAPTER 3

MATHEMATICAL MODELLING

3.1 Introduction

A mathematical model of a dynamic system is defined as a set of equations that represent dynamics of system accurately or at least fairly well. A mathematical system is not unique to a given mechanical system. A system may be represented in different ways and therefore may have many mathematical models, depending on one's perspective.

The dynamics of a mathematical model can be described in terms of differential equations. Such differential equations may be obtained by using physical laws governing particular system for example Newton's used in case of mechanical system and Renold's equation in hydraulic system. Mathematical model as you may give many different forms. Depending on the particular system and the particular circumstances, one mathematical model may be better suited than other models. Once a mathematical model of a system is obtained various analytical and Computer tools can be used for analysis and synthesis purposes.

3.2 Rayleigh beam model

As the bond graph model of our shaft is based on Rayleigh beam model. One may describe the mathematical modelling of Rayleigh beam.

The following assumptions are taken into consideration:

- i. The beam is prismatic and has a straight centroidal axis (which we will label the x-axis),
- ii. The beam's cross-section has an axis of symmetry (which we will label the y axis)
- iii. All transverse loading act in the plane of symmetry (x-y plane),
- iv. Plane sections perpendicular to the centroidal axis remains plane after deformation,
- v. The material is elastic, isotropic and homogeneous,
- vi. Transverse deflections are small.

.

The physical situation is drawn schematically in Figure 2.1. One may denote the internal bending moment by M , the internal shear force by V and external distributed loading by w .

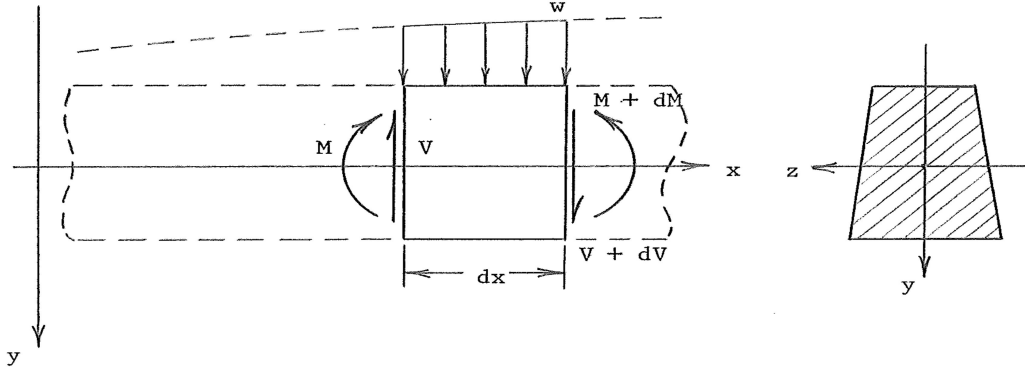


Fig 3.1: Beam element with generalized forces and displacement

The elementary Euler-Bernoulli beam theory has some serious shortcomings for high frequency motion. One may make here a refinement in the story to account for the rotary motion of beam elements. This rotary connection was first applied by Lord Rayleigh and hence one will use the terminology Rayleigh beam theory.

The place where the rotary motion, i.e., the angular acceleration of beam elements, would be incorporated into the analysis lies in the moment equation (3.1)

$$\frac{\partial M}{\partial x} = V \quad (3.1)$$

Taking this motion into account, (3.1) now can be written as,

$$\frac{\partial M}{\partial x} = V - \rho I \frac{\partial^2 \theta}{\partial t^2} \quad (3.2)$$

where θ is the angle of rotation of the beam element, and ρ and I as before being the material density and cross sectional area moment of inertia respectively.

For small deformation $\cong \frac{dy}{dx}$, and so (3.2) becomes

$$\frac{\partial M}{\partial x} = V - \rho I \frac{\partial^3 \theta}{\partial t^2 \partial x} \quad (3.3)$$

$$\frac{\partial M}{\partial x} = -w + \rho A \frac{\partial^2 y}{\partial t^2} \quad (3.4)$$

Combining equation (3.3) and (3.4) with (3.1) gives

$$b^2 \frac{\partial^4 y}{\partial x^4} - a^2 \frac{\partial^4 y}{\partial x^2 \partial t^2} + \frac{\partial^2 y}{\partial t^2} = 0 \quad (3.5)$$

Where, we have taken the zero external loading case, $b^2 = \frac{EI}{\rho A}$ and $a^2 = \frac{I}{A}$. Equation (3.5) is then the governing relations for Rayleigh beam theory.

The separation of variables method may also be applied successfully to equation (3.5). Putting in the product form $y = X(x)T(t)$, gives

$$X'''' + \frac{\gamma^2 a^2}{b^2} X'' - \frac{\gamma^2}{b^2} X = 0 \quad (3.6)$$

$$\ddot{T} + \gamma^2 T = 0 \quad (3.7)$$

Here γ is again the Separation constant.

The solution to (3.6) and (3.7) is the same as for the Euler-Bernoulli case, the solution is not quite so easy, but can be handled by putting in a solution form Ae^{rx} . After cancelling the common terms, this produces the characteristic equation.

The roots of this equation are

$$r^4 + \frac{\gamma^2 a^2}{b^2} r^2 - \frac{\gamma^2}{b^2} = 0 \quad (3.8)$$

$$r_{1,2} = \pm \left\{ -\frac{\gamma^2 a^2}{2b^2} - \left\{ \frac{\gamma^4 a^4}{4b^4} + \frac{\gamma^2}{b^2} \right\}^{1/2} \right\}^{1/2} = 0 \quad (3.9)$$

$$r_{3,4} = \pm \left\{ -\frac{\gamma^2 a^2}{2b^2} + \left\{ \frac{\gamma^4 a^4}{4b^4} + \frac{\gamma^2}{b^2} \right\}^{1/2} \right\}^{1/2} = 0$$

So the solution may be written as

$$X(x) = A_1 e^{r_1 x} + A_2 e^{r_2 x} + A_3 e^{r_3 x} + A_4 e^{r_4 x} \quad (3.10)$$

or by letting $r_{1,2} = \pm im_1$ and $r_{3,4} = \pm im_2$, we write

$$X(x) = c_1 \sin m_1 x + c_2 \cos m_1 x \quad (3.11)$$

$$= c_3 \sin hm_2 x + c_4 \cos hm_2 x$$

Notice that the Rayleigh solution from, (3.11) is quite similar to the Euler-Bernouli results. However, a detailed comparison of the frequencies and mode shapes would show a difference between the two theories.

3.3 Summary of chapter

In this chapter mathematical modelling of different components used in our analysis is done. The mathematical modelling of eccentricity is done with the help of Reynolds equation. The mathematical modelling of rotor shaft is done based on Rayleigh beam model. The nomenclature presents the entire notation used in the mathematical model. The mathematical model obtained in this chapter is used in bondgraph modelling of components in the next chapter.

CHAPTER 4

BONDGRAPH MODELLING

4.1 Introduction

A bondgraph is a graphical representation of a physical dynamic system. It is similar to the better known block diagram and signal-flow graph, with the major difference that the arcs in bondgraphs represent bi-directional exchange of physical energy, while those in block diagrams and signal-flow graphs represent uni-directional flow of information. Also, bondgraphs are multi-energy domain (e.g. mechanical, electrical, hydraulic, etc.) are domain neutral. This means a bondgraph can incorporate multiple domains seamlessly.

The bondgraph is composed of the "bonds" which link together "single port", "double port" and "multi port" elements (see below for details). Each bond represents an instantaneous flow of energy (dE/dt) or power. The flow in each bond is denoted by a pair of variables called 'power variables' whose product is the instantaneous power of the bond. For example, the bond of an electrical system would represent the flow of electrical energy and the power variables would be voltage and current, whose product is power. Each domain's power variables are broken into two types: "effort" and "flow". Effort multiplied by flow produces power, thus the term power variables. Every domain has a pair of power variables with a corresponding effort and flow variable. Examples of effort include force, torque, voltage, or pressure; while flow examples include velocity, current, and volumetric flow. The table below contains the most common energy domains and the corresponding "effort" and "flow".

A bondgraph has two other features which is derived describe briefly here, and further discussed in more details. One is the "half Arrow" sign convection, which defines the assumed directions of positive energy flow. As with free body diagrams and electrical circuit diagrams, the choice of positive direction is arbitrary with a caveat that analyst must be consistent throughout with chosen definitions. The other feature is the "causal stroke" which is a vertical bar placed on only one end of the bond and it is not arbitrary. There are rules for signing the proper causality to a given port and rules for the precedence among ports. In Bondgraph any port (single, double or multiple) attached to the bond will specify either "flow" or "effort" by its causal stroke but not both. The port attached at the end of the bond with a "causal stroke" specifies the "flow" of the bond and the bond imposes "effort" upon that port. Similarly the port at the end of without the "causal stroke" imposes "effort" to the bond, whereas the bond imposes "flow" to that port.

The power term is denoted by the product of effort and flow, i.e

$$\text{Power} = \text{Effort (e)} \times \text{Flow (f)}$$

Table 4.1: Power terms in terms of effort and flow

Systems	Efforts (e)	Flow (f)
Mechanical	Force (F)	Velocity (V)
	Torque (τ)	Angular Velocity (ω)
Electrical	Voltage (V)	Current (I)
Hydraulic	Pressure (P)	Volume flow rate (dQ/dt)
Thermal	Temperature (T)	Entropy change rate (dS/dt)
	Pressure (P)	Volume change rate (dV/dt)
Chemical	Chemical potential (μ)	Mole flow rate (dN/dt)
	Enthalpy (h)	Mass flow rate (dm/dt)
	Magnetic-motive force (e_m)	Magnetic flux (φ)

Let us now see the difference between a classical approach of physical modelling and a bondgraph approach for modelling a system.

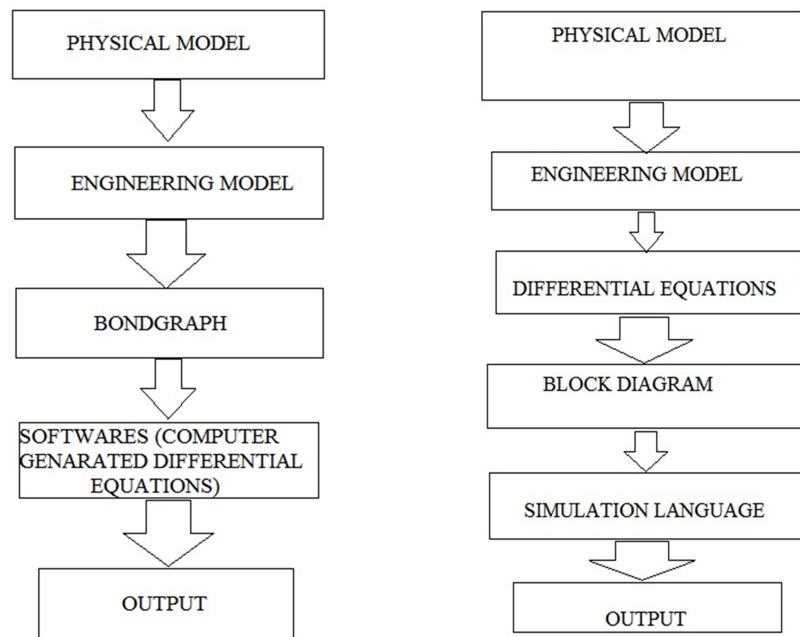


Fig. 4.1 (a) Bondgraph Approach

(b) Classical Approach

4.1.1 Basics of bondgraph modelling

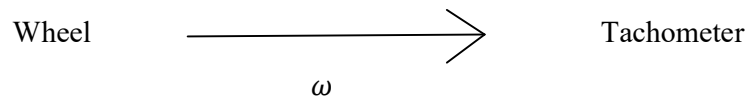
The fundamental idea of the bond graph is that power is transmitted between connected components by combination of “flow” and “efforts” (generalized flow and generalized effort). Refer to the table 4.1 for examples flow and efforts in different domains can be ascertained. If an engine is connected to wheel through a shaft, the power in the rotational mechanical domain, which means that the flow and efforts are angular velocity (ω) and torque (τ) respectively. The word bondgraph is first step towards the bondgraph, in which words define the components. As the word bondgraph, this will look like:

$$\text{engine} \xrightarrow[\omega]{\tau} \text{wheel}$$

To provide a sign convention half arrow is used. If the engine is doing work when τ and ω are positive, then the diagram would be drawn as:

$$\text{engine} \xrightarrow[\omega]{\tau} \text{wheel}$$

To indicate a measurement of full arrow is used and is referred as single bonds, because the amount of power flowing through the bond is insignificant. However, it may be useful to certain physical components. For example, the power required to activate a relay in orders of magnitude smaller than the power through the itself; making it relevant only to convey whether the which is on, not the power consumed by it.



4.1.2 Junction structure in bondgraph modelling

Power bonds can join at one of two kinds of junctions i.e. a 1 junction and a 0 junction.

- In a 1 junction, the flows are equal and effort sum to zero. This corresponds to a force balance at a mass in a mechanical system or to electrical loop.
- In a 0 junction the effort are equal and sums to zero. This corresponds to a mechanical “stack” in which all forces are equal or to a node in an electrical circuit (where the Kirchhoff’s law is applied).

Consider a resistor in series, for an example of a 1 junction:

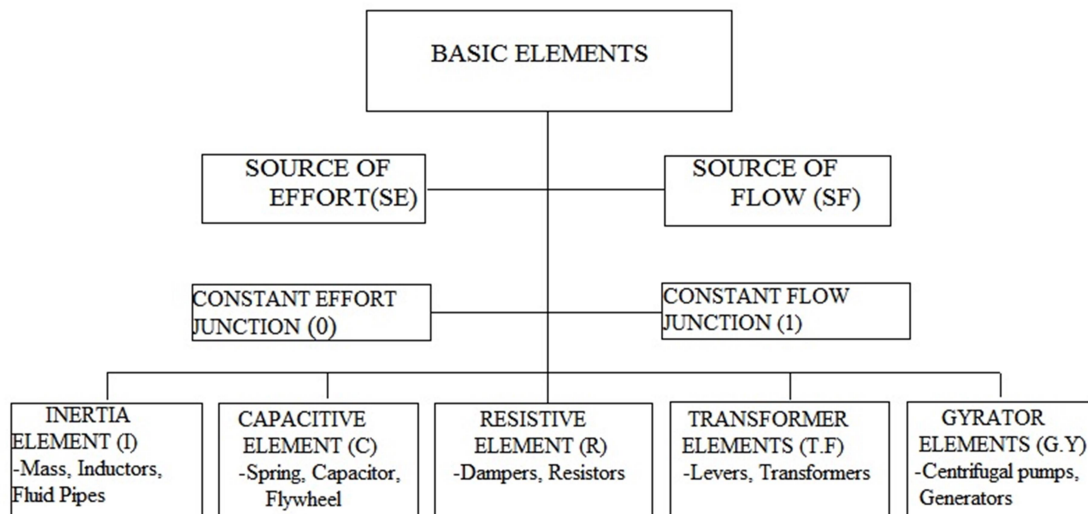
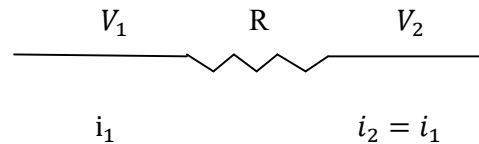
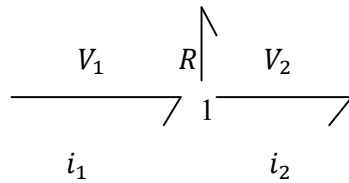


Fig.4.2 Basic elements

In this case, the flow (current) is constrained to be same at all points, and the efforts sum to zero when the implied current return path is included. Power can be computed at points 1 and 2, whereas in general some power will be dissipated in resistor. Bondgraph of this system becomes



This diagram may seem counter intuitive in that flow which is not preserved in the same way across the diagram, from electrical point of view. It will be helpful to consider the 1 junction as a daisy chaining the bonds it connects to and the power bond up to R as resistor with a lead turning down. Bond graph modelling proceeds from the identification of key 0 and 1 junctions associated with identifiable flows and efforts in the system, after that indentifying the storage element (I and C) and dissipative (R), power sources, and drawing bonds wherever the information or power flows between the junctions, sources and dissipative/storage components. The sign conventions (arrow heads), and causality are assigned and finally the questions which is describing the behaviour of a system can be derived using the graph as a kind of map or guide.

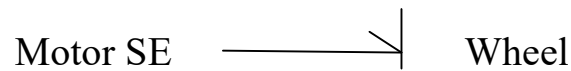
4.1.3 Concept of causality in bondgraph modelling

Bondgraph have a notion of causality that indicate which side of bond determines the instantaneous flow and with which side determines the instantaneous efforts. While formulating the dynamic equation which describes the system, causality for each modelling element, which variable is independent and which is dependent. Analysis of a large scale model becomes easier by propagating the causation graphically from one modelling element to other. In a bondgraph model, completing causal assignment will allow the detection of a modelling situation where an algebraic loop exists i.e. the situation when a variable is defined recursively as the function of itself.

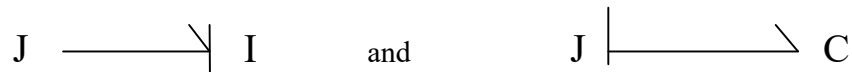
Considered a capacitor in series with a battery as an example of causality. To charge a capacitor instantly is not physically possible therefore anything connected in parallel with a capacitor should necessarily have the same voltage (effort variable) as that of the capacitor. Similarly, an inductor cannot change flux instantly therefore any component connected in series with an inductor should necessarily have the same flow as that at of the inductor.

Because inductors and capacitors are passive devices, therefore they cannot maintain their respective flow and voltage indefinitely the components to which they are connected will affect their respective flow and voltage, but only indirectly by affecting their voltage and current respectively. Causality is basically a symmetric relationship. When one side causes flow, the other side causes effort. Active components such as an ideal current or voltage source are also causal.

In a bondgraph notation, a causal stroke can be added to one end of the power bond which indicates that the bond opposite end is defining the effort. For example, consider a constant torque Motors which is driving a wheel which is a source of effort (SE) may be drawn as follows:



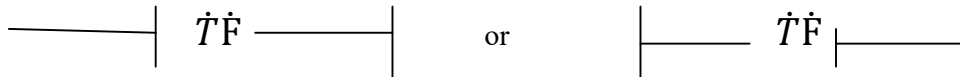
Similarly, the side causal stroke (in case of wheel) defines the flow for the bond. Causality results in the compatibility constraints. It is clear that only one end of the power bond can define the effort therefore only one end of a bond can have a causal stroke. The two passive components with time dependent behaviour, C and I, can only have one sort of causation i.e a C component define effort and I component define flow. Therefore from a Junction J, the only legal configuration for C and I are



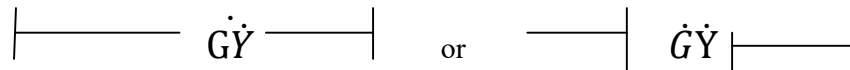
A resistor has no time-dependent behaviour therefore or voltage can be applied to get flow instantly or be applied to get a voltage instantly. Hence a resistor can be at either end of a causal.



Source of effort (SE) define effort, sources of flow (SF) define flow. Transformers are passive, neither storing energy nor dissipating. So, the causality passes through them.

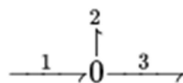


A gyrator transforms effort to flow and flow to effort, so if effort is caused on one side, flow is caused on the other side and vice versa.



4.1.4 Junction and causality

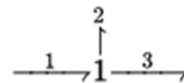
In a 1-junction, flows are equal and in a 0-junction efforts are equal. Thus, with causal bonds only one bond can cause the flow in a 1- junction and only one can cause the effort in 0-junction. Therefore, if the causality of others is also known, that bond is known as strong bond.



Resulting equations:

$$e_1 = e_2 = e_3$$

$$f_1 = f_2 + f_3$$



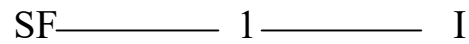
Resulting equations:

$$f_1 = f_2 = f_3$$

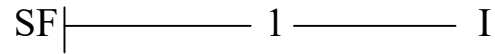
$$e_1 = e_2 + e_3$$

Using the above our rules one can continue to assign the causality. If any model which results in inconsistent causality therefore, it is not physically valid. For example, considered an

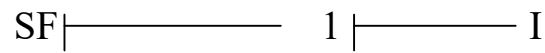
inductor in series with an ideal current source which is physically impossible configuration and the bondgraph looks like:



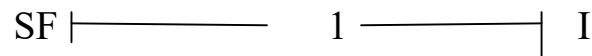
Assigning causality to source bond we get,



Propagating the causality through the junction will give,



But assigning causality to inductor will give,



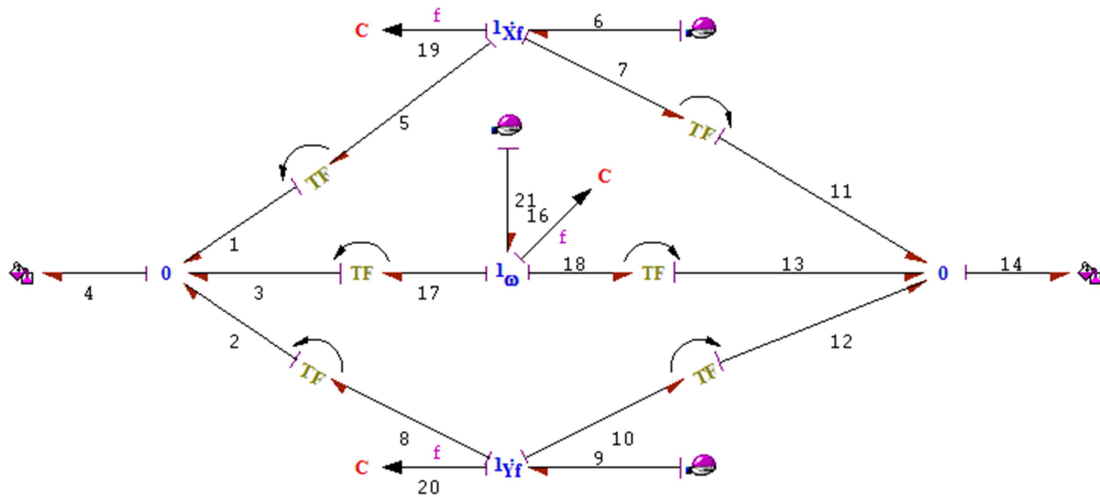
The causality on the right bond is redundant therefore this is valid disability which leads to automatically identify impossible configuration is a major advantage of bondgraph.

4.2 Assumptions taken during modelling through bondgraph

The following assumptions are being made during bondgraph modelling of rotor with eccentricity:

1. The rotor is rigid and symmetric.
2. The angular speed of rotation is kept constant during each eccentric values of rotor.
3. The gyroscopic effect is considered.
4. Displacement of the rotor in the axial direction is considered.

The shaft model is based on the Rayleigh beam model where inertia rotary inertia of the speed is included. Shaft elements with shear forces and moments acting on it can be modelled where the stiffness of the shaft elements relates the generalized Newtonian forces to generalize displacement at the ends of element. The stiffness Matrix can be modelled as a 4-port compliance field storing energy due to the four generalized displacement.



The fixed to rotating frame velocity transformer capsule has been used four times to transform $\dot{X}_f, \dot{Y}_f, \dot{\omega}_f, \dot{\theta}_f$ to rotating frame to model internal damping of the shaft in rotating frame through the R- fields, which brings out the tensorial nature of the rotating internal damping.

4.4 Bondgraph model of shaft:

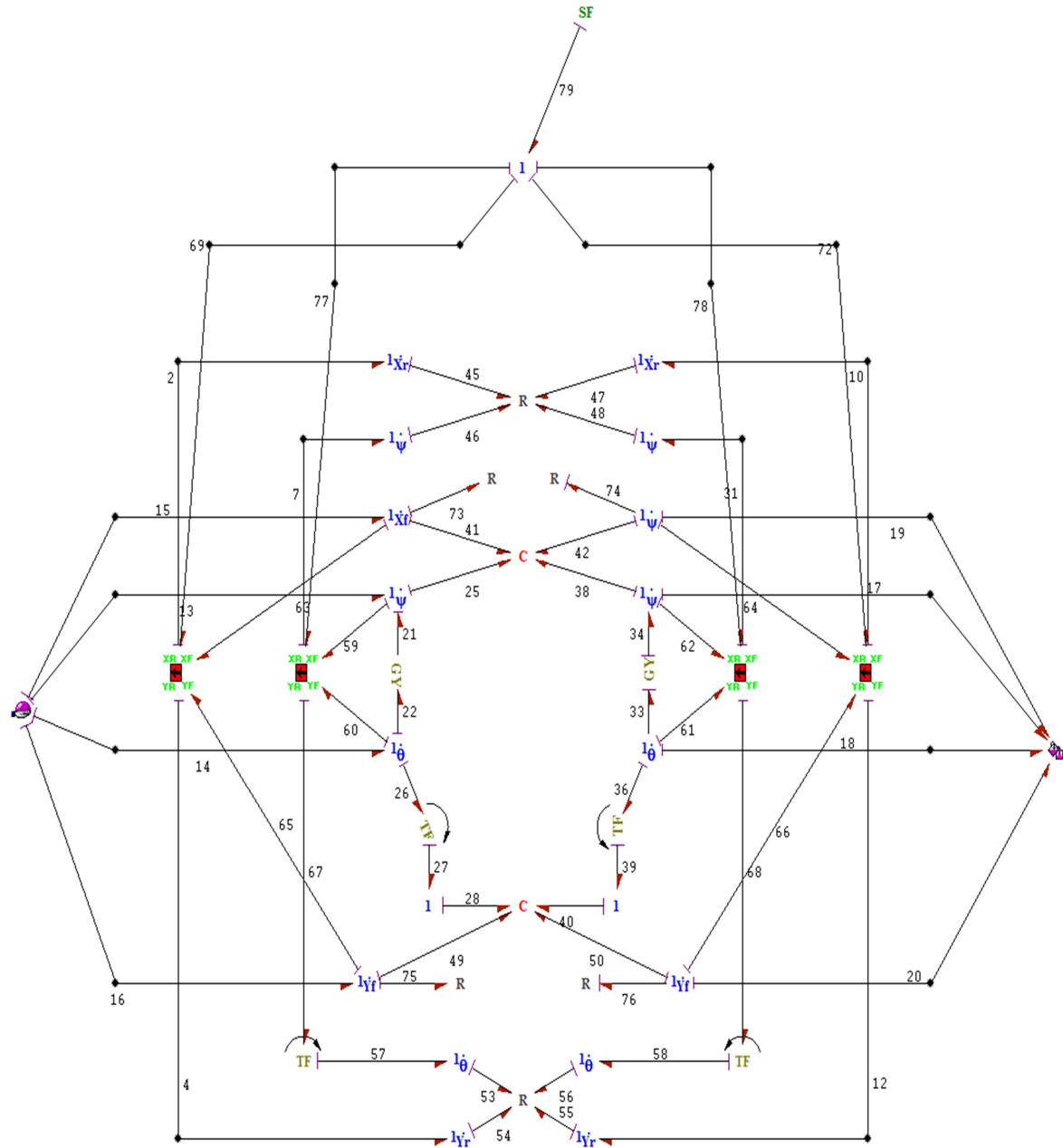






Fig.4.4 Shaft Capsule

The following glue ports have been used in the bond graph modelling of the components. Glue ports are the connecting link between two capsules which enables transfer of flow and effort between capsules.

 is effort input glue port. It is used to give effort into a sub model (capsule). The effort coming from a sub system can be transfer to other sub model with the help of this glue port.

 is the flow input glue port .It is used to give flow into a sub model(capsule). The flow coming from a subsystem can be transfer to other sub model with help of this glue port.

 is the effort output glue port . It is used to take out the effort from a sub model (capsule).

 is the flow output glue port . It is used to take out the flow from a sub model (capsule). In the bond graph model of shaft, flow input glue port is used to give flow to shaft in two linear velocity motion in x and y and two velocity component in angular motion in figure 4.5. The output from the capsule is taken with the flow output glue port similarly from two linear components and two angular components.

4.5 Bondgraph model of spinning hub

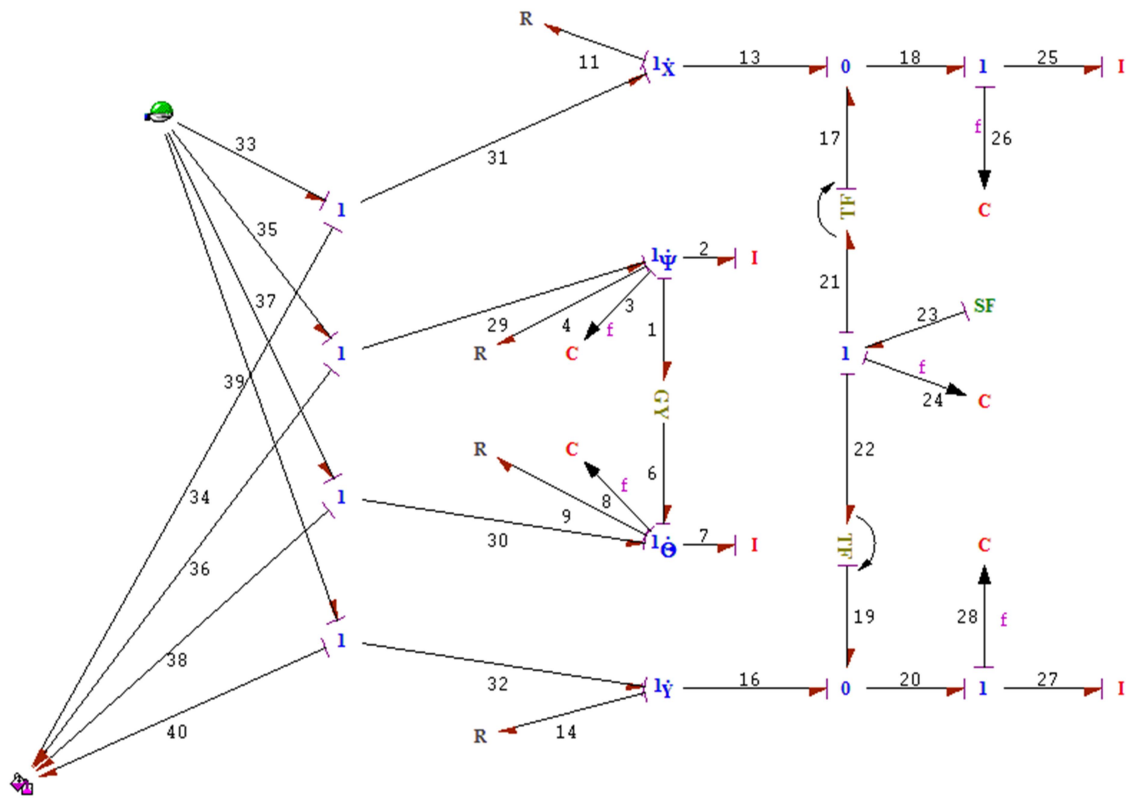


Fig.4.5 Spinning hub

The spinning hub in figure 4.5 is used to model the annular disks. The model incooperates the eccentricity of hub centre of mass and its angular orientation is recorded by the flow-

activated element. The expressions of the mass and the rotary inertia contribution from the interfacing shaft element are added to those of the hub. Flow activated elements records the displacement of the hub centre of mass with zero initial condition of the corresponding state vectors give the displacement of the hub axis.

In the bond graph model of spinning hub effort is taken with the help of effort glue port and the output from the capsule is in the form of flow which is taken to other capsule with the help of flow output glue port.

4.6 Summary of chapter

In this chapter the bond graph model of different component is made using symbol sonata software. The bondgraphs are connected to form rig in the next chapter and simulation of the rig is carried out using simulator of symbols sonata.

CHAPTER 5

SIMULATION STUDY

5.1 INTRODUCTION

Computer simulation can compress the performance of a system over years into a few minutes of computer running time. Simulation models are comparatively flexible and can be modified to accommodate changing environment to real situation. There is no area, where the technique of computer simulations cannot be applied as the complexities of problem increases the scope of application of simulation equations. At present, most of the simulation models are made by means of differential equations. In this research, analysis of rotor with eccentricity is done with various parameters using bondgraph and simulator of SYMBOLS-Sonata Software is used.

5.2 Simulation environment

This simulator of symbols Sonata, which is the base post-processing module of SYMBOLS Sonata, is used for rotor with eccentricity introduced.

SYMBOLS Sonata software

SYMBOLS Sonata is the next generation of SYMBOLS software (Symbols Modelling by Bond graph language and simulation) running in Microsoft Windows 95/ 98/ XP/ NT 4.0 environment. It is a modelling, simulation and control system software for a variety of scientific and engineering applications. Being a powerful research tool, it can help avoid unaffordable, sophisticated fabrications. Yet, one may know precisely the response characteristics of the simulated system. A model in SYMBOLS sonata may be created using combination of Bond graphic elements, block diagram elements in capsulated form or other capsules. Even model can be created purely using capsules. Sub-model capsules can be imported from the huge capsules library or can even be created by modeller. The pre-cast capsules are not Pandora's boxes. They can be opened using Bond pad editor and customised according to the modeller's need. Modeller may personalize and organise capsule created by them to separate their capsule group from other users.

Few features of SYMBOLS Sonata Software are as follows:

- Drawing a bondgraph model.
- Augmenting the model by numbering the bonds, assigning power direction.
- Causality, module of 2- port elements, bond activation etc.

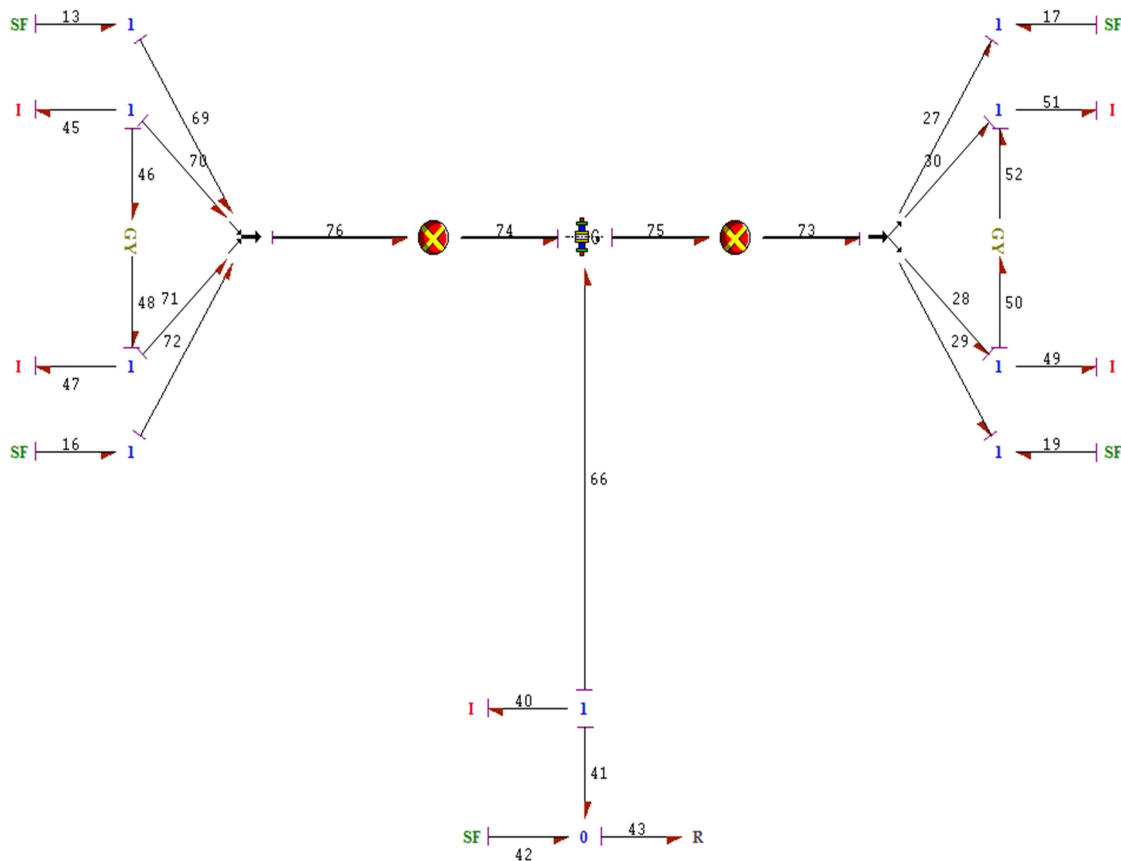
- Validation of bondgraph. Bondgraph's integrity is validated after the model is created.
- Creation of non-integrated observers in the form of detectors.
- Equations can be generated and displayed on single pallets.
- Creation of expressions.
- Generation of program code.
- Creation of sub-system models henceforth called as capsules and incorporation of capsules in a bond graph model.
- Fault diagnosis.
- Preparing models for simulator and control modules.
- Export of sub system and Systems model to MATLAB/simulink environment.
- Integrated simulation environment.
- Easy to access control panels.
- Multiple and intelligent entry mode.
- Online plotting, pause, stop and resume option.
- Online parameter variation through slider during simulation.
- Continuous Run simulation, multiple simulations of different systems at the same time.
- Simulation extension facility.
- Advanced post simulation plotting facilities.
- Online code editing and compilation.
- Different integration methods for stiff equations.
- Multi-run facility with interpolated or discrete parameter values.
- Event handlers and notification messages.
- Direct debugging and variable tracking.
- Improved external data and chart interpretation routine.
- Export routines for Microsoft Excel database.

5.3 Simulation properties

The bondgraph model of the rigid rotor with eccentricity is simulated for 2 seconds to obtain different output responses. Total 8194 records are used in simulation and simulation error is kept in order of 5×10^{-4} . Runge-Kutta Gill method of fifth order is used in present work to solve the differential equations generated through bondgraph model.

Ranga-Kutta methods propagate a solution over an interval by combining the information from several Euler-style steps (each involving one evolution of state equations), and then using the information obtained to match a Taylor series expansion up to some higher order. This method treats every step in a sequence of steps in identical manner. This is mathematically correct, since any point along the trajectory of an ordinary Differential equation can serve as an initial point. Fifth-order Ranga-Kutta method, is used in present simulation work.

In this setup, one may have x and y rotational motion with different dampings connected at either ends of the shafts. On one end, we have connected it to shaft and then the shaft is connected to another shaft with the help of spinning hub which is then connected to a bond which provides rotor excitation. The experimental rig is shown in figure 5.1:



37

5.5 Simulation parameters

Following are the parameters used for shaft simulation. These parameters are used to populate the state space representation of the bond graph model.

Table 5.1: Parameter values for simulation

Parameter	Value
Spinning Hub	
Angular speed	16-70 rad/s
Material density	4420 kg/m ³
Inner radius of end of spinning hub	1x 10 ⁻² m
Mass of spinning hub	0.60 kg
Eccentricity of hub	0.001-0.005 m
Rotational damping about diametrical axes	1.25e ⁻⁴ Ns/m
Rotational damping about mass centre	1.25e ⁻⁴ Ns/m
Polar moment of Inertia	0.0003675 kgm ²
Shaft	
Length of shaft	1 m
Thickness of shaft	0.01 m
Young's modulus (E)	104.5e ⁹
Outer radius of shaft	0.02 m
Inner radius of shaft	0.01 m
Material damping coefficient of shaft	2.25

CHAPTER 6

RESULTS AND DISCUSSION

6.1 Introduction

This chapter presents the simulation results of bondgraph model of rigid rotor on squeeze film damper having centralizing springs. In this, we have taken into consideration the motion of centre of mass of rigid rotor with change in various parameters.

6.2 Various variable parameters

We have changed various parameters related to the shaft and observed its effect on Vibration amplitude of centre of mass of rigid rotor. The variable parameters are discussed below:

6.2.1 Angular speed with low eccentricity

The angular speed of rotation of the shaft has been changed from minimum value of 16 rad/s to maximum value of 70 rad/sec. The eccentricity of the shaft is kept at 0.001 m and the effect of which on the displacement of centre of mass at different angular velocities has been observed as follows:

Case I:

At angular speed=16 rad/s and eccentricity= 0.001 m. The following graph has been obtained between X-coordinate of centre of mass of rotor vs. Y-coordinate of the centre of mass of rotor.

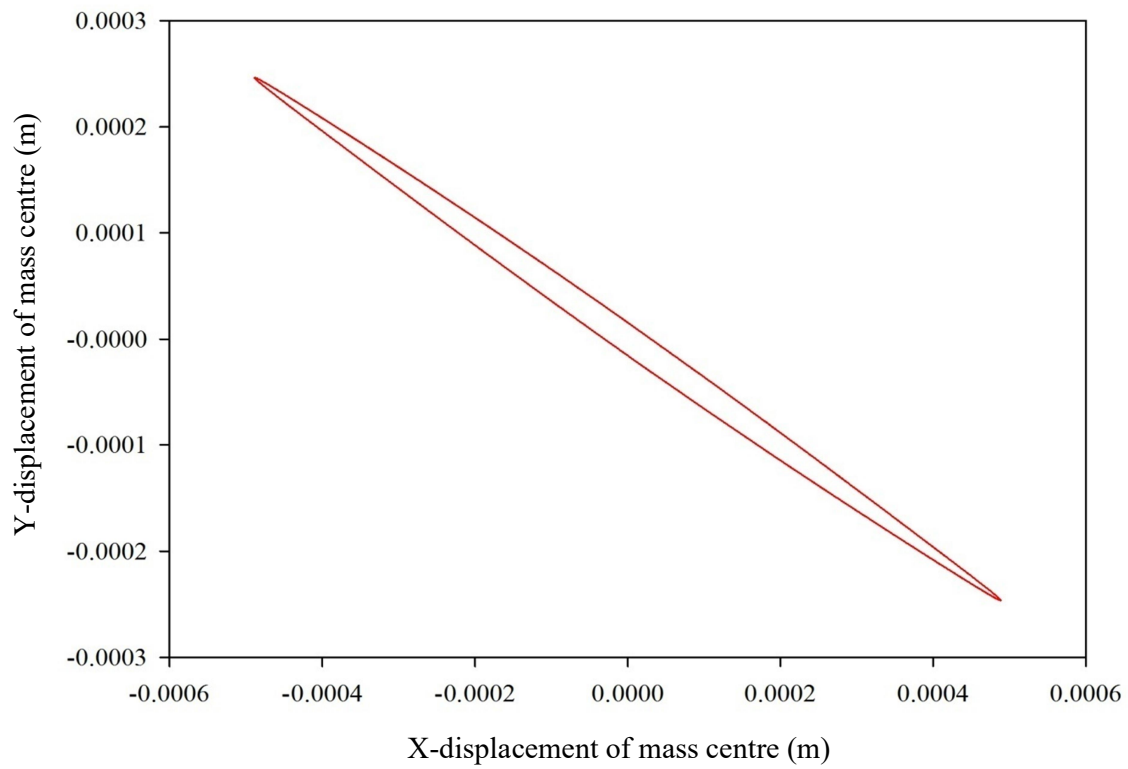


Fig 6.1: Displacement of rotor about X vs. Y axes about the centre of mass at Eccentricity= 0.001 and Angular velocity= 16 rad/sec

Case II:

Again changing angular speed=40 rad/s and eccentricity= 0.001 m, we get the following curve:

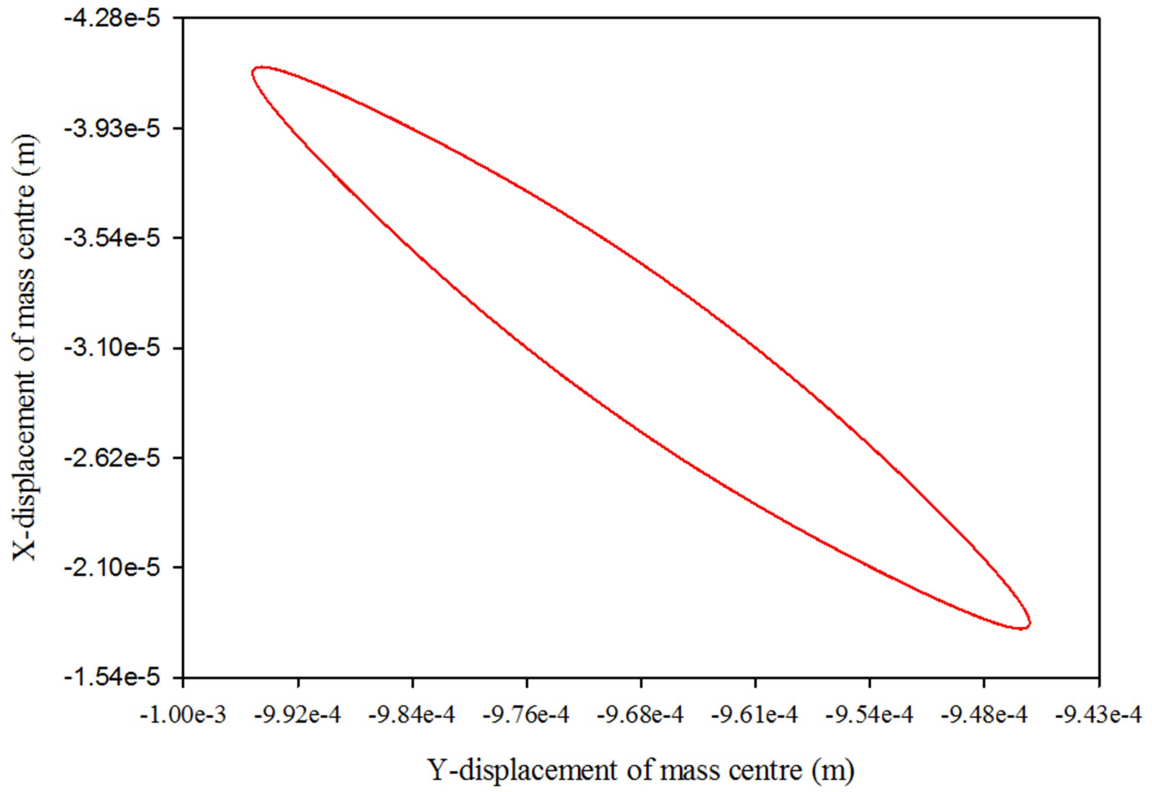


Fig 6.2: Displacement of rotor about X vs. Y axes about the centre of mass at eccentricity= 0.001 and angular velocity= 40 rad/sec

Case III:

Again changing angular speed=70 rad/s and eccentricity= 0.001 m, we get the following curve:

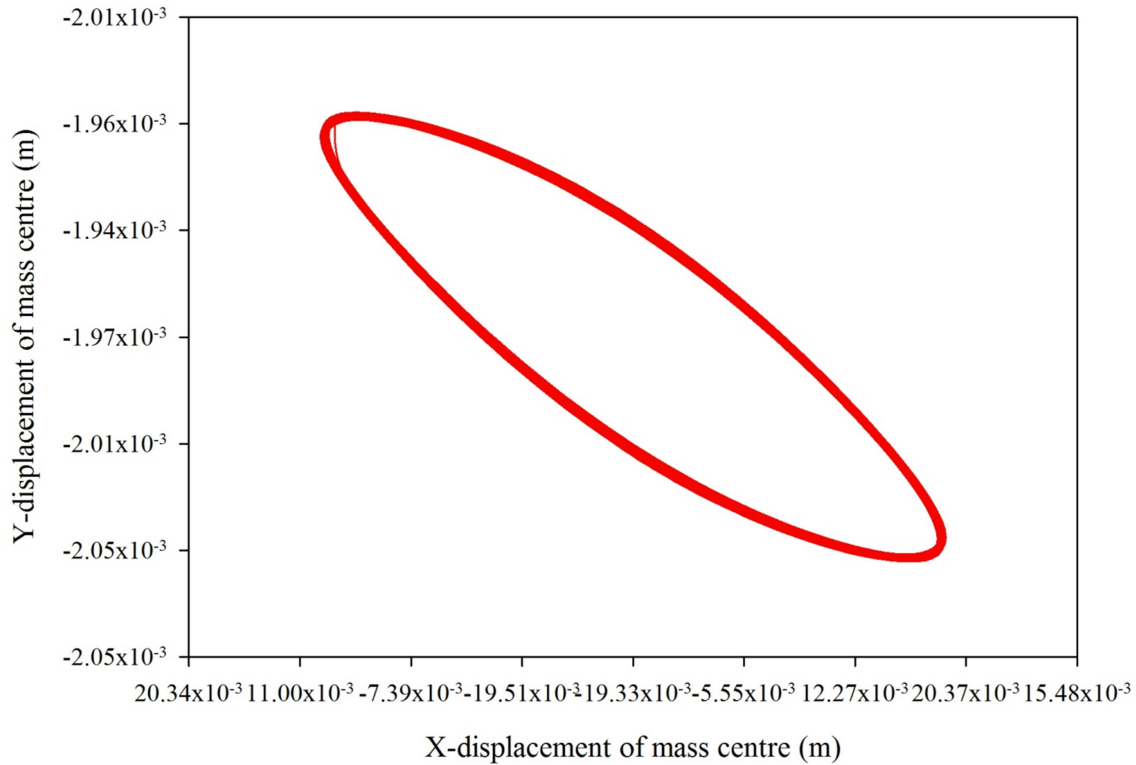


Fig 6.3: Displacement of rotor about X vs. Y axes about the centre of mass at eccentricity= 0.001 and angular velocity= 70 rad/sec

6.2.2 Angular velocity at comparatively high eccentricity

The eccentricity of the shaft is now changed to 0.005, the effect of which has been observed. For low value of eccentricity, the shaft does not have much variation in the amplitude of vibration of mass centre of rotor as compared to the higher value of eccentricity whose variations are observed as follows:

Case I:

Angular speed=16 rad/s, eccentricity=0.005 m. The following plot has been obtained between X-coordinate of centre of mass of rotor vs. Y- coordinate of the centre of mass of rotor.

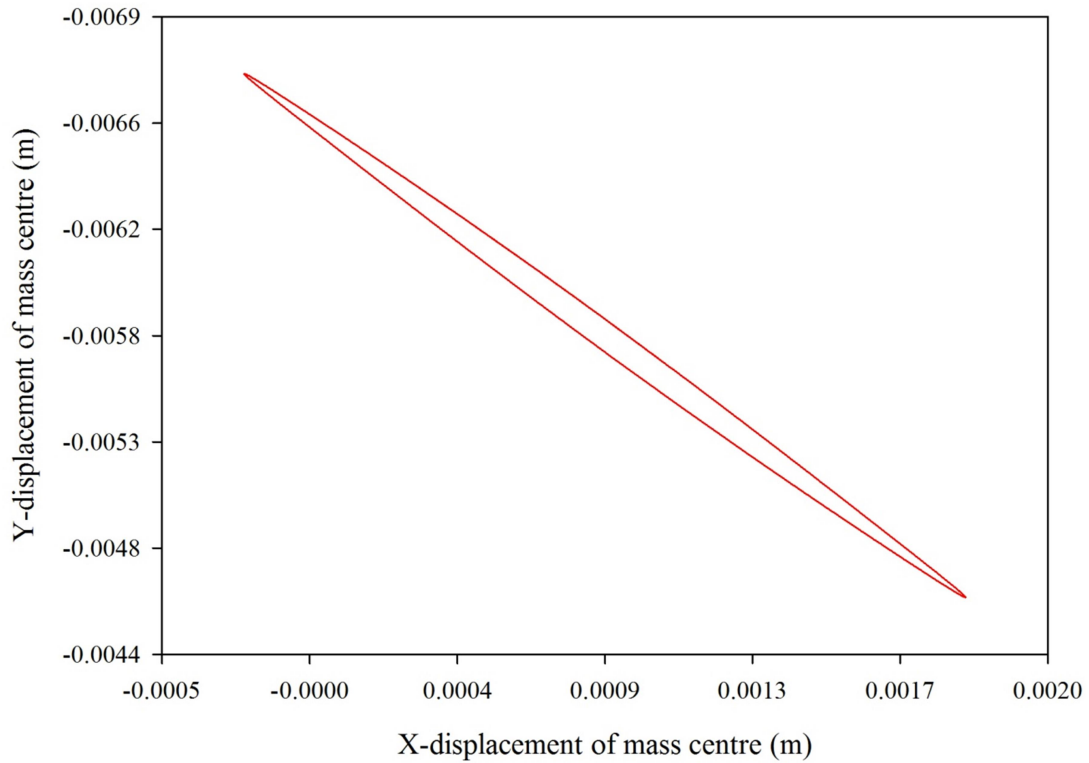


Fig 6.4: Displacement of rotor about X vs. Y axes about the centre of mass at eccentricity= 0.005 and angular velocity= 16 rad/sec

Case II:

Angular speed=40 rad/s, eccentricity=0.005. The following plot has been obtained between X-coordinate of centre of mass of rotor vs Y- coordinate of the centre of mass of rotor.

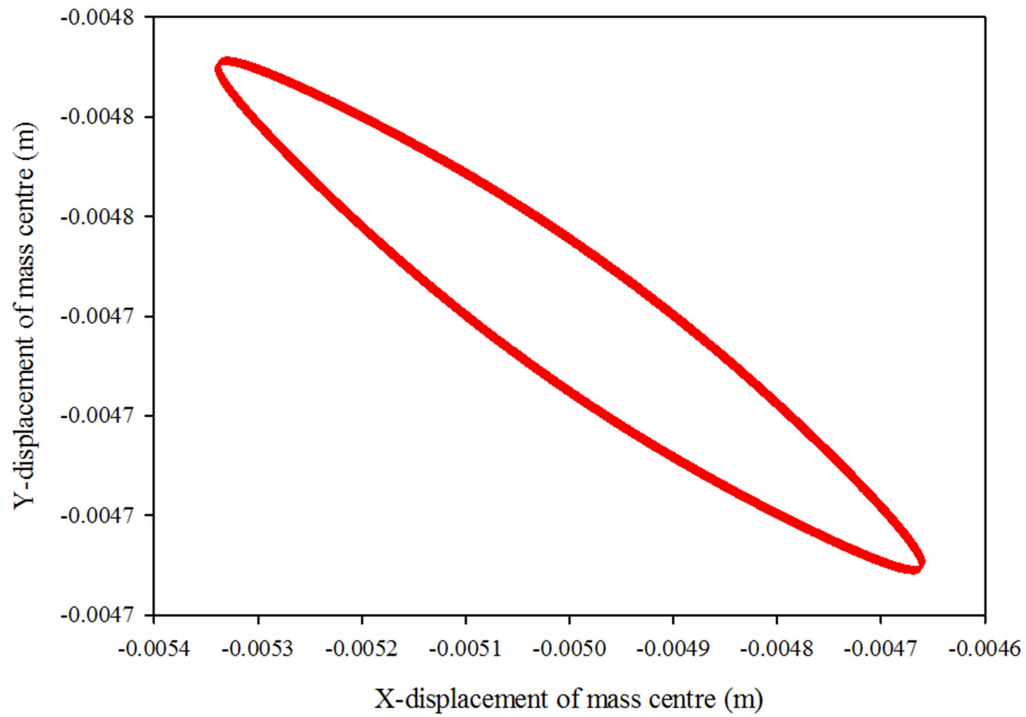


Fig 6.5: Displacement of rotor about X vs. Y axes about the centre of mass at eccentricity= 0.005 and angular velocity= 40 rad/sec

Case III:

Angular speed=70 rad/s, eccentricity=0.005. The following plot has been obtained between X-coordinate of centre of mass of rotor vs. Y- coordinate of the centre of mass of rotor.

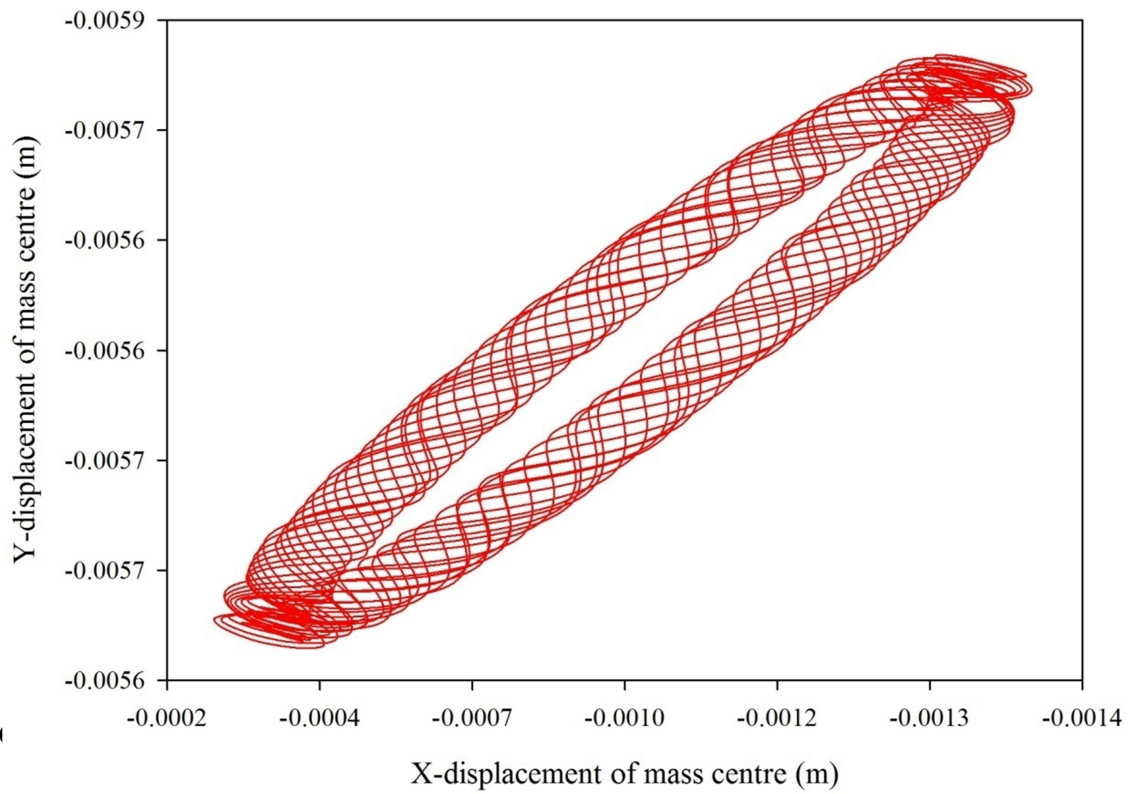


Fig 6.6: Displacement of rotor about X vs. Y axes about the centre of mass at eccentricity= 0.005 and angular velocity= 70 rad/sec

Now, the rotational effect of the shaft at different axes is seen at different angular speeds and different eccentricities. The effect of which has been observed:

Case I:

Angular speed=16 rad/s and eccentricity=0.001 m. The following plot has been obtained between X-coordinate vs. time for a period of 2 seconds.

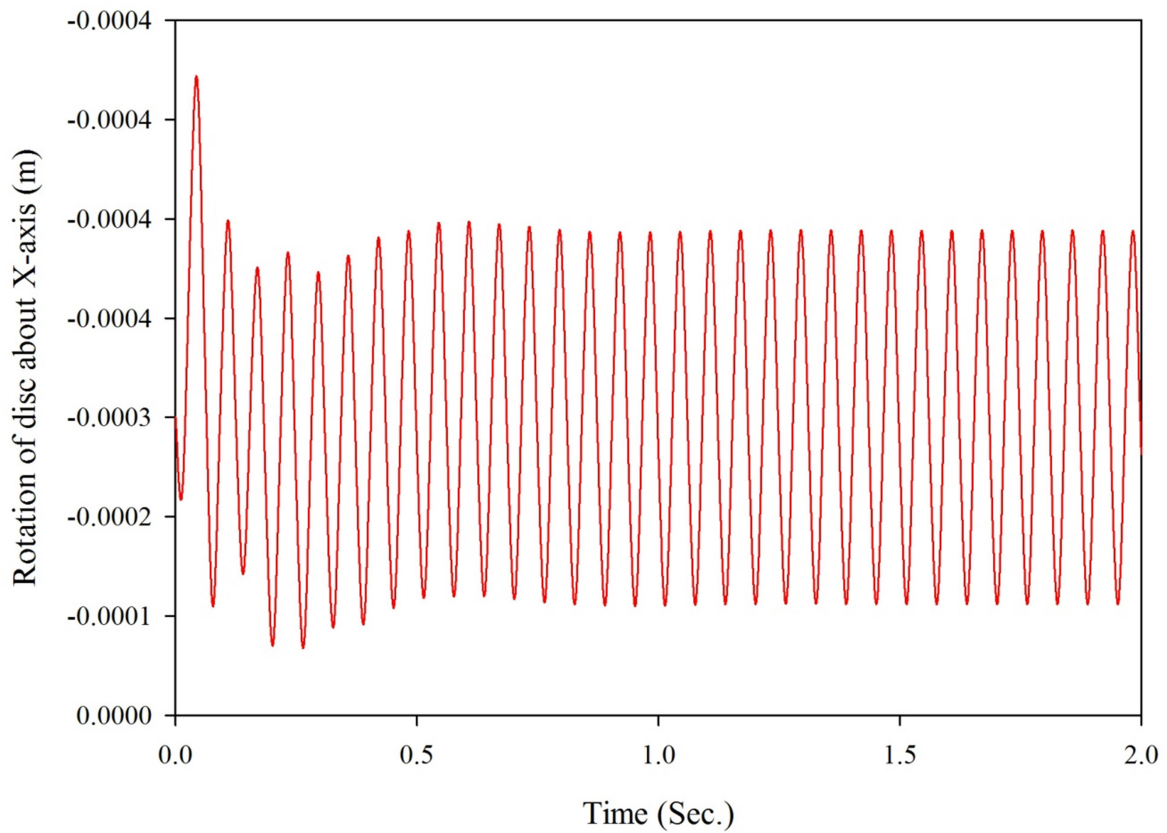


Fig 6.7: Displacement of rotor about X-axis vs. time at eccentricity= 0.001 and angular velocity= 16 rad/sec

Case II:

Angular speed=16 rad/s and eccentricity=0.005 m. The following plot has been obtained between X-coordinate vs. time for a period of 2 seconds.

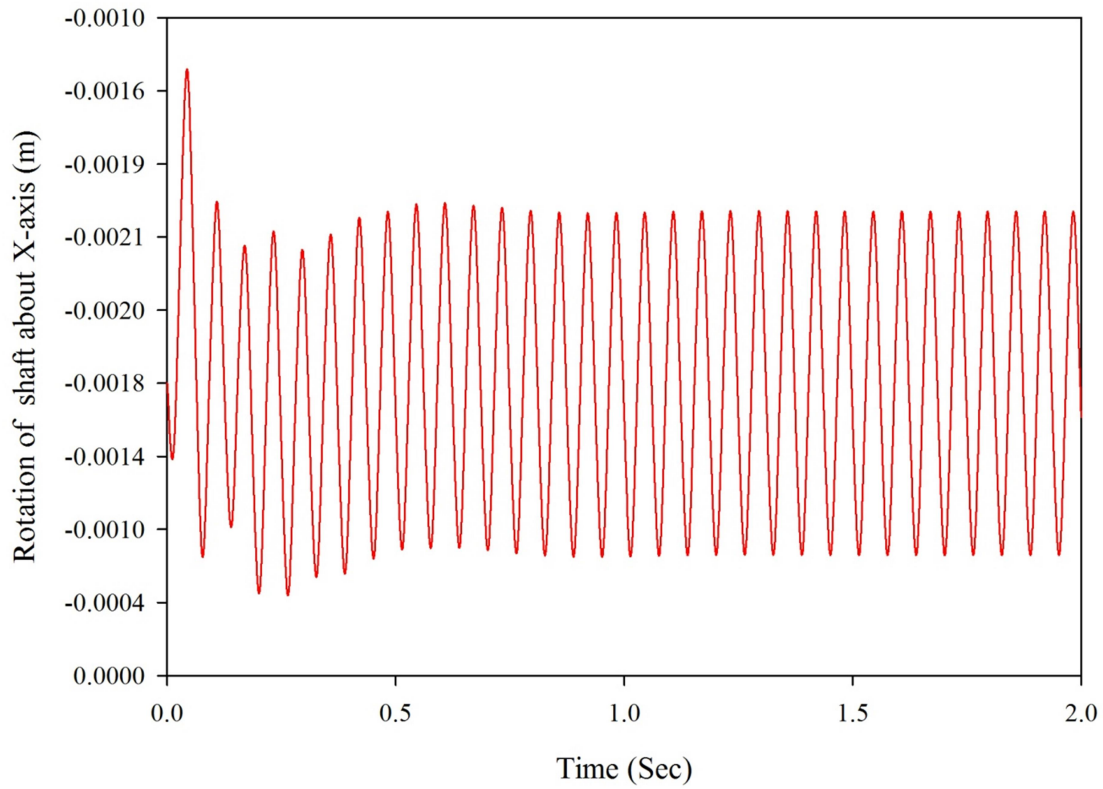


Fig 6.8: Displacement of rotor about X-axis vs. time at eccentricity= 0.005 and angular velocity= 16 rad/sec

Case III:

Angular speed=16 rad/s and eccentricity=0.001 m. The following plot has been obtained between Y-coordinate vs. time for a period of 2 seconds.

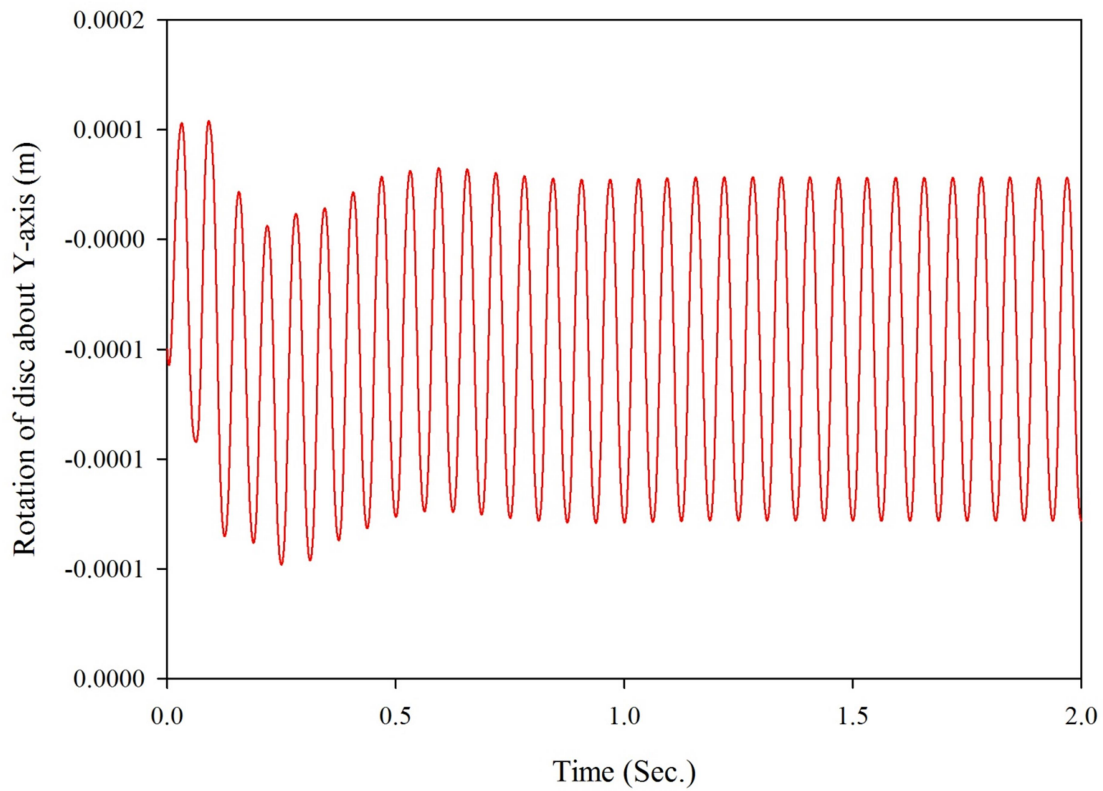


Fig 6.9: Displacement of rotor about Y-axis vs. time at eccentricity= 0.001 and angular velocity= 16 rad/sec

Case IV:

Angular speed=16 rad/s and eccentricity=0.001 m. The following plot has been obtained between Y-coordinate vs. time for a period of 2 seconds.

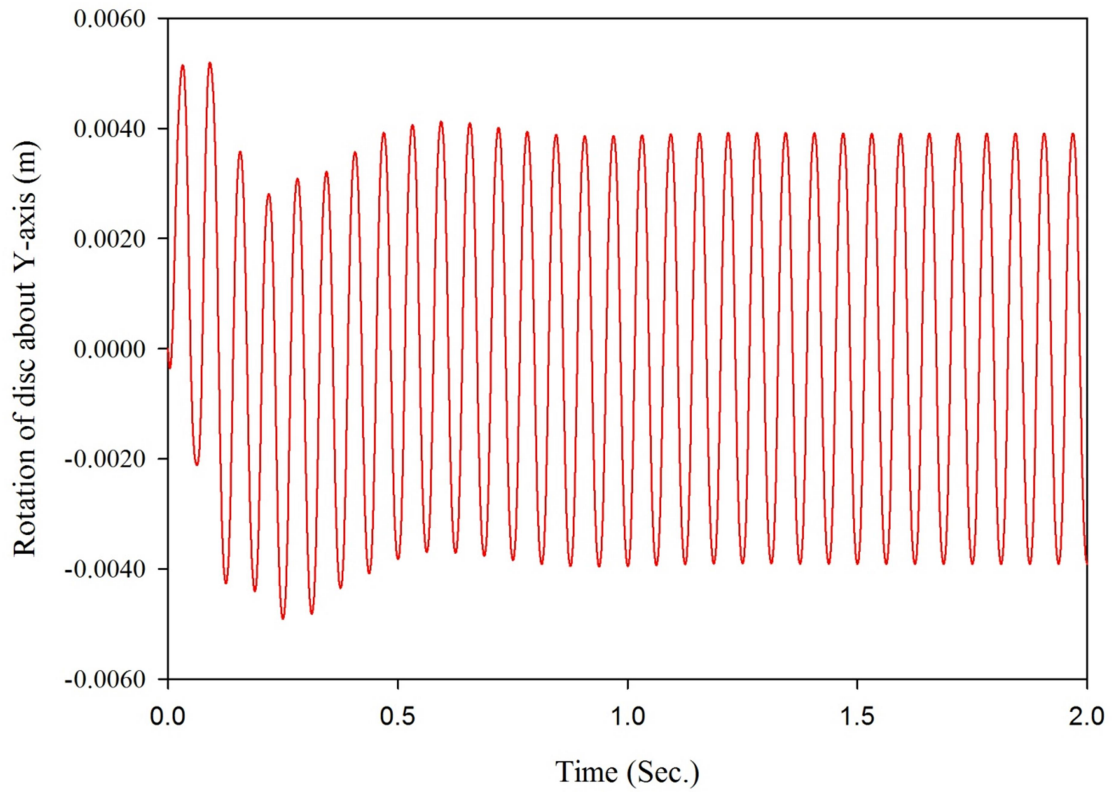


Fig 6.10: Displacement of rotor about X-axis vs. time at eccentricity= 0.001 and angular velocity= 16 rad/sec

Case V:

Angular speed=40 rad/s and eccentricity=0.001 m. The following plot has been obtained between X-coordinate vs. time for a period of 2 seconds.

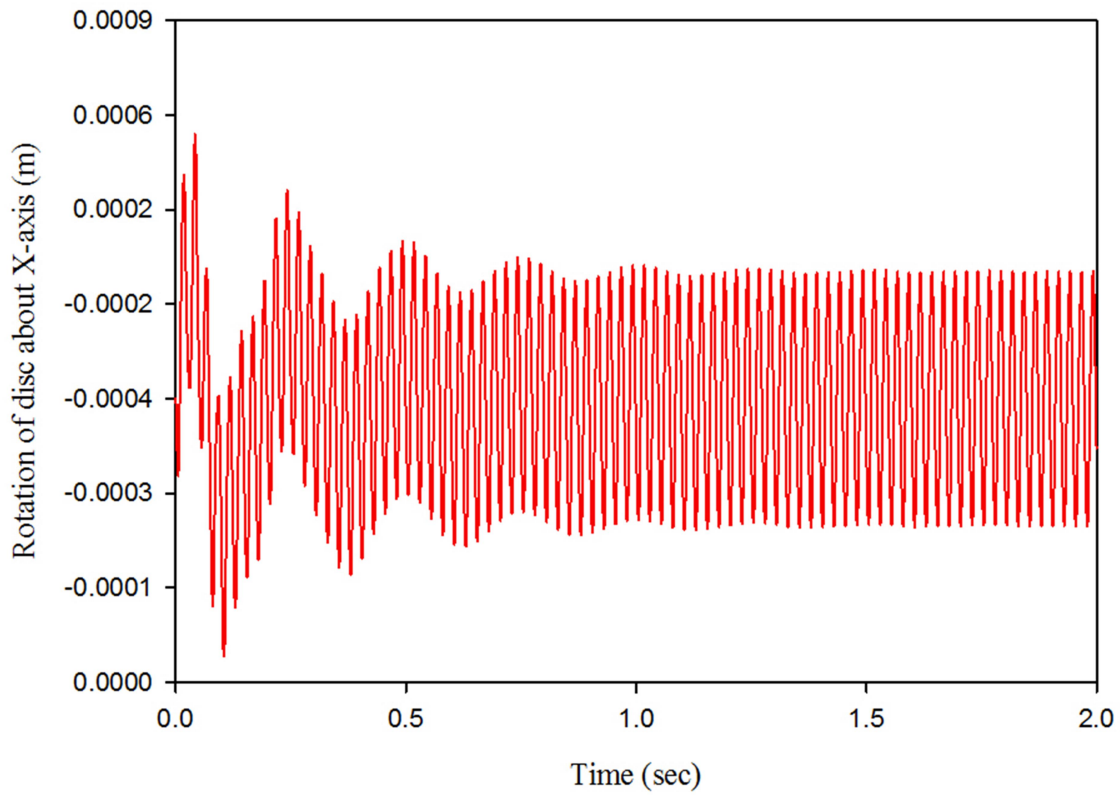


Fig 6.11: Displacement of rotor about X-axis vs. time at eccentricity= 0.001 and angular velocity= 40 rad/sec

Case VI:

Angular speed=40 rad/s and eccentricity=0.005 m. The following plot has been obtained between X-coordinate vs. time for a period of 2 seconds.

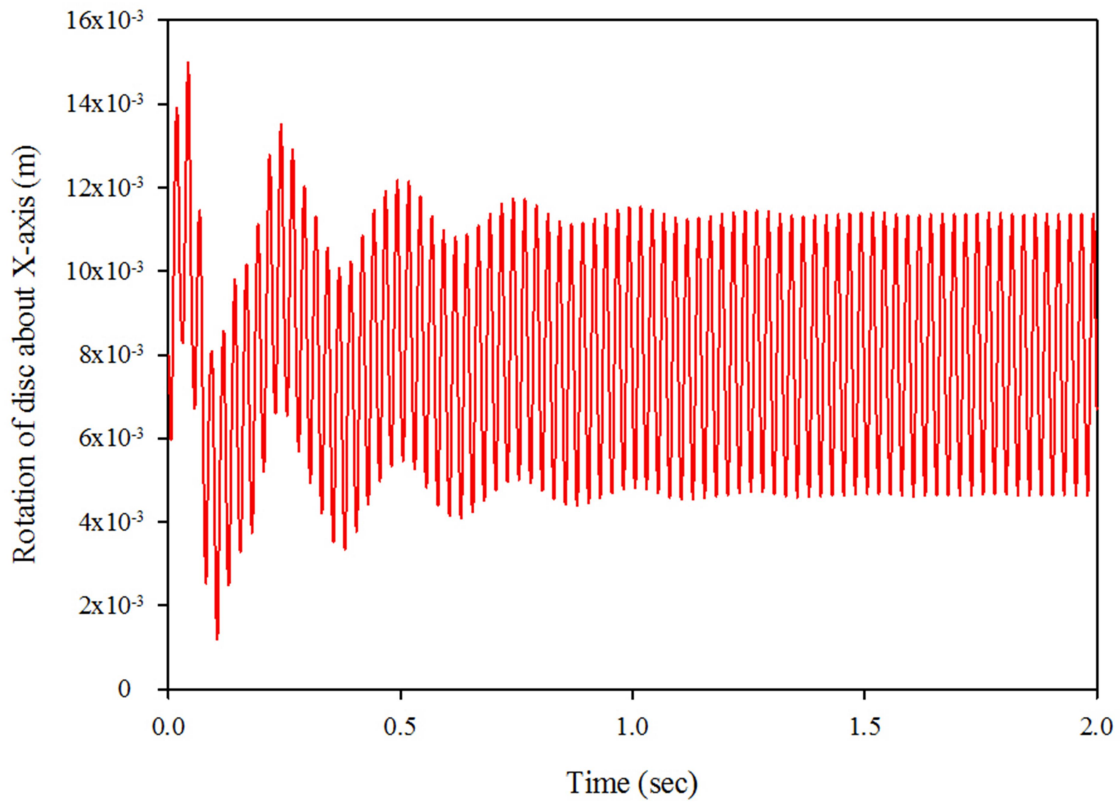


Fig 6.12: Displacement of rotor about X-axis vs. time at eccentricity= 0.005 and angular velocity= 40 rad/sec

Case VII:

Angular speed=40 rad/s and eccentricity=0.001 m. The following plot has been obtained between Y-coordinate vs. time for a period of 2 seconds.

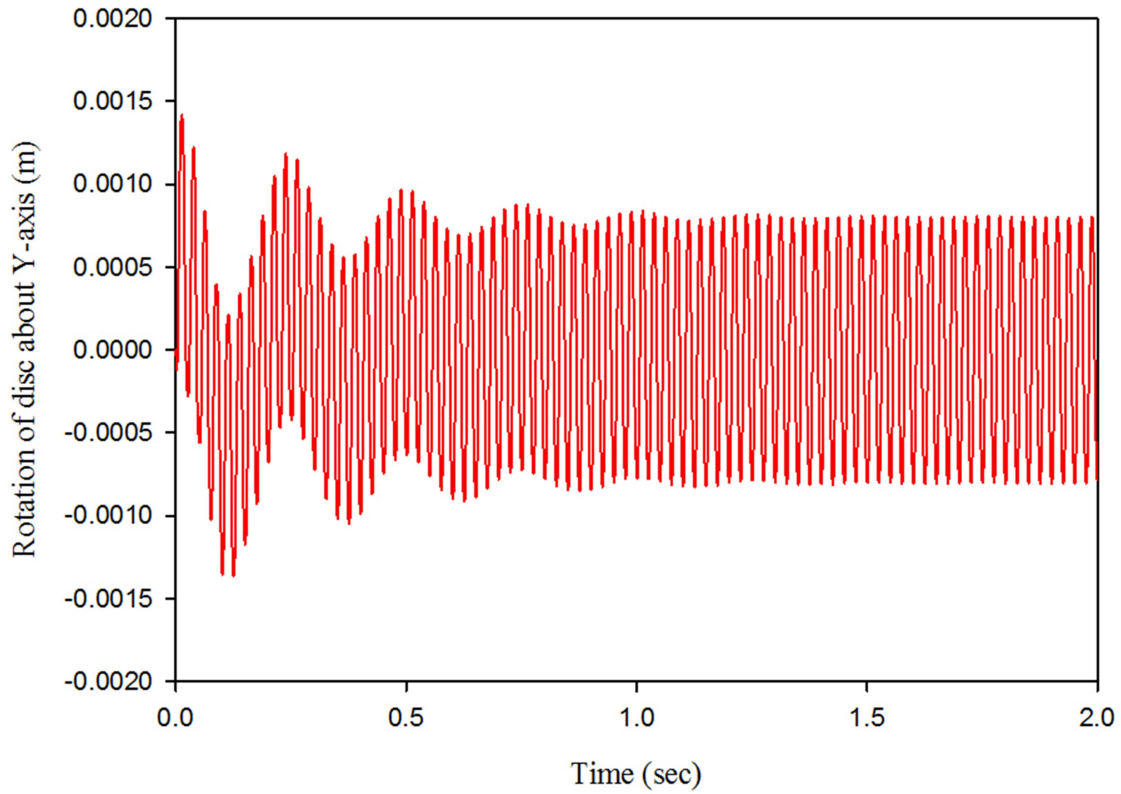


Fig 6.13: Displacement of rotor about Y-axis vs. time at eccentricity= 0.001 and angular velocity= 40 rad/sec

Case VIII:

Angular speed=40 rad/s and eccentricity=0.005 m. The following plot has been obtained between Y-coordinate vs. time for a period of 2 seconds.

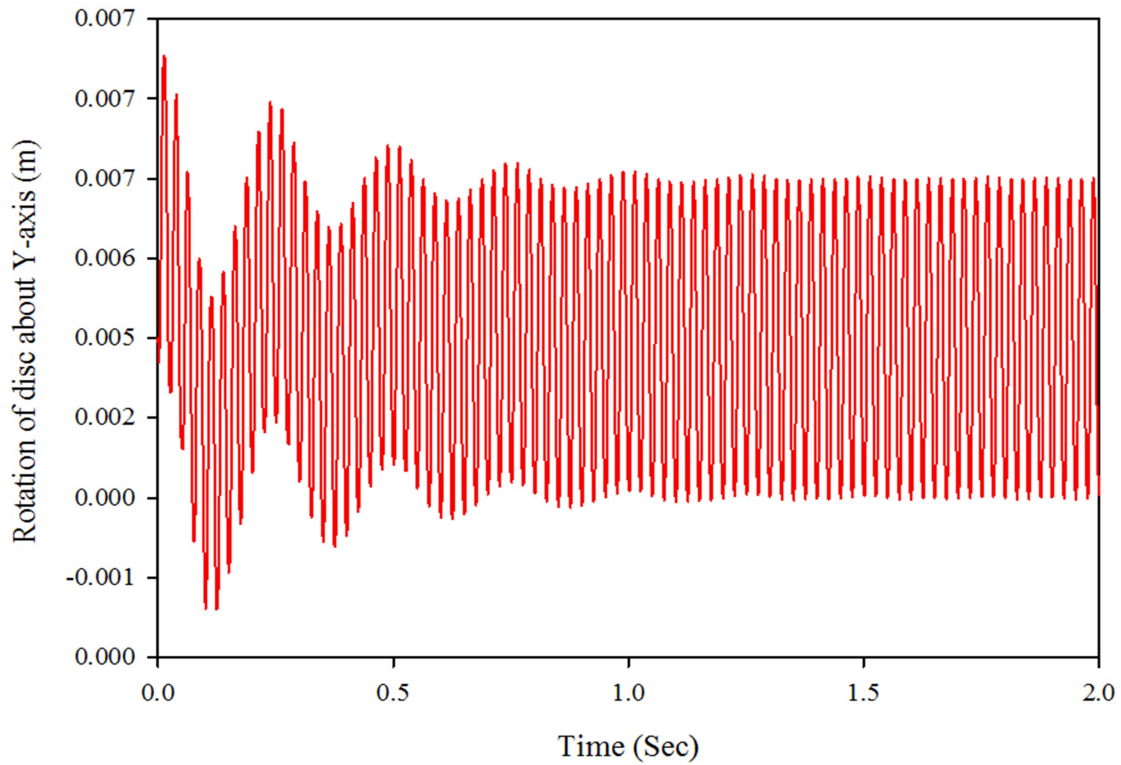


Fig 6.14: Displacement of rotor about Y-axis vs. time at eccentricity= 0.005 and angular velocity= 40 rad/sec

Case IX:

Angular speed=70 rad/s and eccentricity=0.001 m. The following plot has been obtained between X-coordinate vs. time for a period of 2 seconds.

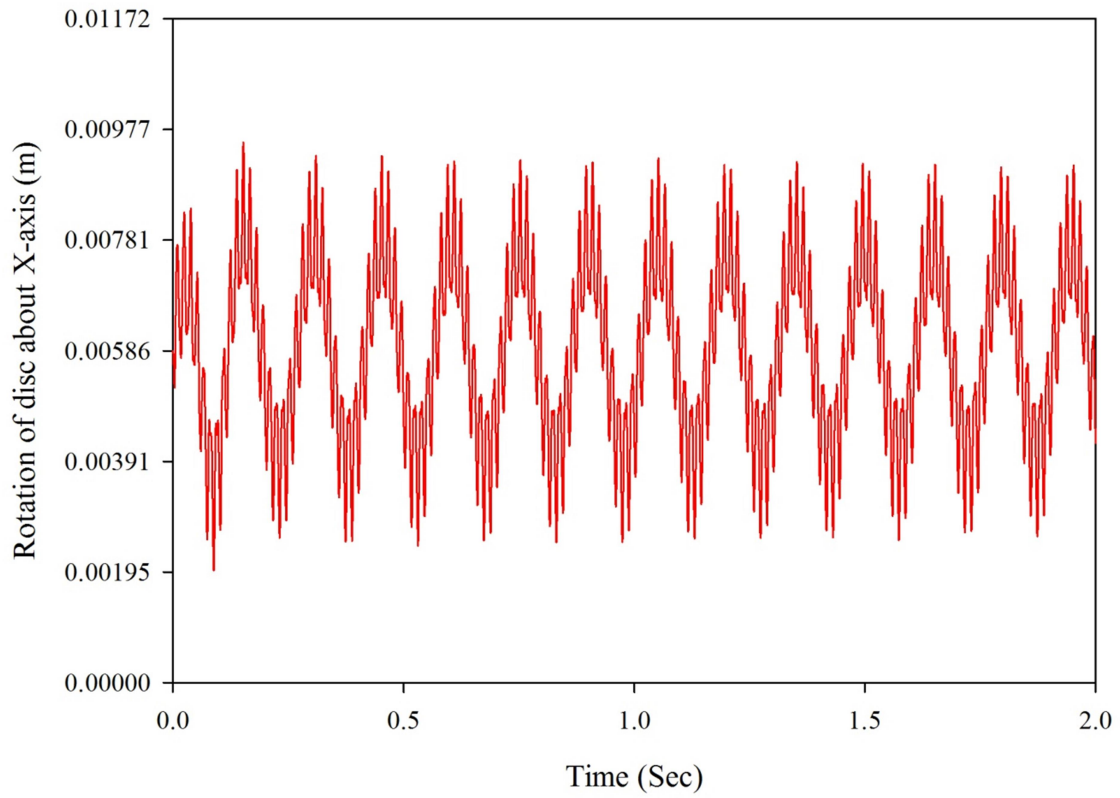


Fig 6.15: Displacement of rotor about X-axis vs. time at eccentricity= 0.001 and angular velocity= 70 rad/sec

Case X:

Angular speed=70 rad/s and eccentricity=0.005 m. The following plot has been obtained between X-coordinate vs. time for a period of 2 seconds.

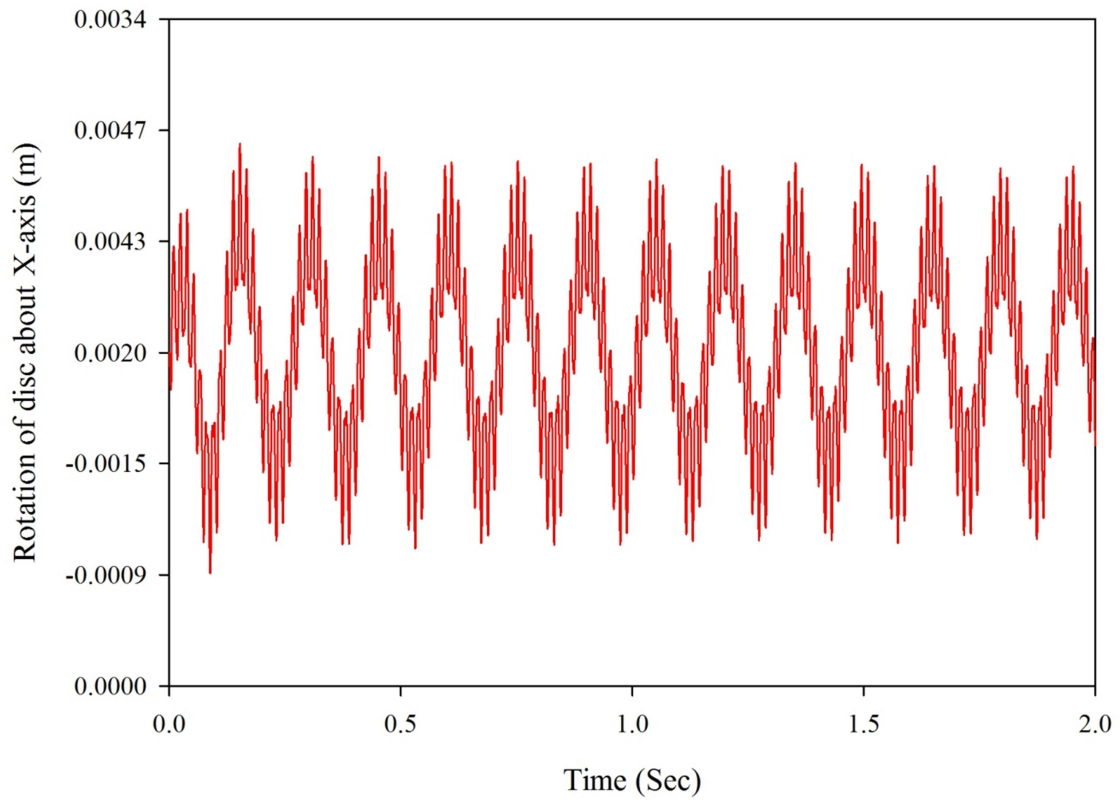


Fig 6.16: Displacement of rotor about X-axis vs. time at eccentricity= 0.005 and angular velocity= 70 rad/sec

Case XI:

Angular speed=70 rad/s and eccentricity=0.001 m. The following plot has been obtained between Y-coordinate vs. time for a period of 2 seconds.

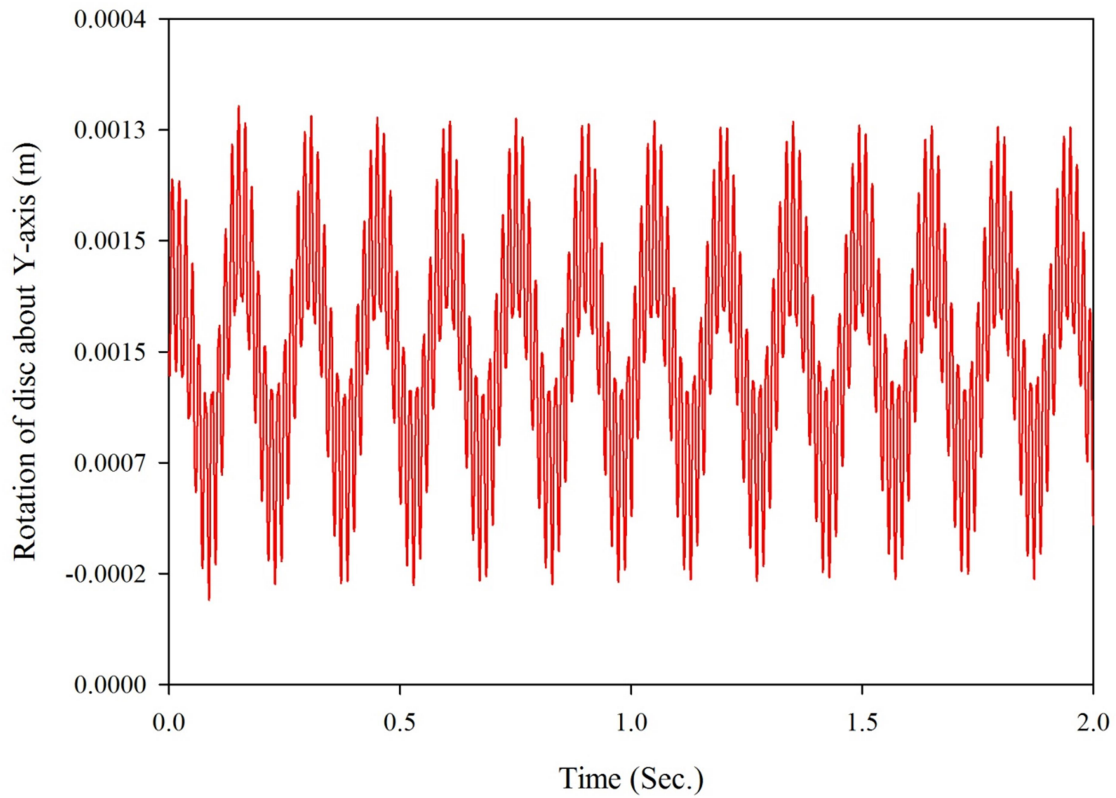


Fig 6.17: Displacement of rotor about Y-axis vs. time at eccentricity= 0.001 and angular velocity= 70 rad/sec

Case XII:

Angular speed=70 rad/s and eccentricity=0.005 m. The following plot has been obtained between Y-coordinate vs. time for a period of 2 seconds.

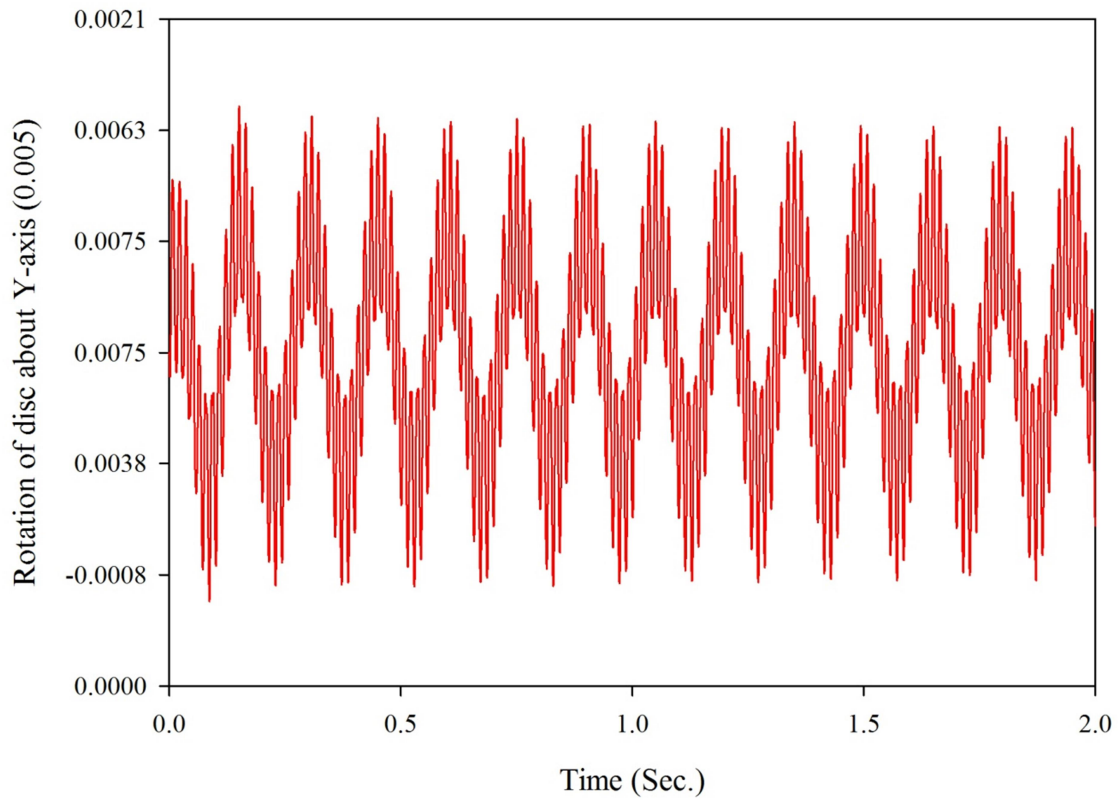


Fig 6.18: Displacement of rotor about Y-axis vs. time at eccentricity= 0.005 and angular velocity= 70 rad/sec

Table 6.1 Comparison among displacement and angular speed at different eccentricity

Sl. No.	Eccentricity (m)	Angular Speed (rad/sec)	Displacement (m)	
			X- direction	Y- direction
1.	0.001	16	-0.0005 to 0.0005	0.00025 to -0.00025
		40	-0.00092 to -0.00095	-0.00041 to -0.00017
		70	-0.00739 to 0.00203	-0.00197 to -0.00205
2.	0.005	16	-0.0001 to 0.0017	-0.0046 to -0.0067
		40	-0.0053 to -0.0046	-0.0048 to -0.0046
		70	-0.0002 to -0.0014	-0.0056 to -0.0057

6.3 Results and discussion

From the above graphs we can make the conclusions that

1) Variation in speed :-

Due to increase in speed, vibration amplitude of centre of mass of rigid rotor starts increasing continuously.

2) Variation in eccentricity :-

For less value of eccentricity, the system works with very less deviation in earlier stages but with 0.005 m of eccentricity, the centre of mass about X and Y axis further increases, increasing the vibration with more magnitude.

CHAPTER 7

CONCLUSION AND FUTURE SCOPE

7.1 Conclusion

This dissertation work has been attempted to obtain the dynamic behaviour of Rotor on changing the eccentricity of the rotor through bond graph modelling and also evaluate the effect of various parameters through simulation.

The simulation study of variation in the amplitude of centre of mass of rigid rotor is done with change in parameters such as angular speed and eccentricity of the shaft.

The following conclusions have been made:

- Vibration amplitude increases with increase in speed.
- Effect of vibration depends on its eccentric value from the mass centre of the rotor.

7.2 Future scope

Following future scope has been proposed for further analysis.

- In this model only the vibration amplitude of the centre mass of rotor has been investigated.
- The forces experienced by the centre of mass due to vibration may also be considered in future.
- In present work, only effect of few parameters is considered, further investigation with varying some other parameters can be done.
- Some experimental investigations can be attempted in future.

REFERENCES

- [1] J. J. Beaman, H. M. Paynter, *Modeling of Physical Systems*, 1993, unpublished, pp. 6.22–6.35.
- [2] Hinrichsen D, Pritchard AJ. On the transient behaviour of stable linear systems. In: Proceedings of the fourteenth international symposium of mathematical theory of networks and systems, 2000. o<http://www.univ-perp.fr/mtns2000/4>.
- [3] Trefethen LN, Trefethen AE, Reddy SC, Driscoll TA. Hydrodynamic stability without eigenvalues. *Science* 1993;261(5121):578–84.
- [4] Higham DJ, Trefethen LN. Stiffness of ODEs. *BIT* 1992; 33: 285–303.
- [5] R. G. Loewy and V. J. Piarulli, *[SVM-4] Dynamics of Rotating Shafts*. Washington, D.C.: The Shock and Vibration Information Center, U.S. Department of Defense, 1969, pp. 1–4.
- [6] D. Childs, *Turbomachinery Rotordynamics—Phenomena, Modeling and Analysis*. New York: Wiley, 1993, pp. 2–8.
- [7] R. G. Loewy and V. J. Piarulli, *[SVM-4] Dynamics of Rotating Shafts*. Washington, D.C.: The Shock and Vibration Information Center, U.S. Department of Defense, 1969, pp. 6–10.
- [8] J. M. Vance, *Rotordynamics of Turbomachinery*. New York: Wiley, 1988, p. 295.
- [9] J. J. Beaman and H. M. Paynter, *Modeling of Physical Systems*, 1993, unpublished, pp. 3.69–3.71.
- [10] D. C. Karnopp, D. L. Margolis, and R. C. Rosenberg, *System Dynamics: A Unified Approach*, 2nd, ed. New York: Wiley, 1990, pp. 316–317.
- [11] M. Hubbard, “Whirl dynamics of pendulous flywheels using bondgraphs,” *J. Franklin Inst.*, vol. 308, no. 4, pp. 505–421, Oct. 1979.
- [13] Gebhardt T, Grossmann S. Chaos transition despite linear stability. *Physical Review E* 1994; 50(5):3705–11.

- [14] Schweizer B. Total instability of turbocharger rotors - physical explanation of the dynamic failure of rotors with full-floating ring bearings. *Journal of Sound and Vibration* 2009; 328, p. 156-190.
- [15] Schweizer B. Oil whirl, oil whip and whirl/whip synchronization occurring in rotor systems with full-floating ring bearings. *Nonlinear Dynamics* 2009; 57, p. 509-532.
- [16] Sundararajan P, Noah ST. Dynamics of forced nonlinear systems using shooting/arc-length continuation method - application to rotor systems. *Journal of Vibration and Acoustics* 1997; 119, p. 9-20.
- [17] van de Vrande, BL. *Nonlinear dynamics of elementary rotor systems with compliant plain journal bearings*. Proefschrift, Technische Universiteit Eindhoven; 2001.
- [18] Woschke E, Göbel S, Nitzschke S, Daniel C, Strackeljan J. Influence of bearing geometry of automotive turbochargers on the nonlinear vibrations during run-up. In: *Proceedings of the 9th IFToMM International Conference on Rotordynamics, Volume 21 of the series Mechanisms and Machine Science*. Springer International Publishing; 2015. p. 835-844.
- [19] Zhao, JY, Hahn, EJ. Subharmonic, quasiperiodic and chaotic motions of a rigid rotor supported by an eccentric squeeze film damper. *Proceedings of the Institution of Mechanical Engineers, Part C: Journal of Mechanical Engineering Science* 1993; 207, p. 383-392.
- [20] G.H. Tidbury, Analytical treatment of beam vibrations, *Machine Design Eng.* (November) (1964), p. 53–62.
- [21] N.O. Myklestad, A new method for calculating natural modes of uncoupled bending vibration of airplane wings, *J. Aeronaut. Sci.* (1944) 153–162.
- [22] J.W. Lund, Stability and Damped Critical Speeds of a Flexible Rotor on Fluid Film Bearings, ASME 73-DET-103, ASME Design-Technology Conference, Cincinnati, USA, Sept. 1973.
- [23] J.P. Den Hartog, *Mechanical Vibrations*, McGraw-Hill, New York, 1956.
- [24] J.M. Vance, H.R. Simmons, Computer Analysis of the Transient Dynamics of Rigid and Flexible Rotors with Bearing Dampers, Report FTDM-301, Pratt and Whitney Inc., Conn. September, 1969.
- [25] H.D. Nelson, J.M. McVaugh, The dynamics of rotor-bearing systems using finite elements, *Trans. ASME J. Eng.* 98 (1976) 593–600.

- [26] K.E. Rouch, J.S. Kao, Dynamic reduction in rotor dynamics by the finite element method, *Trans. ASME, J. Mech. Design* 102 (1980) 360–367.
- [27] Y.D. Kim, C.W. Lee, Finite element analysis of rotor bearing systems using a modal transformation matrix, *J. Sound Vibration* 111 (3) (1986) 441–456.
- [28] M. Aleyaasin, M. Ebrahimi, Flexural vibration of rotating shafts by frequency domain hybrid modelling, *Comput. Struct.* 79 (39) (2000) 319–331.
- [29] D.G. Hibner, Dynamic response of viscous damped multi-shaft jet engines, *J. Aircraft* 12 (1975) 13–19.
- [30] J. Hannah, R.C. Stephens, *Mechanics of Machines*, Edward Arnold, London, 1997.

APPENDIX A

State equations of rotor with eccentricity:

$$\begin{aligned}
 e40 = & -R43*(P40/M40+SF42)-SPINNIN1_mepsnth*(-SPINNIN1_R11*(- \\
 & SPINNIN1_mepsnth*SPINNIN1_SF41+SPINNIN1_P25/SPINNIN1_M25)- \\
 & Rishspi1_K38_41*Rishspi1_Q41-Rishspi1_K38_42 *Rishspi1_Q42-Rishspi1_K38_25*Rishspi1_Q25- \\
 & Rishspi1_K38_38*Rishspi1_Q38 \\
 & +Rishspi1_Gyrator2*SPINNIN1_P2/SPINNIN1_M2-Rishspi1_Fixedto3_cst*(Rishspi1_R48_45 \\
 & *(Rishspi1_Fixedto1_cst*SF13+Rishspi1_Fixedto1_snt*SF16+Rishspi1_Fixedto1_Od1) \\
 & +Rishspi1_R48_46*(Rishspi1_Fixedto2_cst*P45/M45+Rishspi1_Fixedto2_snt*P47 \\
 & /M47+Rishspi1_Fixedto2_Od1)+Rishspi1_R48_47*(Rishspi1_Fixedto4_cst*SPINNIN1_P7 \\
 & /SPINNIN1_M7+Rishspi1_Fixedto4_snt*(-SPINNIN1_epcsth*SPINNIN1_SF41+SPINNIN1_P27 \\
 & /SPINNIN1_M27)+Rishspi1_Fixedto4_Od1)+Rishspi1_R48_48*(Rishspi1_Fixedto3_cst \\
 & *(-SPINNIN1_mepsnth*SPINNIN1_SF41+SPINNIN1_P25/SPINNIN1_M25)+Rishspi1_Fixedto3_snt \\
 & *SPINNIN1_P2/SPINNIN1_M2+Rishspi1_Fixedto3_Od1))-Rishspi1_Fixedto3_msnt \\
 & *Rishspi1_Tf_yr2*(Rishspi1_R56_53*Rishspi1_TF_yr*(Rishspi1_Fixedto2_msnt \\
 & *P45/M45+Rishspi1_Fixedto2_cst*P47/M47+Rishspi1_Fixedto2_Od2)+Rishspi1_R56_54 \\
 & *(Rishspi1_Fixedto1_msnt*SF13+Rishspi1_Fixedto1_cst*SF16+Rishspi1_Fixedto1_Od2) \\
 & +Rishspi1_R56_55*(Rishspi1_Fixedto4_msnt*SPINNIN1_P7/SPINNIN1_M7+Rishspi1_Fixedto4_cst \\
 & *(-SPINNIN1_epcsth*SPINNIN1_SF41+SPINNIN1_P27/SPINNIN1_M27)+Rishspi1_Fixedto4_Od2) \\
 & +Rishspi1_R56_56*Rishspi1_Tf_yr2*(Rishspi1_Fixedto3_msnt*(-SPINNIN1_mepsnth \\
 & *SPINNIN1_SF41+SPINNIN1_P25/SPINNIN1_M25)+Rishspi1_Fixedto3_cst*SPINNIN1_P2 \\
 & /SPINNIN1_M2+Rishspi1_Fixedto3_Od2))-Rishspi2_K41_41*Rishspi2_Q41-Rishspi2_K41_42 \\
 & *Rishspi2_Q42-Rishspi2_K41_25*Rishspi2_Q25-Rishspi2_K41_38*Rishspi2_Q38 \\
 & -Rishspi2_Fixedto1_cst*(Rishspi2_R45_45*(Rishspi2_Fixedto1_cst*(-SPINNIN1_mepsnth \\
 & *SPINNIN1_SF41+SPINNIN1_P25/SPINNIN1_M25)+Rishspi2_Fixedto1_snt*(-SPINNIN1_epcsth \\
 & *SPINNIN1_SF41+SPINNIN1_P27/SPINNIN1_M27)+Rishspi2_Fixedto1_Od1)+Rishspi2_R45_46 \\
 & *(Rishspi2_Fixedto2_cst*SPINNIN1_P2/SPINNIN1_M2+Rishspi2_Fixedto2_snt*SPINNIN1_P7 \\
 & /SPINNIN1_M7+Rishspi2_Fixedto2_Od1)+Rishspi2_R45_47*(Rishspi2_Fixedto4_cst \\
 & *P49/M49+Rishspi2_Fixedto4_snt*SF19+Rishspi2_Fixedto4_Od1)+Rishspi2_R45_48 \\
 & *(Rishspi2_Fixedto3_cst*SF17+Rishspi2_Fixedto3_snt*P51/M51+Rishspi2_Fixedto3_Od1)) \\
 & -Rishspi2_Fixedto1_msnt*(Rishspi2_R54_53*Rishspi2_TF_yr*(Rishspi2_Fixedto2_msnt \\
 & *SPINNIN1_P2/SPINNIN1_M2+Rishspi2_Fixedto2_cst*SPINNIN1_P7/SPINNIN1_M7+Rishspi2_Fixed
 \end{aligned}$$

to2_Od2) +Rishspi2_R54_54*(Rishspi2_Fixedto1_msnt*(-SPINNIN1_mepsnth*SPINNIN1_SF41
+SPINNIN1_P25/SPINNIN1_M25)+Rishspi2_Fixedto1_cst*(-SPINNIN1_epcsth*SPINNIN1_SF41
+SPINNIN1_P27/SPINNIN1_M27)+Rishspi2_Fixedto1_Od2)+Rishspi2_R54_55*(Rishspi2_Fixedto4_ms
nt *P49/M49+Rishspi2_Fixedto4_cst*SF19+Rishspi2_Fixedto4_Od2)+Rishspi2_R54_56
Rishspi2_Tf_yr2(Rishspi2_Fixedto3_msnt*SF17+Rishspi2_Fixedto3_cst*P51
/M51+Rishspi2_Fixedto3_Od2))-Rishspi2_R73*(-SPINNIN1_mepsnth*SPINNIN1_SF41
+SPINNIN1_P25/SPINNIN1_M25))-SPINNIN1_epcsth*(-SPINNIN1_R14*(-SPINNIN1_epcsth
*SPINNIN1_SF41+SPINNIN1_P27/SPINNIN1_M27)-Rishspi1_K50_28*Rishspi1_Q28-
Rishspi1_K50_40 *Rishspi1_Q40-Rishspi1_K50_49*Rishspi1_Q49-Rishspi1_K50_50*Rishspi1_Q50
-Rishspi1_Fixedto4_snt*(Rishspi1_R47_45*(Rishspi1_Fixedto1_cst*SF13+Rishspi1_Fixedto1_snt
SF16+Rishspi1_Fixedto1_Od1)+Rishspi1_R47_46(Rishspi1_Fixedto2_cst*P45
/M45+Rishspi1_Fixedto2_snt*P47/M47+Rishspi1_Fixedto2_Od1)+Rishspi1_R47_47
*(Rishspi1_Fixedto4_cst*SPINNIN1_P7/SPINNIN1_M7+Rishspi1_Fixedto4_snt*(
-SPINNIN1_epcsth*SPINNIN1_SF41+SPINNIN1_P27/SPINNIN1_M27)+Rishspi1_Fixedto4_Od1)
+Rishspi1_R47_48*(Rishspi1_Fixedto3_cst*(-SPINNIN1_mepsnth*SPINNIN1_SF41
+SPINNIN1_P25/SPINNIN1_M25)+Rishspi1_Fixedto3_snt*SPINNIN1_P2/SPINNIN1_M2
+Rishspi1_Fixedto3_Od1))-Rishspi1_Fixedto4_cst*(Rishspi1_R55_53*Rishspi1_TF_yr
*(Rishspi1_Fixedto2_msnt*P45/M45+Rishspi1_Fixedto2_cst*P47/M47+Rishspi1_Fixedto2_Od2)
+Rishspi1_R55_54*(Rishspi1_Fixedto1_msnt*SF13+Rishspi1_Fixedto1_cst*SF16
+Rishspi1_Fixedto1_Od2)+Rishspi1_R55_55*(Rishspi1_Fixedto4_msnt*SPINNIN1_P7
/SPINNIN1_M7+Rishspi1_Fixedto4_cst*(-SPINNIN1_epcsth*SPINNIN1_SF41+SPINNIN1_P27
/SPINNIN1_M27)+Rishspi1_Fixedto4_Od2)+Rishspi1_R55_56*Rishspi1_Tf_yr2*(Rishspi1_Fixedto3_m
snt *(-SPINNIN1_mepsnth*SPINNIN1_SF41+SPINNIN1_P25/SPINNIN1_M25)+
Rishspi1_Fixedto3_cst *SPINNIN1_P2/SPINNIN1_M2+Rishspi1_Fixedto3_Od2))-Rishspi1_R76*(-
SPINNIN1_epcsth *SPINNIN1_SF41+SPINNIN1_P27/SPINNIN1_M27)-
Rishspi2_K49_28*Rishspi2_Q28-Rishspi2_K49_40 *Rishspi2_Q40-Rishspi2_K49_49 *Rishspi2_Q49-
Rishspi2_K49_50*Rishspi2_Q50 -Rishspi2_Fixedto1_snt*(Rishspi2_R45_45*(Rishspi2_Fixedto1_cst *(-
SPINNIN1_mepsnth
SPINNIN1_SF41+SPINNIN1_P25/SPINNIN1_M25)+Rishspi2_Fixedto1_snt(-SPINNIN1_epcsth
*SPINNIN1_SF41+SPINNIN1_P27/SPINNIN1_M27)+Rishspi2_Fixedto1_Od1)+Rishspi2_R45_46
*(Rishspi2_Fixedto2_cst*SPINNIN1_P2/SPINNIN1_M2+Rishspi2_Fixedto2_snt*SPINNIN1_P7
/SPINNIN1_M7+Rishspi2_Fixedto2_Od1)+Rishspi2_R45_47*(Rishspi2_Fixedto4_cst
*P49/M49+Rishspi2_Fixedto4_snt*SF19+Rishspi2_Fixedto4_Od1)+Rishspi2_R45_48
*(Rishspi2_Fixedto3_cst*SF17+Rishspi2_Fixedto3_snt*P51/M51+Rishspi2_Fixedto3_Od1))

$$\begin{aligned}
& -\text{Rishspi2_Fixedto1_cst} * (\text{Rishspi2_R54_53} * \text{Rishspi2_TF_yr} * (\text{Rishspi2_Fixedto2_msnt} \\
& * \text{SPINNIN1_P2/SPINNIN1_M2} + \text{Rishspi2_Fixedto2_cst} * \text{SPINNIN1_P7/SPINNIN1_M7} + \text{Rishspi2_Fixed} \\
& \text{to2_Od2}) \\
& + \text{Rishspi2_R54_54} * (\text{Rishspi2_Fixedto1_msnt} * (-\text{SPINNIN1_mepsnth} * \text{SPINNIN1_SF41} \\
& + \text{SPINNIN1_P25/SPINNIN1_M25}) + \text{Rishspi2_Fixedto1_cst} * (-\text{SPINNIN1_epcsth} * \text{SPINNIN1_SF41} \\
& + \text{SPINNIN1_P27/SPINNIN1_M27}) + \text{Rishspi2_Fixedto1_Od2}) + \text{Rishspi2_R54_55} * (\text{Rishspi2_Fixedto4_ms} \\
& \text{nt} \\
& * \text{P49/M49} + \text{Rishspi2_Fixedto4_cst} * \text{SF19} + \text{Rishspi2_Fixedto4_Od2}) + \text{Rishspi2_R54_56} \\
& * \text{Rishspi2_Tf_yr2} * (\text{Rishspi2_Fixedto3_msnt} * \text{SF17} + \text{Rishspi2_Fixedto3_cst} * \text{P51} \\
& / \text{M51} + \text{Rishspi2_Fixedto3_Od2})) - \text{Rishspi2_R75} * (-\text{SPINNIN1_epcsth} * \text{SPINNIN1_SF41} \\
& + \text{SPINNIN1_P27/SPINNIN1_M27})) \\
\end{aligned}$$

e49=

$$\begin{aligned}
& -\text{Rishspi2_K42_41} * \text{Rishspi2_Q41} - \text{Rishspi2_K42_42} * \text{Rishspi2_Q42} - \text{Rishspi2_K42_25} \\
& * \text{Rishspi2_Q25} - \text{Rishspi2_K42_38} * \text{Rishspi2_Q38} - \text{Rishspi2_Fixedto4_cst} * (\text{Rishspi2_R47_45} \\
& * (\text{Rishspi2_Fixedto1_cst} * (-\text{SPINNIN1_mepsnth} * \text{SPINNIN1_SF41} + \text{SPINNIN1_P25/SPINNIN1_M25}) \\
& + \text{Rishspi2_Fixedto1_snt} * (-\text{SPINNIN1_epcsth} * \text{SPINNIN1_SF41} + \text{SPINNIN1_P27/SPINNIN1_M27}) \\
& + \text{Rishspi2_Fixedto1_Od1}) + \text{Rishspi2_R47_46} * (\text{Rishspi2_Fixedto2_cst} * \text{SPINNIN1_P2} \\
& / \text{SPINNIN1_M2} + \text{Rishspi2_Fixedto2_snt} * \text{SPINNIN1_P7/SPINNIN1_M7} + \text{Rishspi2_Fixedto2_Od1}) \\
& + \text{Rishspi2_R47_47} * (\text{Rishspi2_Fixedto4_cst} * \text{P49/M49} + \text{Rishspi2_Fixedto4_snt} * \text{SF19} \\
& + \text{Rishspi2_Fixedto4_Od1}) + \text{Rishspi2_R47_48} * (\text{Rishspi2_Fixedto3_cst} * \text{SF17} + \text{Rishspi2_Fixedto3_snt} \\
& * \text{P51/M51} + \text{Rishspi2_Fixedto3_Od1})) - \text{Rishspi2_Fixedto4_msnt} * (\text{Rishspi2_R55_53} \\
& * \text{Rishspi2_TF_yr} * (\text{Rishspi2_Fixedto2_msnt} * \text{SPINNIN1_P2/SPINNIN1_M2} + \text{Rishspi2_Fixedto2_cst} \\
& * \text{SPINNIN1_P7/SPINNIN1_M7} + \text{Rishspi2_Fixedto2_Od2}) + \text{Rishspi2_R55_54} * (\text{Rishspi2_Fixedto1_msnt} \\
& * (-\text{SPINNIN1_mepsnth} * \text{SPINNIN1_SF41} + \text{SPINNIN1_P25/SPINNIN1_M25}) + \text{Rishspi2_Fixedto1_cst} \\
& * (-\text{SPINNIN1_epcsth} * \text{SPINNIN1_SF41} + \text{SPINNIN1_P27/SPINNIN1_M27}) + \text{Rishspi2_Fixedto1_Od2}) \\
& + \text{Rishspi2_R55_55} * (\text{Rishspi2_Fixedto4_msnt} * \text{P49/M49} + \text{Rishspi2_Fixedto4_cst} * \text{SF19} \\
& + \text{Rishspi2_Fixedto4_Od2}) + \text{Rishspi2_R55_56} * \text{Rishspi2_Tf_yr2} * (\text{Rishspi2_Fixedto3_msnt} \\
& * \text{SF17} + \text{Rishspi2_Fixedto3_cst} * \text{P51/M51} + \text{Rishspi2_Fixedto3_Od2})) - \text{Rishspi2_R74} * \text{P49/M49} - \\
& \text{RGyrator} * \text{P51/M51}
\end{aligned}$$

e51=

$$\begin{aligned}
& -\text{Rishspi2_Gyrator2} * \text{SF17} - \text{Rishspi2_trans36} * (\text{Rishspi2_K40_28} * \text{Rishspi2_Q28} + \text{Rishspi2_K40_40} \\
& * \text{Rishspi2_Q40} + \text{Rishspi2_K40_49} * \text{Rishspi2_Q49} + \text{Rishspi2_K40_50} * \text{Rishspi2_Q50}) \\
& - \text{Rishspi2_Fixedto3_snt} * (\text{Rishspi2_R48_45} * (\text{Rishspi2_Fixedto1_cst} * (-\text{SPINNIN1_mepsnth} \\
& * \text{SPINNIN1_SF41} + \text{SPINNIN1_P25/SPINNIN1_M25}) + \text{Rishspi2_Fixedto1_snt} * (-\text{SPINNIN1_epcsth}
\end{aligned}$$

*SPINNIN1_SF41+SPINNIN1_P27/SPINNIN1_M27)+Rishspi2_Fixedto1_Od1)+Rishspi2_R48_46
 *(Rishspi2_Fixedto2_cst*SPINNIN1_P2/SPINNIN1_M2+Rishspi2_Fixedto2_snt*SPINNIN1_P7
 /SPINNIN1_M7+Rishspi2_Fixedto2_Od1)+Rishspi2_R48_47*(Rishspi2_Fixedto4_cst
 *P49/M49+Rishspi2_Fixedto4_snt*SF19+Rishspi2_Fixedto4_Od1)+Rishspi2_R48_48
 *(Rishspi2_Fixedto3_cst*SF17+Rishspi2_Fixedto3_snt*P51/M51+Rishspi2_Fixedto3_Od1))
 -
 Rishspi2_Fixedto3_cst*Rishspi2_Tf_yr2*(Rishspi2_R56_53*Rishspi2_TF_yr*(Rishspi2_Fixedto2_msnt
 *SPINNIN1_P2/SPINNIN1_M2+Rishspi2_Fixedto2_cst*SPINNIN1_P7/SPINNIN1_M7+Rishspi2_Fixed
 to2_Od2)
 +Rishspi2_R56_54*(Rishspi2_Fixedto1_msnt*(-SPINNIN1_mepsnth*SPINNIN1_SF41
 +SPINNIN1_P25/SPINNIN1_M25)+Rishspi2_Fixedto1_cst*(-SPINNIN1_epcsth*SPINNIN1_SF41
 +SPINNIN1_P27/SPINNIN1_M27)+Rishspi2_Fixedto1_Od2)+Rishspi2_R56_55*(Rishspi2_Fixedto4_m
 snt *P49/M49+Rishspi2_Fixedto4_cst*SF19+Rishspi2_Fixedto4_Od2)+Rishspi2_R56_56
 Rishspi2_Tf_yr2(Rishspi2_Fixedto3_msnt*SF17+Rishspi2_Fixedto3_cst*P51
 /M51+Rishspi2_Fixedto3_Od2))+RGyrator*P49/M49

 e47= LGyrator*P45/M45-Rishspi1_Gyrator1*P45/M45-Rishspi1_trans26*(Rishspi1_K28_28
 *Rishspi1_Q28+Rishspi1_K28_40*Rishspi1_Q40+Rishspi1_K28_49*Rishspi1_Q49
 +Rishspi1_K28_50*Rishspi1_Q50)-Rishspi1_Fixedto2_snt*(Rishspi1_R46_45*(Rishspi1_Fixedto1_cst
 *SF13+Rishspi1_Fixedto1_snt*SF16+Rishspi1_Fixedto1_Od1)+Rishspi1_R46_46
 *(Rishspi1_Fixedto2_cst*P45/M45+Rishspi1_Fixedto2_snt*P47/M47+Rishspi1_Fixedto2_Od1)
 +Rishspi1_R46_47*(Rishspi1_Fixedto4_cst*SPINNIN1_P7/SPINNIN1_M7+Rishspi1_Fixedto4_snt
 *(-SPINNIN1_epcsth*SPINNIN1_SF41+SPINNIN1_P27/SPINNIN1_M27)+Rishspi1_Fixedto4_Od1)
 +Rishspi1_R46_48*(Rishspi1_Fixedto3_cst*(-SPINNIN1_mepsnth*SPINNIN1_SF41
 +SPINNIN1_P25/SPINNIN1_M25)+Rishspi1_Fixedto3_snt*SPINNIN1_P2/SPINNIN1_M2
 +Rishspi1_Fixedto3_Od1))-Rishspi1_Fixedto2_cst*Rishspi1_TF_yr*(Rishspi1_R53_53
 Rishspi1_TF_yr(Rishspi1_Fixedto2_msnt*P45/M45+Rishspi1_Fixedto2_cst*P47
 /M47+Rishspi1_Fixedto2_Od2)+Rishspi1_R53_54*(Rishspi1_Fixedto1_msnt*SF13
 +Rishspi1_Fixedto1_cst*SF16+Rishspi1_Fixedto1_Od2)+Rishspi1_R53_55*(Rishspi1_Fixedto4_msnt
 SPINNIN1_P7/SPINNIN1_M7+Rishspi1_Fixedto4_cst(-SPINNIN1_epcsth*SPINNIN1_SF41
 +SPINNIN1_P27/SPINNIN1_M27)+Rishspi1_Fixedto4_Od2)+Rishspi1_R53_56*Rishspi1_Tf_yr2
 (Rishspi1_Fixedto3_msnt(-SPINNIN1_mepsnth*SPINNIN1_SF41+SPINNIN1_P25/SPINNIN1_M25)
 +Rishspi1_Fixedto3_cst*SPINNIN1_P2/SPINNIN1_M2+Rishspi1_Fixedto3_Od2))

$$\begin{aligned}
e45 = & -L\text{Gyrator} * P47 / M47 - \text{Rishspi1_K25_41} * \text{Rishspi1_Q41} - \text{Rishspi1_K25_42} * \text{Rishspi1_Q42} \\
& - \text{Rishspi1_K25_25} * \text{Rishspi1_Q25} - \text{Rishspi1_K25_38} * \text{Rishspi1_Q38} + \text{Rishspi1_Gyrator1} \\
& * P47 / M47 - \text{Rishspi1_Fixedto2_cst} * (\text{Rishspi1_R46_45} * (\text{Rishspi1_Fixedto1_cst} * \text{SF13} \\
& + \text{Rishspi1_Fixedto1_snt} * \text{SF16} + \text{Rishspi1_Fixedto1_Od1}) + \text{Rishspi1_R46_46} * (\text{Rishspi1_Fixedto2_cst} \\
& * P45 / M45 + \text{Rishspi1_Fixedto2_snt} * P47 / M47 + \text{Rishspi1_Fixedto2_Od1}) + \text{Rishspi1_R46_47} \\
& * (\text{Rishspi1_Fixedto4_cst} * \text{SPINNIN1_P7} / \text{SPINNIN1_M7} + \text{Rishspi1_Fixedto4_snt} * (\\
& - \text{SPINNIN1_epcsth} * \text{SPINNIN1_SF41} + \text{SPINNIN1_P27} / \text{SPINNIN1_M27}) + \text{Rishspi1_Fixedto4_Od1}) \\
& + \text{Rishspi1_R46_48} * (\text{Rishspi1_Fixedto3_cst} * (-\text{SPINNIN1_mepsnth} * \text{SPINNIN1_SF41} \\
& + \text{SPINNIN1_P25} / \text{SPINNIN1_M25}) + \text{Rishspi1_Fixedto3_snt} * \text{SPINNIN1_P2} / \text{SPINNIN1_M2} \\
& + \text{Rishspi1_Fixedto3_Od1})) - \text{Rishspi1_Fixedto2_msnt} * \text{Rishspi1_TF_yr} * (\text{Rishspi1_R53_53} \\
& * \text{Rishspi1_TF_yr} * (\text{Rishspi1_Fixedto2_msnt} * P45 / M45 + \text{Rishspi1_Fixedto2_cst} * P47 \\
& / M47 + \text{Rishspi1_Fixedto2_Od2}) + \text{Rishspi1_R53_54} * (\text{Rishspi1_Fixedto1_msnt} * \text{SF13} \\
& + \text{Rishspi1_Fixedto1_cst} * \text{SF16} + \text{Rishspi1_Fixedto1_Od2}) + \text{Rishspi1_R53_55} * (\text{Rishspi1_Fixedto4_msnt} \\
& * \text{SPINNIN1_P7} / \text{SPINNIN1_M7} + \text{Rishspi1_Fixedto4_cst} * (-\text{SPINNIN1_epcsth} * \text{SPINNIN1_SF41} \\
& + \text{SPINNIN1_P27} / \text{SPINNIN1_M27}) + \text{Rishspi1_Fixedto4_Od2}) + \text{Rishspi1_R53_56} * \text{Rishspi1_Tf_yr2} \\
& * (\text{Rishspi1_Fixedto3_msnt} * (-\text{SPINNIN1_mepsnth} * \text{SPINNIN1_SF41} + \text{SPINNIN1_P25} / \text{SPINNIN1_M25}) \\
& + \text{Rishspi1_Fixedto3_cst} * \text{SPINNIN1_P2} / \text{SPINNIN1_M2} + \text{Rishspi1_Fixedto3_Od2}))
\end{aligned}$$

$$\text{Rishspi2_f50} = \text{SF19}$$

$$\text{Rishspi2_f49} = -\text{SPINNIN1_epcsth} * \text{SPINNIN1_SF41} + \text{SPINNIN1_P27} / \text{SPINNIN1_M27}$$

$$\text{Rishspi2_f40} = \text{Rishspi2_trans36} * P51 / M51$$

$$\text{Rishspi2_f28} = \text{Rishspi2_trans26} * \text{SPINNIN1_P7} / \text{SPINNIN1_M7}$$

$$\text{Rishspi2_f38} = \text{SF17}$$

$$\text{Rishspi2_f25} = \text{SPINNIN1_P2} / \text{SPINNIN1_M2}$$

$$\text{Rishspi2_f42} = P49 / M49$$

$$\text{Rishspi2_f41} = -\text{SPINNIN1_mepsnth} * \text{SPINNIN1_SF41} + \text{SPINNIN1_P25} / \text{SPINNIN1_M25}$$

$$\text{Rishspi2_Fixedto4_f20} = \text{SF19}$$

$$\text{Rishspi2_Fixedto4_f19} = P49 / M49$$

$\text{Rishspi2_Fixedto4_f16} = \text{Rishspi2_Fixedto4_SF15}$
 $\text{Rishspi2_Fixedto3_f20} = \text{P51/M51}$
 $\text{Rishspi2_Fixedto3_f19} = \text{SF17}$
 $\text{Rishspi2_Fixedto3_f16} = \text{Rishspi2_Fixedto3_SF15}$
 $\text{Rishspi2_Fixedto2_f20} = \text{SPINNIN1_P7/SPINNIN1_M7}$
 $\text{Rishspi2_Fixedto2_f19} = \text{SPINNIN1_P2/SPINNIN1_M2}$
 $\text{Rishspi2_Fixedto2_f16} = \text{Rishspi2_Fixedto2_SF15}$
 $\text{Rishspi2_Fixedto1_f20} = -\text{SPINNIN1_epcsth} * \text{SPINNIN1_SF41} + \text{SPINNIN1_P27/SPINNIN1_M27}$
 $\text{Rishspi2_Fixedto1_f19} = -\text{SPINNIN1_mepsnth} * \text{SPINNIN1_SF41} + \text{SPINNIN1_P25/SPINNIN1_M25}$
 $\text{Rishspi2_Fixedto1_f16} = \text{Rishspi2_Fixedto1_SF15}$
 $\text{Rishspi1_f50} = -\text{SPINNIN1_epcsth} * \text{SPINNIN1_SF41} + \text{SPINNIN1_P27/SPINNIN1_M27}$
 $\text{Rishspi1_f49} = \text{SF16}$
 $\text{Rishspi1_f40} = \text{Rishspi1_trans36} * \text{SPINNIN1_P2/SPINNIN1_M2}$
 $\text{Rishspi1_f28} = \text{Rishspi1_trans26} * \text{P47/M47}$
 $\text{Rishspi1_f38} = -\text{SPINNIN1_mepsnth} * \text{SPINNIN1_SF41} + \text{SPINNIN1_P25/SPINNIN1_M25}$
 $\text{Rishspi1_f25} = \text{P45/M45}$
 $\text{Rishspi1_f42} = \text{SPINNIN1_P7/SPINNIN1_M7}$
 $\text{Rishspi1_f41} = \text{SF13}$
 $\text{Rishspi1_Fixedto4_f20} = -\text{SPINNIN1_epcsth} * \text{SPINNIN1_SF41} + \text{SPINNIN1_P27/SPINNIN1_M27}$
 $\text{Rishspi1_Fixedto4_f19} = \text{SPINNIN1_P7/SPINNIN1_M7}$
 $\text{Rishspi1_Fixedto4_f16} = \text{Rishspi1_Fixedto4_SF15}$
 $\text{Rishspi1_Fixedto3_f20} = \text{SPINNIN1_P2/SPINNIN1_M2}$

Rishspi1_Fixedto3_f19= -SPINNIN1_mepsnth*SPINNIN1_SF41+SPINNIN1_P25/SPINNIN1_M25

Rishspi1_Fixedto3_f16= Rishspi1_Fixedto3_SF15

Rishspi1_Fixedto2_f20= P47/M47

Rishspi1_Fixedto2_f19= P45/M45

Rishspi1_Fixedto2_f16= Rishspi1_Fixedto2_SF15

Rishspi1_Fixedto1_f20= SF16

Rishspi1_Fixedto1_f19= SF13

Rishspi1_Fixedto1_f16= Rishspi1_Fixedto1_SF15

SPINNIN1_e7= SPINNIN1_pmiomeg*SPINNIN1_P2/SPINNIN1_M2SPINNIN1_R9*SPINNIN1_P7/SPINNIN1_M7 -Rishspi1_K42_41*Rishspi1_Q41-Rishspi1_K42_42*Rishspi1_Q42-Rishspi1_K42_25
*Rishspi1_Q25-Rishspi1_K42_38*Rishspi1_Q38-Rishspi1_Fixedto4_cst*(Rishspi1_R47_45
*(Rishspi1_Fixedto1_cst*SF13+Rishspi1_Fixedto1_snt*SF16+Rishspi1_Fixedto1_Od1)
+Rishspi1_R47_46*(Rishspi1_Fixedto2_cst*P45/M45+Rishspi1_Fixedto2_snt*P47
/M47+Rishspi1_Fixedto2_Od1)+Rishspi1_R47_47*(Rishspi1_Fixedto4_cst*SPINNIN1_P7
/SPINNIN1_M7+Rishspi1_Fixedto4_snt*(-SPINNIN1_epcsth*SPINNIN1_SF41+
SPINNIN1_P27 /SPINNIN1_M27)+Rishspi1_Fixedto4_Od1)+Rishspi1_R47_48*(Rishspi1_Fixe
dto3_cst *(-SPINNIN1_mepsnth*SPINNIN1_SF41+SPINNIN1_P25/SPINNIN1_M25)+
Rishspi1_Fixedto3_snt *SPINNIN1_P2/SPINNIN1_M2+Rishspi1_Fixedto3_Od1))-
Rishspi1_Fixedto4_msnt *(Rishspi1_R55_53*Rishspi1_TF_yr*(Rishspi1_Fixedto2_msnt*P45/M
45+Rishspi1_Fixedto2_cst *P47/M47+Rishspi1_Fixedto2_Od2)+Rishspi1_R55_54*(Rishspi1_Fi
xedto1_msnt *SF13+Rishspi1_Fixedto1_cst*SF16+Rishspi1_Fixedto1_Od2)+Rishspi1_R55_55
*(Rishspi1_Fixedto4_msnt*SPINNIN1_P7/SPINNIN1_M7+Rishspi1_Fixedto4_cst*(-
SPINNIN1_epcsth*SPINNIN1_SF41+SPINNIN1_P27/SPINNIN1_M27)+Rishspi1_Fixedto4_Od
2)+Rishspi1_R55_56*Rishspi1_Tf_yr2*(Rishspi1_Fixedto3_msnt*(-SPINNIN1_mepsnth *
SPINNIN1_SF41+SPINNIN1_P25/SPINNIN1_M25)+Rishspi1_Fixedto3_cst*SPINNIN1_P2 /S
PINNIN1_M2+Rishspi1_Fixedto3_Od2))-Rishspi1_R74*SPINNIN1_P7/SPINNIN1_M7
-Rishspi2_Gyrator1*SPINNIN1_P2/SPINNIN1_M2-Rishspi2_trans26*(Rishspi2_K28_28
*Rishspi2_Q28+Rishspi2_K28_40*Rishspi2_Q40+Rishspi2_K28_49*Rishspi2_Q49
+Rishspi2_K28_50*Rishspi2_Q50)-Rishspi2_Fixedto2_snt*(Rishspi2_R46_45*
(Rishspi2_Fixedto1_cst*(-SPINNIN1_mepsnth*SPINNIN1_SF41+SPINNIN1_P25/

$$\begin{aligned}
& SPINNIN1_M25)+Rishspi2_Fixedto1_snt*(-SPINNIN1_epcsth*SPINNIN1_SF41+ \\
& SPINNIN1_P27/SPINNIN1_M27)+Rishspi2_Fixedto1_Od1) +Rishspi2_R46_46*(Rishspi2_Fixe \\
& dto2_cst*SPINNIN1_P2/SPINNIN1_M2+Rishspi2_Fixedto2_snt *SPINNIN1_P7/SPINNIN1_M \\
& 7+Rishspi2_Fixedto2_Od1)+Rishspi2_R46_47*(Rishspi2_Fixedto4_cst *P49/M49+Rishspi2_Fix \\
& edto4_snt*SF19+Rishspi2_Fixedto4_Od1)+Rishspi2_R46_48 *(Rishspi2_Fixedto3_cst*SF17+Ri \\
& shspi2_Fixedto3_snt*P51/M51+Rishspi2_Fixedto3_Od1)) - \\
& Rishspi2_Fixedto2_cst*Rishspi2_TF_yr*(Rishspi2_R53_53*Rishspi2_TF_yr*(Rishspi2_Fixedto \\
& 2_msnt *SPINNIN1_P2/SPINNIN1_M2+Rishspi2_Fixedto2_cst*SPINNIN1_P7/SPINNIN1_M7 \\
& +Rishspi2_Fixedto2_Od2) +Rishspi2_R53_54*(Rishspi2_Fixedto1_msnt*(- \\
& SPINNIN1_mepsnth*SPINNIN1_SF41+SPINNIN1_P25/SPINNIN1_M25)+Rishspi2_Fixedto1_ \\
& cst*(-SPINNIN1_epcsth*SPINNIN1_SF41+SPINNIN1_P27/SPINNIN1_M27)+ \\
& Rishspi2_Fixedto1_Od2)+Rishspi2_R53_55*(Rishspi2_Fixedto4_msnt *P49/M49+Rishspi2_Fix \\
& edto4_cst*SF19+Rishspi2_Fixedto4_Od2)+Rishspi2_R53_56*Rishspi2_Tf_yr2*(Rishspi2_Fixed \\
& to3_msnt*SF17+Rishspi2_Fixedto3_cst*P51/M51+Rishspi2_Fixedto3_Od2))
\end{aligned}$$

$$\begin{aligned}
SPINNIN1_e2= & -SPINNIN1_pmiomeg*SPINNIN1_P7/SPINNIN1_M7-SPINNIN1_R4*SPINNIN1_P2/ \\
& SPINNIN1_M2 -Rishspi1_Gyrator2*(-SPINNIN1_mepsnth*SPINNIN1_SF41+ \\
& SPINNIN1_P25/SPINNIN1_M25)-Rishspi1_trans36*(Rishspi1_K40_28*Rishspi1_Q28+ \\
& Rishspi1_K40_40*Rishspi1_Q40 +Rishspi1_K40_49*Rishspi1_Q49+Rishspi1_K40_50*Rish \\
& spi1_Q50)-Rishspi1_Fixedto3_snt *(Rishspi1_R48_45*(Rishspi1_Fixedto1_cst*SF13+ \\
& Rishspi1_Fixedto1_snt*SF16+Rishspi1_Fixedto1_Od1)+Rishspi1_R48_46*(Rishspi1_Fixedt \\
& o2_cst*P45/M45+Rishspi1_Fixedto2_snt *P47/M47+Rishspi1_Fixedto2_Od1)+Rishspi1_R48 \\
& _47*(Rishspi1_Fixedto4_cst*SPINNIN1_P7/SPINNIN1_M7+Rishspi1_Fixedto4_snt*(- \\
& SPINNIN1_epcsth*SPINNIN1_SF41+SPINNIN1_P27/SPINNIN1_M27)+Rishspi1_Fixedto4 \\
& _Od1)+Rishspi1_R48_48*(Rishspi1_Fixedto3_cst *(SPINNIN1_mepsnth*SPINNIN1_SF41+ \\
& SPINNIN1_P25/SPINNIN1_M25)+Rishspi1_Fixedto3_snt *SPINNIN1_P2/SPINNIN1_M2+ \\
& Rishspi1_Fixedto3_Od1))-Rishspi1_Fixedto3_cst*Rishspi1_Tf_yr2 *(Rishspi1_R56_53* \\
& Rishspi1_TF_yr*(Rishspi1_Fixedto2_msnt*P45/M45+Rishspi1_Fixedto2_cst *P47/M47+ \\
& Rishspi1_Fixedto2_Od2)+Rishspi1_R56_54*(Rishspi1_Fixedto1_msnt *SF13+Rishspi1_Fixe \\
& dto1_cst*SF16+Rishspi1_Fixedto1_Od2)+Rishspi1_R56_55 *(Rishspi1_Fixedto4_msnt*SPI \\
& NNIN1_P7/SPINNIN1_M7+Rishspi1_Fixedto4_cst*(-SPINNIN1_epcsth*SPINNIN1_SF41+ \\
& SPINNIN1_P27/SPINNIN1_M27)+Rishspi1_Fixedto4_Od2) +Rishspi1_R56_56*Rishspi1_T \\
& f_yr2*(Rishspi1_Fixedto3_msnt*(-SPINNIN1_mepsnth *SPINNIN1_SF41+SPINNIN1_P25 \\
& /SPINNIN1_M25)+Rishspi1_Fixedto3_cst*SPINNIN1_P2 /SPINNIN1_M2+Rishspi1_Fixedt \\
& o3_Od2))-Rishspi2_K25_41*Rishspi2_Q41-Rishspi2_K25_42*Rishspi2_Q42-
\end{aligned}$$

$$\begin{aligned}
& \text{Rishspi2_K25_25} * \text{Rishspi2_Q25} - \text{Rishspi2_K25_38} * \text{Rishspi2_Q38} + \text{Rishspi2_Gyrator1} \\
& * \text{SPINNIN1_P7} / \text{SPINNIN1_M7} \text{Rishspi2_Fixedto2_cst} * (\text{Rishspi2_R46_45} * (\text{Rishspi2_Fixedto1_cst} * (-\text{SPINNIN1_mepsnth} * \text{SPINNIN1_SF41} + \text{SPINNIN1_P25} / \text{SPINNIN1_M25}) + \\
& \text{Rishspi2_Fixedto1_snt} * (-\text{SPINNIN1_epcsth} * \text{SPINNIN1_SF41} + \text{SPINNIN1_P27} / \text{SPINNIN1_M27}) + \text{Rishspi2_Fixedto1_Od1}) + \text{Rishspi2_R46_46} * (\text{Rishspi2_Fixedto2_cst} \\
& * \text{SPINNIN1_P2} / \text{SPINNIN1_M2} + \text{Rishspi2_Fixedto2_snt} * \text{SPINNIN1_P7} / \text{SPINNIN1_M7} + \\
& \text{Rishspi2_Fixedto2_Od1}) + \text{Rishspi2_R46_47} * (\text{Rishspi2_Fixedto4_cst} * \text{P49} / \text{M49} + \text{Rishspi2_Fixedto4_snt} * \text{SF19} + \text{Rishspi2_Fixedto4_Od1}) + \text{Rishspi2_R46_48} * (\text{Rishspi2_Fixedto3_cst} * \text{SF17} \\
& + \text{Rishspi2_Fixedto3_snt} * \text{P51} / \text{M51} + \text{Rishspi2_Fixedto3_Od1})) - \text{Rishspi2_Fixedto2_msnt} \\
& * \text{Rishspi2_TF_yr} * (\text{Rishspi2_R53_53} * \text{Rishspi2_TF_yr} * (\text{Rishspi2_Fixedto2_msnt} * \text{SPINNIN1_P2} / \text{SPINNIN1_M2} + \text{Rishspi2_Fixedto2_cst} * \text{SPINNIN1_P7} / \text{SPINNIN1_M7} + \text{Rishspi2_Fixedto2_Od2}) + \text{Rishspi2_R53_54} * (\text{Rishspi2_Fixedto1_msnt} * (\text{SPINNIN1_mepsnth} * \text{SPINNIN1_SF41} + \text{SPINNIN1_P25} / \text{SPINNIN1_M25}) + \text{Rishspi2_Fixedto1_cst} * (\text{SPINNIN1_epcsth} * \text{SPINNIN1_SF41} + \text{SPINNIN1_P27} / \text{SPINNIN1_M27}) + \text{Rishspi2_Fixedto1_Od2}) + \text{Rishspi2_R53_55} * (\text{Rishspi2_Fixedto4_msnt} * \text{P49} / \text{M49} + \text{Rishspi2_Fixedto4_cst} * \text{SF19} + \text{Rishspi2_Fixedto4_Od2}) + \text{Rishspi2_R53_56} * \text{Rishspi2_TF_yr}^2 * (\text{Rishspi2_Fixedto3_msnt} * \text{SF17} + \text{Rishspi2_Fixedto3_cst} * \text{P51} / \text{M51} + \text{Rishspi2_Fixedto3_Od2}))
\end{aligned}$$

$$\begin{aligned}
\text{SPINNIN1_e27} = & -\text{SPINNIN1_R14} * (-\text{SPINNIN1_epcsth} * \text{SPINNIN1_SF41} + \text{SPINNIN1_P27} / \text{SPINNIN1_M27}) \\
& - \text{Rishspi1_K50_28} * \text{Rishspi1_Q28} - \text{Rishspi1_K50_40} * \text{Rishspi1_Q40} - \text{Rishspi1_K50_49} \\
& * \text{Rishspi1_Q49} - \text{Rishspi1_K50_50} * \text{Rishspi1_Q50} - \text{Rishspi1_Fixedto4_snt} * (\text{Rishspi1_R47_45} \\
& * (\text{Rishspi1_Fixedto1_cst} * \text{SF13} + \text{Rishspi1_Fixedto1_snt} * \text{SF16} + \text{Rishspi1_Fixedto1_Od1}) \\
& + \text{Rishspi1_R47_46} * (\text{Rishspi1_Fixedto2_cst} * \text{P45} / \text{M45} + \text{Rishspi1_Fixedto2_snt} * \text{P47} / \text{M47} + \text{Rishspi1_Fixedto2_Od1}) + \text{Rishspi1_R47_47} * (\text{Rishspi1_Fixedto4_cst} * \text{SPINNIN1_P7} / \text{SPINNIN1_M7} + \text{Rishspi1_Fixedto4_snt} * (-\text{SPINNIN1_epcsth} * \text{SPINNIN1_SF41} + \text{SPINNIN1_P27} / \text{SPINNIN1_M27}) + \text{Rishspi1_Fixedto4_Od1}) + \text{Rishspi1_R47_48} * (\text{Rishspi1_Fixedto3_cst} * (\text{SPINNIN1_mepsnth} * \text{SPINNIN1_SF41} + \text{SPINNIN1_P25} / \text{SPINNIN1_M25}) + \text{Rishspi1_Fixedto3_snt} * \text{SPINNIN1_P2} / \text{SPINNIN1_M2} + \text{Rishspi1_Fixedto3_Od1})) - \\
& \text{Rishspi1_Fixedto4_cst} * (\text{Rishspi1_R55_53} * \text{Rishspi1_TF_yr} * (\text{Rishspi1_Fixedto2_msnt} * \text{P45} / \text{M45} + \text{Rishspi1_Fixedto2_cst} * \text{P47} / \text{M47} + \text{Rishspi1_Fixedto2_Od2}) + \text{Rishspi1_R55_54} * (\text{Rishspi1_Fixedto1_msnt} * \text{SF13} + \text{Rishspi1_Fixedto1_cst} * \text{SF16} + \text{Rishspi1_Fixedto1_Od2}) + \text{Rishspi1_R55_55} * (\text{Rishspi1_Fixedto4_msnt} * \text{SPINNIN1_P7} / \text{SPINNIN1_M7} + \text{Rishspi1_Fixedto4_cst} * (-\text{SPINNIN1_epcsth} * \text{SPINNIN1_SF41} + \text{SPINNIN1_P27} / \text{SPINNIN1_M27}) + \text{Rishspi1_Fixedto4_Od2}) + \text{Rishspi1_R55_56} * \text{Rishspi1_TF_yr}^2 * (\text{Rishspi1_Fixedto3_msnt} * (-
\end{aligned}$$

SPINNIN1_mepsnth*SPINNIN1_SF41+SPINNIN1_P25/SPINNIN1_M25) +Rishspi1_Fixedt
 o3_cst*SPINNIN1_P2/SPINNIN1_M2+Rishspi1_Fixedto3_Od2))-Rishspi1_R76 *(-
 SPINNIN1_epcsth*SPINNIN1_SF41+SPINNIN1_P27/SPINNIN1_M27)-Rishspi2_K49_28
 *Rishspi2_Q28-Rishspi2_K49_40*Rishspi2_Q40-Rishspi2_K49_49*Rishspi2_Q49-
 Rishspi2_K49_50*Rishspi2_Q50-Rishspi2_Fixedto1_snt*(Rishspi2_R45_45*
 (Rishspi2_Fixedto1_cst *(-SPINNIN1_mepsnth*SPINNIN1_SF41+SPINNIN1_P25
 /SPINNIN1_M25)+Rishspi2_Fixedto1_snt *(-SPINNIN1_epcsth*SPINNIN1_SF41+
 SPINNIN1_P27/SPINNIN1_M27)+Rishspi2_Fixedto1_Od1) +Rishspi2_R45_46*(Rishspi2_
 Fixedto2_cst*SPINNIN1_P2/SPINNIN1_M2+Rishspi2_Fixedto2_snt *SPINNIN1_P7/SPIN
 NIN1_M7+Rishspi2_Fixedto2_Od1)+Rishspi2_R45_47*(Rishspi2_Fixedto4_cst *P49/M49+
 Rishspi2_Fixedto4_snt*SF19+Rishspi2_Fixedto4_Od1)+Rishspi2_R45_48
 *(Rishspi2_Fixedto3_cst*SF17+Rishspi2_Fixedto3_snt*P51/M51+Rishspi2_Fixedto3_Od1))
 -Rishspi2_Fixedto1_cst*(Rishspi2_R54_53*Rishspi2_TF_yr*(Rishspi2_Fixedto2_msnt
 *SPINNIN1_P2/SPINNIN1_M2+Rishspi2_Fixedto2_cst*SPINNIN1_P7/SPINNIN1_M7+Ris
 hspi2_Fixedto2_Od2) +Rishspi2_R54_54*(Rishspi2_Fixedto1_msnt*(-SPINNIN1_mepsnth*
 SPINNIN1_SF41 +SPINNIN1_P25/SPINNIN1_M25)+Rishspi2_Fixedto1_cst*(-SPINNIN1
 _epcsth*SPINNIN1_SF41+SPINNIN1_P27/SPINNIN1_M27)+Rishspi2_Fixedto1_Od2)
 +Rishspi2_R54_55*(Rishspi2_Fixedto4_msnt *P49/M49+Rishspi2_Fixedto4_cst*SF19+Rish
 spi2_Fixedto4_Od2)+Rishspi2_R54_56 *Rishspi2_Tf_yr2*(Rishspi2_Fixedto3_msnt*SF17+
 Rishspi2_Fixedto3_cst*P51 /M51+Rishspi2_Fixedto3_Od2))-Rishspi2_R75*(-SPINNIN1_
 epcsth*SPINNIN1_SF41 +SPINNIN1_P27/SPINNIN1_M27)

SPINNIN1_e25= -SPINNIN1_R11*(-SPINNIN1_mepsnth*SPINNIN1_SF41+SPINNIN1_P25/
 SPINNIN1_M25)-Rishspi1_K38_41*Rishspi1_Q41-Rishspi1_K38_42*Rishspi1_Q42-
 Rishspi1_K38_25
 *Rishspi1_Q25-Rishspi1_K38_38*Rishspi1_Q38+Rishspi1_Gyrator2*SPINNIN1_P2
 /SPINNIN1_M2-Rishspi1_Fixedto3_cst*(Rishspi1_R48_45*(Rishspi1_Fixedto1_cst
 *SF13+Rishspi1_Fixedto1_snt*SF16+Rishspi1_Fixedto1_Od1)+Rishspi1_R48_46
 *(Rishspi1_Fixedto2_cst*P45/M45+Rishspi1_Fixedto2_snt*P47/M47+Rishspi1_Fixedto2_O
 d1) +Rishspi1_R48_47*(Rishspi1_Fixedto4_cst*SPINNIN1_P7/SPINNIN1_M7+Rishspi1_Fi
 xedto4_snt *(-SPINNIN1_epcsth*SPINNIN1_SF41+SPINNIN1_P27/SPINNIN1_M27)
 +Rishspi1_Fixedto4_Od1) +Rishspi1_R48_48*(Rishspi1_Fixedto3_cst*(-
 SPINNIN1_mepsnth*SPINNIN1_SF41 +SPINNIN1_P25/SPINNIN1_M25)+Rishspi1_Fixedt
 o3_snt*SPINNIN1_P2/SPINNIN1_M2 +Rishspi1_Fixedto3_Od1))-Rishspi1_Fixedto3_msnt
 Rishspi1_Tf_yr2(Rishspi1_R56_53 *Rishspi1_TF_yr*(Rishspi1_Fixedto2_msnt*P45/M45

$$\begin{aligned}
& +\text{Rishspi1_Fixedto2_cst}*\text{P47}/\text{M47}+\text{Rishspi1_Fixedto2_Od2})+\text{Rishspi1_R56_54}*(\text{Rishspi1_} \\
& \text{Fixedto1_msnt}*\text{SF13}+\text{Rishspi1_Fixedto1_cst}*\text{SF16}+\text{Rishspi1_Fixedto1_Od2})+\text{Rishspi1_R5} \\
& \text{6_55}*(\text{Rishspi1_Fixedto4_msnt}*\text{SPINNIN1_P7}/\text{SPINNIN1_M7}+\text{Rishspi1_Fixedto4_cst}*(- \\
& \text{SPINNIN1_epcsth}*\text{SPINNIN1_SF41}+\text{SPINNIN1_P27}/\text{SPINNIN1_M27})+\text{Rishspi1_Fixedto4} \\
& \text{_Od2})+\text{Rishspi1_R56_56}*\text{Rishspi1_Tf_yr2}*(\text{Rishspi1_Fixedto3_msnt}*(- \\
& \text{SPINNIN1_mepsnth}*\text{SPINNIN1_SF41}+\text{SPINNIN1_P25}/\text{SPINNIN1_M25}) \\
& +\text{Rishspi1_Fixedto3_cst}*\text{SPINNIN1_P2}/\text{SPINNIN1_M2}+\text{Rishspi1_Fixedto3_Od2}))- \\
& \text{Rishspi2_K41_41}*\text{Rishspi2_Q41}-\text{Rishspi2_K41_42}*\text{Rishspi2_Q42}\text{Rishspi2_K41_25}* \\
& \text{Rishspi2_Q25}-\text{Rishspi2_K41_38}*\text{Rishspi2_Q38}-\text{Rishspi2_Fixedto1_cst}*(\text{Rishspi2_R45_45} \\
& *(\text{Rishspi2_Fixedto1_cst}*(-\text{SPINNIN1_mepsnth}*\text{SPINNIN1_SF41}+\text{SPINNIN1_P25} \\
& /\text{SPINNIN1_M25})+\text{Rishspi2_Fixedto1_snt}*(-\text{SPINNIN1_epcsth}*\text{SPINNIN1_SF41} \\
& +\text{SPINNIN1_P27}/\text{SPINNIN1_M27})+\text{Rishspi2_Fixedto1_Od1})+\text{Rishspi2_R45_46}*(\text{Rishspi2} \\
& \text{_Fixedto2_cst}*\text{SPINNIN1_P2}/\text{SPINNIN1_M2}+\text{Rishspi2_Fixedto2_snt}*\text{SPINNIN1_P7}/\text{SPIN} \\
& \text{NIN1_M7}+\text{Rishspi2_Fixedto2_Od1})+\text{Rishspi2_R45_47}*(\text{Rishspi2_Fixedto4_cst}*\text{P49}/\text{M49}+ \\
& \text{Rishspi2_Fixedto4_snt}*\text{SF19}+\text{Rishspi2_Fixedto4_Od1})+\text{Rishspi2_R45_48}*(\text{Rishspi2_Fixedt} \\
& \text{o3_cst}*\text{SF17}+\text{Rishspi2_Fixedto3_snt}*\text{P51}/\text{M51}+\text{Rishspi2_Fixedto3_Od1}))- \text{Rishspi2_} \\
& \text{Fixedto1_msnt}*(\text{Rishspi2_R54_53}*\text{Rishspi2_Tf_yr}*(\text{Rishspi2_Fixedto2_msnt}*\text{SPINNIN1_} \\
& \text{P2}/\text{SPINNIN1_M2}+\text{Rishspi2_Fixedto2_cst}*\text{SPINNIN1_P7}/\text{SPINNIN1_M7}+\text{Rishspi2_Fixedt} \\
& \text{o2_Od2})+\text{Rishspi2_R54_54}*(\text{Rishspi2_Fixedto1_msnt}*(\text{SPINNIN1_mepsnth}*\text{SPINNIN1_S} \\
& \text{F41}+\text{SPINNIN1_P25}/\text{SPINNIN1_M25})+\text{Rishspi2_Fixedto1_cst}*(-\text{SPINNIN1_epcsth} \\
& * \text{SPINNIN1_SF41}+\text{SPINNIN1_P27}/\text{SPINNIN1_M27})+\text{Rishspi2_Fixedto1_Od2})+\text{Rishspi2_} \\
& \text{R54_55}*(\text{Rishspi2_Fixedto4_msnt}*\text{P49}/\text{M49}+\text{Rishspi2_Fixedto4_cst}*\text{SF19}+\text{Rishspi2_Fixedt} \\
& \text{o4_Od2})+\text{Rishspi2_R54_56}*\text{Rishspi2_Tf_yr2}*(\text{Rishspi2_Fixedto3_msnt}*\text{SF17}+\text{Rishspi2_Fi} \\
& \text{xedto3_cst}*\text{P51}/\text{M51}+\text{Rishspi2_Fixedto3_Od2}))- \text{Rishspi2_R73}*(-\text{SPINNIN1_mepsnth} \\
& * \text{SPINNIN1_SF41}+\text{SPINNIN1_P25}/\text{SPINNIN1_M25})
\end{aligned}$$

SPINNIN1_f28= SPINNIN1_P27/SPINNIN1_M27

SPINNIN1_f26= SPINNIN1_P25/SPINNIN1_M25

SPINNIN1_f3= SPINNIN1_P2/SPINNIN1_M2

SPINNIN1_f8= SPINNIN1_P7/SPINNIN1_M7


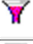






























SPINNIN1_f24= SPINNIN1_SF41






























APPENDIX B

























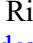


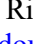

Various expressions used in Simulation rig modelling:















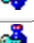



















Variable	Assignment
 pi (double)	pi=3.141592653;
 Omega (double)	Omega=2*pi*Rps;
 AngSpeed (double)	AngSpeed=Omega;
 SPINNIN1_AngSpeed (double) : Angular Speed rad/s	SPINNIN1_AngSpeed=AngSpeed;
 Rho (double)	
 SPINNIN1_Rho (double) : Material Density	SPINNIN1_Rho=Rho;
 Ri (double)	
 SPINNIN1_Ri (double) : Inner Rad. of Right End of Previous Int.face Shaft (Note Cyl. or Cone)	SPINNIN1_Ri=Ri;
 SPINNIN1_Riprv (double) : Inner Rad. of Left End of Previous Int.face Shaft (Note Cyl. or Cone)(Zero if non- existant)	SPINNIN1_Riprv=Ri;
 SPINNIN1_L_Prev (double) : Length of Previous Int. face Shaft(Zero if non-existant)	SPINNIN1_L_Prev=Lelem;
 SPINNIN1_Th_Prev (double) : Thickness of Previous Int. face Shaft (Zero if non-existant)	SPINNIN1_Th_Prev=(Ro-Ri);
 SPINNIN1_Rinext (double) : Inner Rad. of Left End of Next Int.face Shaft (Note Cyl. or Cone)(Zero if non-existant)	SPINNIN1_Rinext=Ri;
 SPINNIN1_Rrhnext (double) : Inner Rad. of Right End of Next Int.face Shaft (Note Cyl. or Cone)(Zero if non-existant)	SPINNIN1_Rrhnext=Ri;
 SPINNIN1_L_Next (double) : Length of Next Int. face Shaft(Zero if non-existant)	SPINNIN1_L_Next=Lelem;
 SPINNIN1_Th_Next (double) :	SPINNIN1_Th_Next=(Ro-Ri);
































Variable	Assignment
Thickness of Next Int. face Shaft (Zero if non-existant)	
 SPINNIN1_MconPrv (double)	
 SPINNIN1_MiconPrv (double)	
 SPINNIN1_MconNext (double)	
 SPINNIN1_MiconNext (double)	
 Rex (double)	
 SPINNIN1_HubMass (double)	
 SPINNIN1_Ecc (double) : Eccentricity of the Hub	
 SPINNIN1_AnglEcc (double) : Angle of Eccentricity from X Axis(vertical) in Degrees.	
 SPINNIN1_RotDmp (double) : Rotational Damping about diametrical axes	
 SPINNIN1_TransDmp (double) : Translational Damping of Mass centre	SPINNIN1_TransDmp=0.0;
 SPINNIN1_HubPolMI (double)	
 SPINNIN1_SF41 (double)	SPINNIN1_SF41=Omega;
 Rishspi1_Fixedto1_AngSpeed (double): Angular speed of the rotating frame	Rishspi1_Fixedto1_AngSpeed=Omega;
 Rishspi1_Fixedto2_AngSpeed (double): Angular speed of the rotating frame	Rishspi1_Fixedto2_AngSpeed=Omega;
 Rishspi1_Fixedto4_AngSpeed (double): Angular speed of the rotating frame	Rishspi1_Fixedto4_AngSpeed=Omega;
 Rishspi1_Fixedto3_AngSpeed (double): Angular speed of the	Rishspi1_Fixedto3_AngSpeed=Omega;






















Variable	Assignment
rotating frame	
 Rishspi1_Gyrator1 (double)	
 Rishspi1_trans26 (double)	
 Rishspi1_Gyrator2 (double)	
 Rishspi1_trans36 (double)	
 E (double)	
 Ro (double)	
 Rishspi1_pi (double)	Rishspi1_pi=pi;
 Rishspi1_Ro (double)	Rishspi1_Ro=Ro;
 Rishspi1_Ri (double)	Rishspi1_Ri=Ri;
 Rishspi1_Lt (double)	
 Lelem (double)	
 Rishspi1_L_this (double)	Rishspi1_L_this=Lelem;
 Rishspi1_Coef (double)	
 Rishspi1_E (double)	Rishspi1_E=E;
 Rishspi1_I (double) : Second Moment of Inertia about Diameter	Rishspi1_I=Rishspi1_pi*(Rishspi1_Ro*Rishspi1_Ro*Rishspi1_Ro*Rishspi1_Ro-Rishspi1_Ri*Rishspi1_Ri*Rishspi1_Ri*Rishspi1_Ri)*0.25;
 Rishspi1_K41_41 (double)	Rishspi1_Lt=Rishspi1_L_this; Rishspi1_Coef=Rishspi1_E*Rishspi1_I/(Rishspi1_Lt*Rishspi1_Lt); Rishspi1_K41_41=12*Rishspi1_Coef;
 Rishspi1_K41_42 (double)	Rishspi1_K41_42=6*Rishspi1_Lt*Rishspi1_Coef;
 Rishspi1_K41_25 (double)	Rishspi1_K41_25=-Rishspi1_K41_41;
 Rishspi1_K41_38 (double)	Rishspi1_K41_38=Rishspi1_K41_42;
 Rishspi1_K42_41 (double)	Rishspi1_K42_41=Rishspi1_K41_42;
 Rishspi1_K42_42 (double)	Rishspi1_K42_42=4*Rishspi1_Lt*Rishspi1_Lt*Rishspi1_Coef;
 Rishspi1_K42_25 (double)	Rishspi1_K42_25=-Rishspi1_K41_42;
 Rishspi1_K42_38 (double)	Rishspi1_K42_38=2*Rishspi1_Lt*Rishspi1_Lt*Rishspi1_Coef;
 Rishspi1_K25_41 (double)	Rishspi1_K25_41=-Rishspi1_K41_41;
 Rishspi1_K25_42 (double)	Rishspi1_K25_42=-Rishspi1_K41_42;
 Rishspi1_K25_25 (double)	Rishspi1_K25_25=Rishspi1_K41_41;
 Rishspi1_K25_38 (double)	Rishspi1_K25_38=-Rishspi1_K41_42;
 Rishspi1_K38_41 (double)	Rishspi1_K38_41=Rishspi1_K41_42;
 Rishspi1_K38_42 (double)	Rishspi1_K38_42=Rishspi1_K42_38;
 Rishspi1_K38_25 (double)	Rishspi1_K38_25=-Rishspi1_K41_42;
 Rishspi1_K38_38 (double)	Rishspi1_K38_38=Rishspi1_K42_42;
 Mu0 (double) : Material Damping Parameter	

Variable	Assignment
 Rishspi1_Mu0 (double)	Rishspi1_Mu0=Mu0;
 Rishspi1_R45_45 (double)	Rishspi1_R45_45=Rishspi1_Mu0*Rishspi1_K41_41;
 Rishspi1_R45_46 (double)	Rishspi1_R45_46=Rishspi1_Mu0*Rishspi1_K41_42;
 Rishspi1_R45_47 (double)	Rishspi1_R45_47=Rishspi1_Mu0*Rishspi1_K41_25;
 Rishspi1_R45_48 (double)	Rishspi1_R45_48=Rishspi1_Mu0*Rishspi1_K41_38;
 Rishspi1_R46_45 (double)	Rishspi1_R46_45=Rishspi1_R45_46;
 Rishspi1_R46_46 (double)	Rishspi1_R46_46=Rishspi1_Mu0*Rishspi1_K42_42;
 Rishspi1_R46_47 (double)	Rishspi1_R46_47=Rishspi1_Mu0*Rishspi1_K42_25;
 Rishspi1_R46_48 (double)	Rishspi1_R46_48=Rishspi1_Mu0*Rishspi1_K42_38;
 Rishspi1_R47_45 (double)	Rishspi1_R47_45=Rishspi1_Mu0*Rishspi1_K25_41;
 Rishspi1_R47_46 (double)	Rishspi1_R47_46=Rishspi1_R46_47;
 Rishspi1_R47_47 (double)	Rishspi1_R47_47=Rishspi1_R45_45;
 Rishspi1_R47_48 (double)	Rishspi1_R47_48=Rishspi1_R47_46;
 Rishspi1_R48_45 (double)	Rishspi1_R48_45=Rishspi1_R45_46;
 Rishspi1_R48_46 (double)	Rishspi1_R48_46=Rishspi1_R46_48;
 Rishspi1_R48_47 (double)	Rishspi1_R48_47=Rishspi1_R47_45;
 Rishspi1_R48_48 (double)	Rishspi1_R48_48=Rishspi1_R46_46;
 Rishspi1_K28_28 (double)	Rishspi1_K28_28=Rishspi1_K41_41;
 Rishspi1_K28_40 (double)	Rishspi1_K28_40=Rishspi1_K41_42;
 Rishspi1_K28_49 (double)	Rishspi1_K28_49=Rishspi1_K41_25;
 Rishspi1_K28_50 (double)	Rishspi1_K28_50=Rishspi1_K41_38;
 Rishspi1_K40_28 (double)	Rishspi1_K40_28=Rishspi1_K42_41;
 Rishspi1_K40_40 (double)	Rishspi1_K40_40=Rishspi1_K42_42;
 Rishspi1_K40_49 (double)	Rishspi1_K40_49=Rishspi1_K42_25;
 Rishspi1_K40_50 (double)	Rishspi1_K40_50=Rishspi1_K42_38;
 Rishspi1_K49_28 (double)	Rishspi1_K49_28=Rishspi1_K25_41;
 Rishspi1_K49_40 (double)	Rishspi1_K49_40=Rishspi1_K25_42;
 Rishspi1_K49_49 (double)	Rishspi1_K49_49=Rishspi1_K25_25;
 Rishspi1_K49_50 (double)	Rishspi1_K49_50=Rishspi1_K25_38;
 Rishspi1_K50_28 (double)	Rishspi1_K50_28=Rishspi1_K38_41;
 Rishspi1_K50_40 (double)	Rishspi1_K50_40=Rishspi1_K38_42;
 Rishspi1_K50_49 (double)	Rishspi1_K50_49=Rishspi1_K38_25;
 Rishspi1_K50_50 (double)	Rishspi1_K50_50=Rishspi1_K38_38;
 Rishspi1_R53_53 (double)	Rishspi1_R53_53=Rishspi1_R45_45;
 Rishspi1_R53_54 (double)	Rishspi1_R53_54=Rishspi1_R45_46;
 Rishspi1_R53_55 (double)	Rishspi1_R53_55=Rishspi1_R45_47;
 Rishspi1_R53_56 (double)	Rishspi1_R53_56=Rishspi1_R45_48;




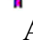

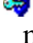

Variable	Assignment
 Rishspi1_R54_53 (double)	Rishspi1_R54_53=Rishspi1_R46_45;
 Rishspi1_R54_54 (double)	Rishspi1_R54_54=Rishspi1_R46_46;
 Rishspi1_R54_55 (double)	Rishspi1_R54_55=Rishspi1_R46_47;
 Rishspi1_R54_56 (double)	Rishspi1_R54_56=Rishspi1_R46_48;
 Rishspi1_R55_53 (double)	Rishspi1_R55_53=Rishspi1_R47_45;
 Rishspi1_R55_54 (double)	Rishspi1_R55_54=Rishspi1_R47_46;
 Rishspi1_R55_55 (double)	Rishspi1_R55_55=Rishspi1_R47_47;
 Rishspi1_R55_56 (double)	Rishspi1_R55_56=Rishspi1_R47_48;
 Rishspi1_R56_53 (double)	Rishspi1_R56_53=Rishspi1_R48_45;
 Rishspi1_R56_54 (double)	Rishspi1_R56_54=Rishspi1_R48_46;
 Rishspi1_R56_55 (double)	Rishspi1_R56_55=Rishspi1_R48_47;
 Rishspi1_R56_56 (double)	Rishspi1_R56_56=Rishspi1_R48_48;
 Rishspi1_TF_yr (double)	
 Rishspi1_Tf_yr2 (double)	
 Rishspi1_R73 (double)	Rishspi1_R73=Rex;
 Rishspi1_R74 (double)	Rishspi1_R74=Rex;
 Rishspi1_R75 (double)	Rishspi1_R75=Rex;
 Rishspi1_R76 (double)	Rishspi1_R76=Rex;
 Rishspi1_Omega (double)	Rishspi1_Omega=Omega;
 Rishspi2_Fixedto1_AngSpeed (double): Angular speed of the rotating frame	Rishspi2_Fixedto1_AngSpeed=Omega;
 Rishspi2_Fixedto2_AngSpeed (double): Angular speed of the rotating frame	Rishspi2_Fixedto2_AngSpeed=Omega;
 Rishspi2_Fixedto4_AngSpeed (double): Angular speed of the rotating frame	Rishspi2_Fixedto4_AngSpeed=Omega;
 Rishspi2_Fixedto3_AngSpeed (double): Angular speed of the rotating frame	Rishspi2_Fixedto3_AngSpeed=Omega;
 Rishspi2_Gyrator1 (double)	
 Rishspi2_trans26 (double)	
 Rishspi2_Gyrator2 (double)	
 Rishspi2_trans36 (double)	
 Rishspi2_Lt (double)	
 Rishspi2_L_this (double)	Rishspi2_L_this=Lelem;

Variable	Assignment
 Rishspi2_Coef (double)	
 Rishspi2_E (double)	Rishspi2_E=E;
 Rishspi2_pi (double)	Rishspi2_pi=pi;
 Rishspi2_Ro (double)	Rishspi2_Ro=Ro;
 Rishspi2_Ri (double)	Rishspi2_Ri=Ri;
 Rishspi2_I (double)	Rishspi2_I=Rishspi2_pi*(Rishspi2_Ro*Rishspi2_Ro*Rishspi2_Ro*Rishspi2_Ro-Rishspi2_Ri*Rishspi2_Ri*Rishspi2_Ri*Rishspi2_Ri)*0.25;
 Rishspi2_K41_41 (double)	Rishspi2_Lt=Rishspi2_L_this; Rishspi2_Coef=Rishspi2_E*Rishspi2_I/(Rishspi2_Lt*Rishspi2_Lt*Rishspi2_Lt); Rishspi2_K41_41=12*Rishspi2_Coef;
 Rishspi2_K41_42 (double)	Rishspi2_K41_42=6*Rishspi2_Lt*Rishspi2_Coef;
 Rishspi2_K41_25 (double)	Rishspi2_K41_25=-Rishspi2_K41_41;
 Rishspi2_K41_38 (double)	Rishspi2_K41_38=Rishspi2_K41_42;
 Rishspi2_K42_41 (double)	Rishspi2_K42_41=Rishspi2_K41_42;
 Rishspi2_K42_42 (double)	Rishspi2_K42_42=4*Rishspi2_Lt*Rishspi2_Lt*Rishspi2_Coef;
 Rishspi2_K42_25 (double)	Rishspi2_K42_25=-Rishspi2_K41_42;
 Rishspi2_K42_38 (double)	Rishspi2_K42_38=2*Rishspi2_Lt*Rishspi2_Lt*Rishspi2_Coef;
 Rishspi2_K25_41 (double)	Rishspi2_K25_41=-Rishspi2_K41_41;
 Rishspi2_K25_42 (double)	Rishspi2_K25_42=-Rishspi2_K41_42;
 Rishspi2_K25_25 (double)	Rishspi2_K25_25=Rishspi2_K41_41;
 Rishspi2_K25_38 (double)	Rishspi2_K25_38=Rishspi2_K25_42;
 Rishspi2_K38_41 (double)	Rishspi2_K38_41=Rishspi2_K41_42;
 Rishspi2_K38_42 (double)	Rishspi2_K38_42=Rishspi2_K42_38;
 Rishspi2_K38_25 (double)	Rishspi2_K38_25=Rishspi2_K42_25;
 Rishspi2_K38_38 (double)	Rishspi2_K38_38=Rishspi2_K42_42;
 Rishspi2_Mu0 (double)	Rishspi2_Mu0=Mu0;
 Rishspi2_R45_45 (double)	Rishspi2_R45_45=Rishspi2_Mu0*Rishspi2_K41_41;
 Rishspi2_R45_46 (double)	Rishspi2_R45_46=Rishspi2_Mu0*Rishspi2_K41_42;
 Rishspi2_R45_47 (double)	Rishspi2_R45_47=Rishspi2_Mu0*Rishspi2_K41_25;
 Rishspi2_R45_48 (double)	Rishspi2_R45_48=Rishspi2_Mu0*Rishspi2_K41_38;
 Rishspi2_R46_45 (double)	Rishspi2_R46_45=Rishspi2_R45_46;
 Rishspi2_R46_46 (double)	Rishspi2_R46_46=Rishspi2_Mu0*Rishspi2_K42_42;
 Rishspi2_R46_47 (double)	Rishspi2_R46_47=Rishspi2_Mu0*Rishspi2_K42_25;
 Rishspi2_R46_48 (double)	Rishspi2_R46_48=Rishspi2_Mu0*Rishspi2_K42_38;
 Rishspi2_R47_45 (double)	Rishspi2_R47_45=Rishspi2_R45_47;
 Rishspi2_R47_46 (double)	Rishspi2_R47_46=Rishspi2_R46_47;
 Rishspi2_R47_47 (double)	Rishspi2_R47_47=Rishspi2_R45_45;








Variable	Assignment
 Rishspi2_R47_48 (double)	Rishspi2_R47_48=Rishspi2_R47_46;
 Rishspi2_R48_45 (double)	Rishspi2_R48_45=Rishspi2_R45_46;
 Rishspi2_R48_46 (double)	Rishspi2_R48_46=Rishspi2_R46_48;
 Rishspi2_R48_47 (double)	Rishspi2_R48_47=Rishspi2_R47_48;
 Rishspi2_R48_48 (double)	Rishspi2_R48_48=Rishspi2_R46_46;
 Rishspi2_K28_28 (double)	Rishspi2_K28_28=Rishspi2_K41_41;
 Rishspi2_K28_40 (double)	Rishspi2_K28_40=Rishspi2_K41_42;
 Rishspi2_K28_49 (double)	Rishspi2_K28_49=Rishspi2_K41_25;
 Rishspi2_K28_50 (double)	Rishspi2_K28_50=Rishspi2_K41_38;
 Rishspi2_K40_28 (double)	Rishspi2_K40_28=Rishspi2_K42_41;
 Rishspi2_K40_40 (double)	Rishspi2_K40_40=Rishspi2_K42_42;
 Rishspi2_K40_49 (double)	Rishspi2_K40_49=Rishspi2_K42_25;
 Rishspi2_K40_50 (double)	Rishspi2_K40_50=Rishspi2_K42_38;
 Rishspi2_K49_28 (double)	Rishspi2_K49_28=Rishspi2_K25_41;
 Rishspi2_K49_40 (double)	Rishspi2_K49_40=Rishspi2_K25_42;
 Rishspi2_K49_49 (double)	Rishspi2_K49_49=Rishspi2_K25_25;
 Rishspi2_K49_50 (double)	Rishspi2_K49_50=Rishspi2_K25_38;
 Rishspi2_K50_28 (double)	Rishspi2_K50_28=Rishspi2_K38_41;
 Rishspi2_K50_40 (double)	Rishspi2_K50_40=Rishspi2_K38_42;
 Rishspi2_K50_49 (double)	Rishspi2_K50_49=Rishspi2_K38_25;
 Rishspi2_K50_50 (double)	Rishspi2_K50_50=Rishspi2_K38_38;
 Rishspi2_R53_53 (double)	Rishspi2_R53_53=Rishspi2_R45_45;
 Rishspi2_R53_54 (double)	Rishspi2_R53_54=Rishspi2_R45_46;
 Rishspi2_R53_55 (double)	Rishspi2_R53_55=Rishspi2_R45_47;
 Rishspi2_R53_56 (double)	Rishspi2_R53_56=Rishspi2_R45_48;
 Rishspi2_R54_53 (double)	Rishspi2_R54_53=Rishspi2_R46_45;
 Rishspi2_R54_54 (double)	Rishspi2_R54_54=Rishspi2_R46_46;
 Rishspi2_R54_55 (double)	Rishspi2_R54_55=Rishspi2_R46_47;
 Rishspi2_R54_56 (double)	Rishspi2_R54_56=Rishspi2_R46_48;
 Rishspi2_R55_53 (double)	Rishspi2_R55_53=Rishspi2_R47_45;
 Rishspi2_R55_54 (double)	Rishspi2_R55_54=Rishspi2_R47_46;
 Rishspi2_R55_55 (double)	Rishspi2_R55_55=Rishspi2_R47_47;
 Rishspi2_R55_56 (double)	Rishspi2_R55_56=Rishspi2_R47_48;
 Rishspi2_R56_53 (double)	Rishspi2_R56_53=Rishspi2_R48_45;
 Rishspi2_R56_54 (double)	Rishspi2_R56_54=Rishspi2_R48_46;
 Rishspi2_R56_55 (double)	Rishspi2_R56_55=Rishspi2_R48_47;
 Rishspi2_R56_56 (double)	Rishspi2_R56_56=Rishspi2_R48_48;
 Rishspi2_TF_yr (double)	

Variable	Assignment
 Rishspi2_Tf_yr2 (double)	
 Rishspi2_R73 (double)	Rishspi2_R73=Rex;
 Rishspi2_R74 (double)	Rishspi2_R74=Rex;
 Rishspi2_R75 (double)	Rishspi2_R75=Rex;
 Rishspi2_R76 (double)	Rishspi2_R76=Rex;
 Rps (double) : Input Rotational Speed	
 Rishspi2_Omega (double)	Rishspi2_Omega=Omega;
 SF13 (double)	SF13=0.0;
 SF16 (double)	SF16=0.0;
 SF17 (double)	SF17=0.0;
 SF19 (double)	SF19=0.0;
 M45 (double)	
 M47 (double)	
 M51 (double)	
 M49 (double)	
 RGyrator (double)	RGyrator=(0.25*SPINNIN1_Rho*pi*(SPINNIN1_L_Prev+SPINNIN1_L_Next)*(Ro*Ro*Ro*Ro-SPINNIN1_Ri*SPINNIN1_Ri*SPINNIN1_Ri*SPINNIN1_Ri))*SPINNIN1_AngSpeed;
 LGyrator (double)	LGyrator=RGyrator;
 M40 (double)	
 SF42 (double)	SF42=Omega;
 Rclp (double) : Coupling Damping	
 R43 (double)	R43=Rclp;








Various expressions used in Transformation element:



















Variable	Assignment
 _cst (double)	_cst=cos(_Q16);
 _snt (double)	_snt=sin(_Q16);
 _msnt (double)	_msnt=-_snt;
 _AngSpeed (double) : Angular speed of the rotating frame	
 _SF15 (double)	_SF15=_AngSpeed;
 _mXsntpYc (double)	_mXsntpYc=-_Q19*_snt+_Q20*_cst;
 _mXcstmYs (double)	_mXcstmYs=-_Q19*_cst-_Q20*_snt;

Various expressions used in Spinning Hub modelling


Variable	Assignment
 _AngSpeed (double) : Angular Speed rad/s	
 _Rho (double) : Material Density	
 _B1 (double) : HubWidth Bi, i=1 to 4	_B1=1.0;
 _B2 (double) : HubWidth Bi, i=1 to 4	_B2=1.0;
 _B3 (double) : HubWidth Bi, i=1 to 4	_B3=1.0;
 _B4 (double) : HubWidth Bi, i=1 to 4	_B4=1.0;
 _R1i (double) : Inner Radius Stage 1	_R1i=0.0;




Variable	Assignment
 _R1o (double) : Outer Radius Stage 1	$_R1o=0.0;$
 _R2o (double) : Outer Radius Stage 2	$_R2o=0.0;$
 _R3o (double) : Outer Radius Stage 3	$_R3o=0.0;$
 _R4o (double) : Outer Radius Stage 4	$_R4o=0.0;$
 _Ri (double) : Inner Rad. of Right End of Previous Int.face Shaft (Note Cyl. or Cone)	
 _RiT (double)	$_RiT=_Ri;$ if ($_Ri==0.0$) $_RiT=1.0;$
 _Riprv (double) : Inner Rad. of Left End of Previous Int.face Shaft (Note Cyl. or Cone)(Zero if non-existent)	
 _L_Prev (double) : Length of Previous Int. face Shaft(Zero if non-existent)	
 _Th_Prev (double) : Thickness of Previous Int. face Shaft (Zero if non-existent)	
 _Rinext (double) : Inner Rad. of Left End of Next Int.face Shaft (Note Cyl. or Cone)(Zero if non-existent)	
 _Rrhnext (double) : Inner Rad. of Right End of Next Int.face Shaft (Note Cyl. or Cone)(Zero if non-existent)	

Variable	Assignment
 _L_Next (double) : Length of Next Int. face Shaft(Zero if non-existant)	
 _Th_Next (double) : Thickness of Next Int. face Shaft (Zero if non-existant)	
 _R2i (double)	_R2i=_R1o;
 _R3i (double)	_R3i=_R2o;
 _R4i (double)	_R4i=_R3o;
 _mprv (double)	
 _L_prvT (double)	_L_prvT=_L_Prev; if (_L_Prev==0.0) _L_prvT=1.0;
 _RiprvT (double)	_RiprvT=_Riprv; if (_Riprv==0.0) _RiprvT=1.0;
 _RrhnextT (double)	_RrhnextT=_Rrhnext; if (_Rrhnext==0.0) _RrhnextT=1.0;
 _RinextT (double)	_RinextT=_Rinext; if (_Rinext==0.0) _RinextT=1.0;
 _L_NextT (double)	_L_NextT=_L_Next; if (_L_Next==0.0) _L_NextT=1.0;
 _L (double)	_L=1.0;
 _m (double)	_m=0.000001;
 _Th (double)	_Th=0.00;
 _mnext (double)	
 _LLip1 (double)	
 _Z4ip1 (double)	
 _Z3ip1 (double)	
 _Z2ip1 (double)	
 _Z1ip1 (double)	

Variable	Assignment
 _LRi (double)	
 _Z4i (double)	
 _Z3i (double)	
 _Z2i (double)	
 _Z1i (double)	
 _LRip1 (double)	
 _LLim1 (double)	
 _Z4im1 (double)	
 _Z3im1 (double)	
 _Z2im1 (double)	
 _Z1im1 (double)	
 _LLi (double)	
 _LRim1 (double)	
 _MconPrv (double)	
 _MiconPrv (double)	
 _MconNext (double)	
 _MiconNext (double)	
 _pi (double)	<pre> _pi=3.141592653; if (first_time) { _mprv=(_RiT-_RiprvT)/_L_prvT; if (_RiT==_RiprvT) _mprv=0.000001; _mnext=(_RrhnextT-_RinextT)/_L_NextT; if (_RrhnextT==_RinextT) _mnext=0.000001; _LLi=(_RiT*_L*0.5+_m*_L*_L/3.0)/(_RiT+_m*_L*0.5); _LRi=_L-_LLi; _LLim1=(_RiprvT*_L_prvT*0.5+_mprv*_L_prvT*_L_prvT/3.0)/ (_RiprvT+_mprv*_L_prvT*0.5); _LLip1=(_RinextT*_L_NextT*0.5+_mnext*_L_NextT*_L_Next T/3.0)/(_RinextT+_mnext*_L_NextT*0.5); _LRim1=_L_prvT-_LLim1; </pre>

Variable	Assignment
	<pre> _LRip1=_L_NextT-_LLip1; _Z1i=(2.0*_RiT*_RiT+3.0*_RiT*_Th)*_RiT; _Z1im1=(2.0*_RiprvT*_RiprvT+3.0*_RiprvT*_Th_Prev)*_RiprvT; _Z1ip1=(2.0*_RinextT*_RinextT+3.0*_RinextT*_Th_Next)*_RinextT; _Z2i=(6.0*_RiT*_RiT+4.0*_RiT*_Th)*_m; _Z2im1=(6.0*_RiprvT*_RiprvT+4.0*_RiprvT*_Th_Prev)*_mprv; _Z2ip1=(6.0*_RinextT*_RinextT+4.0*_RinextT*_Th_Next)*_mnext; _Z3i=(6.0*_RiT+_Th)*_m*_m; _Z3im1=(6.0*_RiprvT+_Th_Prev)*_mprv*_mprv; _Z3ip1=(6.0*_RinextT+_Th_Next)*_mnext*_mnext; _Z4i=2.0*_m*_m*_m; _Z4im1=2.0*_mprv*_mprv*_mprv; _Z4ip1=2.0*_mnext*_mnext*_mnext; _MconPrv=2.0*_pi*_Rho*((_RiT*_LLi+_m*_LLi*_LLi*0.5)*_Th+(_RiprvT*_LRim1+_mprv*_LRim1*_LRim1*0.5)*_Th_Prev); _MiconPrv=_pi*_Rho*((_Z1i*_LLi+_Z2i*_LLi*_LLi*0.5+_Z3i*_LLi*_LLi*_LLi/3.0+_Z4i*_LLi*_LLi*_LLi*_LLi*0.25)*_Th+(_Z1im1*_LLim1+_Z2im1*_LLim1*_LLim1*0.5+_Z3im1*_LLim1*_LLim1*_LLim1/3.0+_Z4im1*_LLim1*_LLim1*_LLim1*_LLim1*0.25)*_Th_Prev); _MconNext=2.0*_pi*_Rho*((_RiT*_LRi+_m*_LRi*_LRi*0.5)*_Th+(_RinextT*_LRip1+_mnext*_LRip1*_LRip1*0.5)*_Th_Next); _MiconNext=_pi*_Rho*((_Z1i*_LRi+_Z2i*_LRi*_LRi*0.5+_Z3i*_LRi*_LRi*_LRi/3.0+_Z4i*_LRi*_LRi*_LRi*_LRi*0.25)*_Th+(_Z1ip1*_LLip1+_Z2ip1*_LLip1*_LLip1*0.5+_Z3ip1*_LLip1*_LLip1*_LLip1/3.0+_Z4ip1*_LLip1*_LLip1*_LLip1*_LLip1*0.25)*_Th_Next)); </pre>
 _HubMass (double)	
 _DiskMass (double)	<pre> _DiskMass=_pi*_Rho*(B1*(R1o*_R1o-_R1i*_R1i)+_B2*(R2o*_R2o-_R2i*_R2i)+_B3*(R3o*_R3o-_R3i*_R3i)+_B4*(R4o*_R4o-_R4i*_R4i))+_MconPrv+_MconNext; _DiskMass=_DiskMass+_HubMass; </pre>

Variable	Assignment
 _Ecc (double) : Eccentricity of the Hub	
 _AnglEcc (double) : Angle of Eccentricity from X Axis(vertical) in Degrees.	
 _RotDmp (double) : Rotational Damping about diametrical axes	
 _TransDmp (double) : Translational Damping of Mass centre	
 _HubPolMI (double)	
 _M25 (double)	_M25=_DiskMass;
 _Hub_DiaMI (double)	_Hub_DiaMI=_HubPolMI*0.5;
 _Dia_MI (double)	$\begin{aligned} _Dia_MI &= 0.25 * _pi * _Rho * (_B1 * (_R1o * _R1o * _R1o * _R1o - \\ &_R1i * _R1i * _R1i * _R1i) \\ &+ _B2 * (_R2o * _R2o * _R2o * _R2o - _R2i * _R2i * _R2i * _R2i) \\ &+ _B3 * (_R3o * _R3o * _R3o * _R3o - \\ &_R3i * _R3i * _R3i * _R3i) + _B4 * (_R4o * _R4o * _R4o * _R4o - \\ &_R4i * _R4i * _R4i * _R4i)) + _MiconPrv + _MiconNext; \\ _Dia_MI &= _Dia_MI + _Hub_DiaMI; \end{aligned}$
 _pmiomeg (double)	_pmiomeg=_HubPolMI*_AngSpeed;
 _R11 (double)	_R11=_TransDmp;
 _R14 (double)	_R14=_R11;
 _PhEcc (double)	
 _mepsnth (double)	$\begin{aligned} _PhEcc &= _AnglEcc * 3.141592653 / 180.0; \\ _mepsnth &= -_Ecc * \sin(_Q24 + _PhEcc); \end{aligned}$
 _epcsth (double)	$_epcsth = _Ecc * \cos(_Q24 + _PhEcc);$
 _M27 (double)	_M27=_M25;
 _M2 (double)	_M2=_Dia_MI;
 _M7 (double)	_M7=_M2;

Variable	Assignment
 _R9 (double)	_R9=_RotDmp;
 _R4 (double)	_R4=_RotDmp;
 _SF41 (double)	